The regulation of PCSK9 structure and function through lipoprotein interactions

SAMANTHA KHADIJA SARKAR

Thesis submitted to the Faculty of Graduate and Postdoctoral Studies

In partial fulfillment of the requirements

For the degree of

Doctorate in Philosophy

Department of Biochemistry, Microbiology and Immunology

University of Ottawa

Ottawa, Ontario, Canada

© Samantha Khadija Sarkar, Ottawa, Canada, 2019

Abstract

Proprotein convertase subtilisin / kexin type 9 (PCSK9) is a negative regulator of the low-density lipoprotein receptor, and PCSK9 inhibition has become an important cholesterol-lowering therapeutic strategy. PCSK9 also associates with LDL particles, and evidence suggests that the activity of PCSK9 may be regulated by LDL binding. We have investigated the biochemistry of the interaction between PCSK9 and lipoproteins. Through mutagenesis and in-vitro binding assays, we found conserved motifs in the PCSK9 N-terminus that play a role in LDL binding. Through secondary structure studies using circular dichroism and computational modelling, we determined that the N-terminal region of the PCSK9 prodomain undergoes an environment-dependent structural shift that affects the ability of PCSK9 to bind LDL. We also found that the commonly found loss-of-function polymorphism R46L is capable of modulating this structural shift. Importantly, we found a surface-exposed region of the PCSK9 prodomain that maps a cluster of gain-of-function mutations (L108R, S127R, and D129G) that severely disrupt LDL binding. Through gel shift assays and density gradient centrifugation, we observed that PCSK9 shows remodeling-dependent ability to bind different classes of lipoprotein particles in vitro, binding strongly to LDL and IDL but showing barely detectable association to VLDL. Further, in human plasma, we found that lipoprotein-bound populations of PCSK9 shifted in response to differences in lipoprotein profiles between normolipidemic and hypercholesterolemic or hypertriglyceridemic subjects. Overall, elucidation of how lipoproteins regulate PCSK9 activity will reveal new targets for designing cholesterol-lowering therapeutics.

Acknowledgements

While the “Contributions of Collaborators” section will detail specific work done by specific people, this section needs to address the kind of help and support I have received that is more difficult to quantify.

I am first and foremost grateful to my supervisor Dr. Thomas Lagace for his many years of support and guidance. Over the years, Tom has done everything from giving me hands-on bench training to providing me with professional growth opportunities, such as conference travel. I also greatly appreciate the considerable amounts of time he allowed me to spend on out-of-lab activities such as teaching assistantships, internships and science outreach volunteering. Tom truly allowed me a full and fruitful graduate student experience.

All my lab-mates over the years have been helpful and delightful to work with. However, I must give special thanks to Tanja Kosenko, our lab manager. From the day I started in this lab, Tanja has been ever-present and ever-ready to help in any way possible, and has always gone above and beyond in helping me do what I needed to do.

I must also thank my thesis advisory committee members and comprehensive examiners Dr. Ruth McPherson, Dr. Alexandre Stewart, Dr. Morgan Fullerton, and Dr. Zemin Yao, for their advice and insight on my project, and guidance in my academic progress.

I would like to add a thank-you to Alex Foo and Saud Ayed, graduate students in the Goto lab at the time that I collaborated there, for taking considerable amounts of their time to teach me circular dichroism from scratch. They also took pity on my lack of muscle and always changed nitrogen tanks for me, and made me feel welcome in their lab with lots of snacks, swords (yes, swords, full size ones), chemical fires and laughter.

Finally, I must thank the people who sustained me throughout the graduate years in ways that they probably do not even realize. My parents continue treat their fully grown daughter as a school-girl, keeping me well fed and allowing me to focus my energies on my work. My closest friends have always lent me their ears at the end of a bad day. Last but not least, thanks to my partner, who made the fretful days of thesis-writing much brighter.

Contributions of Collaborators

Parts of the data presented in this work were obtained in collaboration with different research groups, and some experiments were performed by other members of our lab. These contributions must be clearly acknowledged.

Circular dichroism experiments were performed in the lab of Dr. Natalie Goto at the University of Ottawa, in the Department of Chemistry and Biomolecular Sciences. The experiments were performed by me with the help of Dr. Alex Foo, at the time a graduate student in the Goto lab.

Modeling of the disordered PCSK9 N-terminus by molecular dynamics simulations were done by Dr. Ariela Vergara-Jaques at her lab in Chile, at the Center for Bioinformatics and Molecular Simulation, Universidad de Talca.

C-terminally FLAG-tagged mutant constructs of PCSK9 were generated by me except for the following: R46L – Geoffry LeBlonde, former lab technician in the Lagace lab, R469W – Dr. Curtis Brandt, former postdoctoral fellow in the Lagace lab, mouse A47P – Tanja Kosenko, laboratory manager of the Lagace lab.

The in-vitro binding assays of mutant PCSK9 with LDL were performed by me except for the following: R469W, R496W, F515L – Angela Matyas, graduate student in the Lagace lab.

ELISA measurements of hypercholesterolemic plasma samples were performed by Amy Martinuk, former technician in the Lagace lab, with data compilation and sub-analysis calculations performed by me. Gradient centrifugation and fraction analysis for two hypertriglyceridemic subjects were done by Tanja Kosenko.

The experiment confirming that sodium-bromide-isolated lipoproteins do not contain bound PCSK9 (Figure 10A) was performed by Dr. Lagace.

Data in all other figures were generated by me, with extensive guidance in experimental design and project direction from Dr. Lagace.

Contents

Abbreviations Used

ApoA / B / C	Apolipoprotein A / B / C
ApoB48 / ApoB100	Apolipoprotein B48 or B100
ARH	Autosomal recessive hypercholesterolemia
CETP	Cholesteryl Ester Transferase Protein
CVD	Cardiovascular Disease
DMEM	Dulbecco Modified Eagle Medium
DNA	Deoxyribonucleaic acid
dNTP	Deoxyribonucleotide
EGF	Epidermal growth-factor
ER	Endoplasmic reticulum
FBS	Fetal bovine serum
HBSC	HEPES-buffered saline with calcium
HDL	High density lipoprotein
HEK293	Human embryonic kidney immortalized cell line
HepG2	Human hepatocellular carcinoma immortalized cell line
HMGCoA	3-hydroxy-3-methylglutaryl coenzyme A
HNF1α	Hepatocyte Nuclear factor 1 alpha
HuH7	Human Hepatoma immortalized cell line
IDL	Intermediate density lipoprotein
INSIG	Insulin-induced gene 1
ITS	Insulin – transferrin - selenium
K_i	Inhibitor constant
LDL	Low density lipoprotein
LDL-C	Low density lipoprotein - cholesterol
LDLR	Low density lipoprotein receptor
PBS	Phophate buffered saline
PC	Proprotein convertase
PCR	Polymerase chain reaction
PCSK9	Proprotein convertase subtilisin/ kexin type-9
RNA	Ribonucleic acid
S1P / S2P	Site 1 protease / Site 2 protease
SCAP	SREBP cleavage activating protein
SDS-PAGE	Sodium dodecyl-sulfate - polyacrylamide gel electrophoresis
SEM	Standard error of the mean
SRE	Sterol regulatory element
SREBP	Sterol regulatory element binding protein
SPR	Surface plasmon resonance
TAG	Triacylglycerol
TBSC	Tris-buffered sTransaline with calcium
TFR	Transferrin receptor
TRL	Triglyceride-rich lipoproteins

List of Illustrations, Figures and Tables

Chapter 1: Introduction

Proprotein Convertase Subtilisin Kexin Type – 9 (PCSK9), originally named Neural apoptosis-regulated convertase-1 (NARC-1) at the time of its discovery[1], is a secreted, circulating protein that plays a major role in regulating cholesterol homeostasis in the circulation. PCSK9 is a negative regulator of low-density lipoprotein receptor (LDLR), which is responsible for clearing the majority of the cholesterol-containing particles from the blood. The science of PCSK9 moved rapidly from newly discovered gene in 2003 to FDA-approved target for hypercholesterolemia therapeutics over the course of about 10 years. Inhibiting PCSK9 has been proven in clinical trials to effectively lower blood cholesterol levels[2,3]. However, given the focus on therapeutic development that dominated this time-period, much about the basic biology of PCSK9 still remains to be elucidated.

The studies described herein investigate the interaction between PCSK9 and lipoproteins, and how these interactions may govern reciprocal regulatory mechanisms of PCSK9 activity and plasma cholesterol levels.

1.1 Hypercholesterolemia and PCSK9

1.1.1 Inherited hypercholesterolemia. Familial hypercholesterolemia (FH) is a condition of elevated plasma cholesterol, contained primarily in low density lipoprotein (LDL) particles in the blood. Chronically elevated LDL levels in blood promote the accumulation of modified LDL in the artery walls[4]. LDL moves in and out of arterial walls, and interactions with charged proteoglycans on endothelial cells promote local LDL retention and increase the proximity of these particles to chemical and enzymatic modifications[5-8]. According to the "response-to-retention" hypothesis, this accumulation of LDL in artery walls triggers a cascade of inflammatory responses and formation of atherosclerotic plaques, which impede blood flow and lead to stroke and myocardial infarction[4,9,10]. FH is caused by mutations in various genes involved in clearing LDL particles from circulation. The

majority of FH cases are caused by mutations in the LDL receptor (LDLR) gene (80-85%) followed by mutations in Apolipoprotein B (apoB), a component of LDL particles (5-10%)[11]. More rarely mutations in the Proprotein Convertase Subtilisin / Kexin Type 9 (PCSK9) gene also cause severe FH (<1%)[11]. Remaining FH cases are caused by very rare monogenic mutations in other genes, or are polygenic in nature. These mutations are autosomal dominant, except for mutations in LDLR Adaptor Protein 1 (LDLRAP1), which cause FH in an autosomal recessive manner[12].

1.1.2 PCSK9 in FH. PCSK9 mutations cause FH through PCSK9's role as a negative regulator of LDLR levels. LDLRs are responsible for clearing LDL from the circulation. LDL particles bind to LDLRs on the cell surface and are then endocytosed and directed for catabolism within cells[13]. The apoB moiety on LDL acts as the ligand for LDLR[14]. Thus mutations in the LDLR or apoB gene that disrupt the LDL-LDLR interaction lead to FH through decreased ability to clear LDL from circulation. Circulating PCSK9 can bind cell surface LDLRs as well, and upon internalization of the complex, direct the LDLR for degradation in the lysosome[15-17]. Non-PCSK9 bound LDLR that is endocytosed can typically recycle back to the cell surface several hundred times, allowing for each receptor molecule to clear many LDL particles over the course of its lifetime[13]. However, being directed for degradation by PCSK9 prevents the LDLR from being recycled back to the surface, thus decreasing protein levels of LDLR on the cell surface. Gain-of function mutations that increase the ability of PCSK9 to mediate LDLR degradation thus cause FH, while loss-of-function mutations in PCSK9 lead to lower circulating LDL concentrations in plasma over the course of an individual's life, decreasing their risk of atherosclerosis and cardiovascular disease[18].

The existence of loss-of-function PCSK9 variants in healthy humans validated the idea of PCSK9 inhibition as a therapeutic approach to treat hypercholesterolemia. The nonsense mutations Y142X, C679X, frequently found as heterozygotes in African American populations, have been linked to 30%–40% reductions of plasma LDL-cholesterol, with over 80% reductions in CVD risk[19,20]. Two individual women were identified to be lacking circulating PCSK9 altogether. Both of these women

had less than 15 mg/dL plasma LDL-cholesterol, and neither showed any adverse effects on their health due to the lack of functional PCSK9[21,22].

1.1.3 Statins. PCSK9 inhibition is a relatively new approach to lowering plasma LDL-cholesterol. Up until now, pharmacological treatment of FH has been dominated by statins, inhibitors of the rate-limiting enzyme 3-hydroxy-3-methylglutaryl coenzyme A reductase (HMGCoAR) in the intracellular cholesterol synthesis pathway. Blocking cholesterol biosynthesis triggers a negative feedback mechanism that induces cells to transcriptionally up-regulate expression of the LDLR, decreasing plasma LDL[23].

Stains are a widely prescribed and highly successful class of drugs, reaching 65% reductions in LDL-cholesterol levels and lowering combined risk of death, cardiovascular events and stroke by nearly 40%[24-26]. However, the HMGCoAR reaction occurs upstream of important intermediate metabolite production points. A proportion of patients experience adverse effects associated with statin use, including myopathies, liver toxicity and increased risk of developing diabetes[23]. Many patients are also statin resistant, i.e. they do not achieve the required LDL-cholesterol levels on statins, and require alternate methods of further LDL reductions[27]. Statin resistance is linked with genetic polymorphisms in various genes in the cholesterol homeostasis pathways[28]. These problems mean that there is a need for alternative methods of lowering LDL-cholesterol, to work either alone or in conjunction with statins. Thus, PCSK9 inhibition is currently an active area of both pre-clinical and clinical research and development.

1.1.4 PCSK9 inhibition. Various approaches of PCSK9 inhibition have been under investigation and development. Monoclonal antibodies (mAbs) that block the protein-protein interaction between PCSK9 and LDLR at the cell surface were the first PCSK9 inhibitors to advance successfully through clinical trials and obtain FDA approval. The antibodies Alirocumab (developed by Regeneron pharmaceuticals and Sanofi) and Evolocumab (developed by Amgen) became FDA

approved in 2015, and lead to 50% LDL-cholesterol lowering on PCSK9 inhibitor alone, up to 60% lowering in conjunction with statins and other lipid-lowering agents[2,29,30]. Downstream cardiovascular benefits of these PCSK9 inhibition treatments have also been observed, although in more modest magnitudes, potentially due to limited long-term data. Over a 3 year period, Evolocumab in conjunction with statins was shown to reduce risk of myocardial infarctions, stroke and coronary revascularization by 15% compared to placebo[2]. Recent clinical trial results with Alirocumab showed greatest benefit in patients with the highest LDL cholesterol levels. Similar to Evolocumab, 15% relative risk reduction was seen for the primary composite endpoint (nonfatal myocardial infarction, ischemic stroke, unstable angina and cardiovascular disease-specific mortality) over 4 years[3].

While mAbs are on the market, they remain a highly expensive form of therapy. A report in JAMA calculated that the price of PCSK9 inhibitors needs to decrease by 71% to meet a willingness-to-pay threshold of $100,000 per quality-adjusted life-year[31]. The large antibody molecules also have low tissue distribution[32], and require parenteral administration, usually by injections. Thus, it is desirable to develop more economical small molecule PCSK9 inhibitors. There has been some research into single-domain antibodies, which would be smaller and more cost-effective to produce than the current mAbs[33], although these would still face injection-site issues.

Development of alternative PCSK9-inhibition strategies are underway. Inclisiran, a synthetic liver-specific small interfering RNA (siRNA) against PCSK9 messenger RNA (mRNA), has reached Phase II clinical trials, showing safety and LDL-cholesterol lowering ability comparable to the antibodies[34,35]. An adnectin preventing PCSK9-LDLR binding has undergone phase I trial where LDL-cholesterol lowering was observed[36]. An antisense oligonucleotide against PCSK9 mRNA developed by Santaris Pharma went to Phase I clinical trial, but the trial was discontinued, likely for safety concerns[37]. Two groups have been testing vaccines against PCSK9: The AT04A vaccine is based on a peptide that mimics the PCSK9 N-terminal region, and shows efficacy in

APOE*3Leiden.CETP transgenic mice[38]. Another vaccine based on a virus-like particle lowered plasma cholesterol and plasma PCSK9 levels in Balb/c mice and LDLR+/- mice[39].

Several companies have reported on small organic compounds that increase LDL uptake or LDLR expression in cell culture and mice through unknown mechanisms. Pfizer is working on compounds that selectively inhibit PCSK9 translation[40-42]. In addition, heparan-sulphate proteoglycans have also been found to play a role in PCSK9-induced LDLR-degradation as co-factors, and a heparan-sulphate proteoglycan binding pocket on PCSK9 has been identified[43]. Thus, there is opportunity for heparin mimetics to be investigated as PCSK9 inhibitors.

1.2 PCSK9: A Member of the Proprotein Convertase Family

1.2.1 Proprotein Convertases. Proprotein convertases (PCs) are serine proteases related to bacterial subtilisin and yeast kexin. They play important roles in protein activation through cleavage of precursors of various hormones, growth factors, receptors and enzymes at various intra- and extra-cellular sites. The mammalian PC family has 9 members: PC1, PC2, furin, PC4, PC5, PACE4 (paired basic amino acid cleaving enzyme 4), PC7, SKI1 (subtilisin kexin isozyme 1, also known as S1P), and PCSK9. The first 7 members cleave at single or paired basic residues[44-47], while SKI-1 and PCSK9 play roles in cholesterol and lipid homeostasis via cleavage at non-basic residues[17,48] . All PCs require calcium to cleave their substrates[49,50].

Structurally, PCs begin with a signal sequence, a prodomain and a catalytic domain that contains the aspartate, histidine and serine residues that make up the catalytic triad, as well as an asparagine for the oxyanion hole. Following the catalytic domain, all the PCs have a P-domain that is thought to stabilize the catalytic pocket. However, the two non-basic residue-specific PCs SKI-1 and PCSK9 lack P-domains. The C-terminal of each PC is unique and dictates their trafficking and localization[49].

PCs undergo proteolytic maturation themselves. In the endoplasmic reticulum (ER), they are produced as zymogens that lose their signal peptide through the action of signal peptidase[51]. The

resulting pro-PC is then folded into a conformation that allows the catalytic site to function. The prodomain acts as a chaperone in this folding process[52-54]. The pro-PC then autocatalytically cleaves off its prodomain[55], which remains non-covalently associated with the rest of the protein to keep it in an inactive state. Usually, a second cleavage event in the prodomain releases the prodomain, activating the PC at the appropriate site of cellular localization[51,54]. However, PCSK9 is an exception to this, where the mature PCSK9 protein retains its prodomain permanently [49].

1.2.2 PCSK9 structure and processing. The 692 amino acid (74kDa) PCSK9 zymogen synthesized in the ER contains a signal sequence, a prodomain, a catalytic domain, and a C-terminal domain **(Figure 1)**. In the ER lumen, the 30 amino acid signal peptide at the N-terminal end of the protein is removed. Autocatalytic processing of the 14 kDa prodomain occurs at the site SVFAQ[152]↓SIP[17]. In contrast to other PCs however, no secondary cleavage event occurs in the PCSK9 prodomain due to an apparent lack of the target loop for the second cleavage site[56]. Thus, the cleaved prodomain remains permanently associated with the rest of the protein, preventing mature PCSK9 from acting as a serine protease. No substrates of PCSK9 other than itself have been identified to date. The main apparent physiological function of PCSK9 (*i.e.* mediation of LDLR degradation), occurs independently of the protease activity of PCSK9[57].

The N-terminal 30 residues of the prodomain in mature PCSK9 (amino acids 31-60) are not visible in crystal structures, indicating that the region is structurally disordered[56,58,59] **(Figure 1)**. The remainder of the prodomain is made up of a 5-stranded β-sheet covered on one side by two alpha helices. Residues 61-75 form an extra strand important for self-processing, followed by a helical turn. The strand and turn enlarge the interface of the PCSK9 prodomain with the catalytic domain, helping to retain the prodomain on the mature protein[56]. The catalytic domain is a 7-stranded parallel β-sheet flanked on both sides by alpha helices[58]. The domain contains three disulfide bonds, with two alpha helices forming the interface with the C-terminal domain. Three hydrogen bonds hold the catalytic and C-terminal domain together, in addition to hydrophobic and Van der Waals

forces. The C-terminal domain is made up of three subunits with quasi-three fold internal symmetry, giving the domain an overall cylindrical shape. Each subunit is made up of 6-stranded anti-parallel β-sheets in truncated jelly-roll motifs. The subunits are held together by three internal disulfide bonds each[58,59]. The C-terminal domain also contains many histidine residues, mostly concentrated on the surface of a groove between two of the subunits[58].

PCSK9 contains post-translational modifications at several sites: N-linked glycosylation at asparagine 533[1], two sulfation sites at tyrosine 38 and tyrosine 142[1,17] and two phosphorylation sites at serine 47 and serine 688[60]. The functional purposes of these modifications have yet to be elucidated. Glycosylation and sulfation appear to play no role in PCSK9 activity[61], but phosphorylation may protect the prodomain from proteolysis[60].

1.3 PCSK9 as a regulator of the LDLR

1.3.1 LDLR degradation. Two important reciprocal relationships help maintain LDLR expression homeostasis. Firstly, LDLR-mediated uptake of LDL-cholesterol into cells regulates circulating cholesterol levels while exerting negative feedback on LDLR transcription through regulation of the transcription factor SREBP-2[62,63] . Secondly, circulating PCSK9 post-transcriptionally down-regulates cell surface LDLR levels while the LDLR also acts as the primary clearance pathway for circulating PCSK9[64]. Overexpression and parabiosis studies in hepatocyte cell lines and in mice demonstrated the ability of PCSK9 to reduce LDLR expression and increase plasma LDL-cholesterol[15,65,66]. Studies where gain-of-function PCSK9 mutant D374Y (which exhibits 10-fold - 25 -fold increased affinity for the LDLR at neutral pH[56,67,68]) caused greater PCSK9 uptake and hepatic LDLR degradation support the specificity of the LDLR-PCSK9 interaction[16]. The C-terminal domain of PCSK9 is required for LDLR degradation activity, although it remains unknown whether this is through a structural role or through binding to LDLR or another protein co-factor. It has been

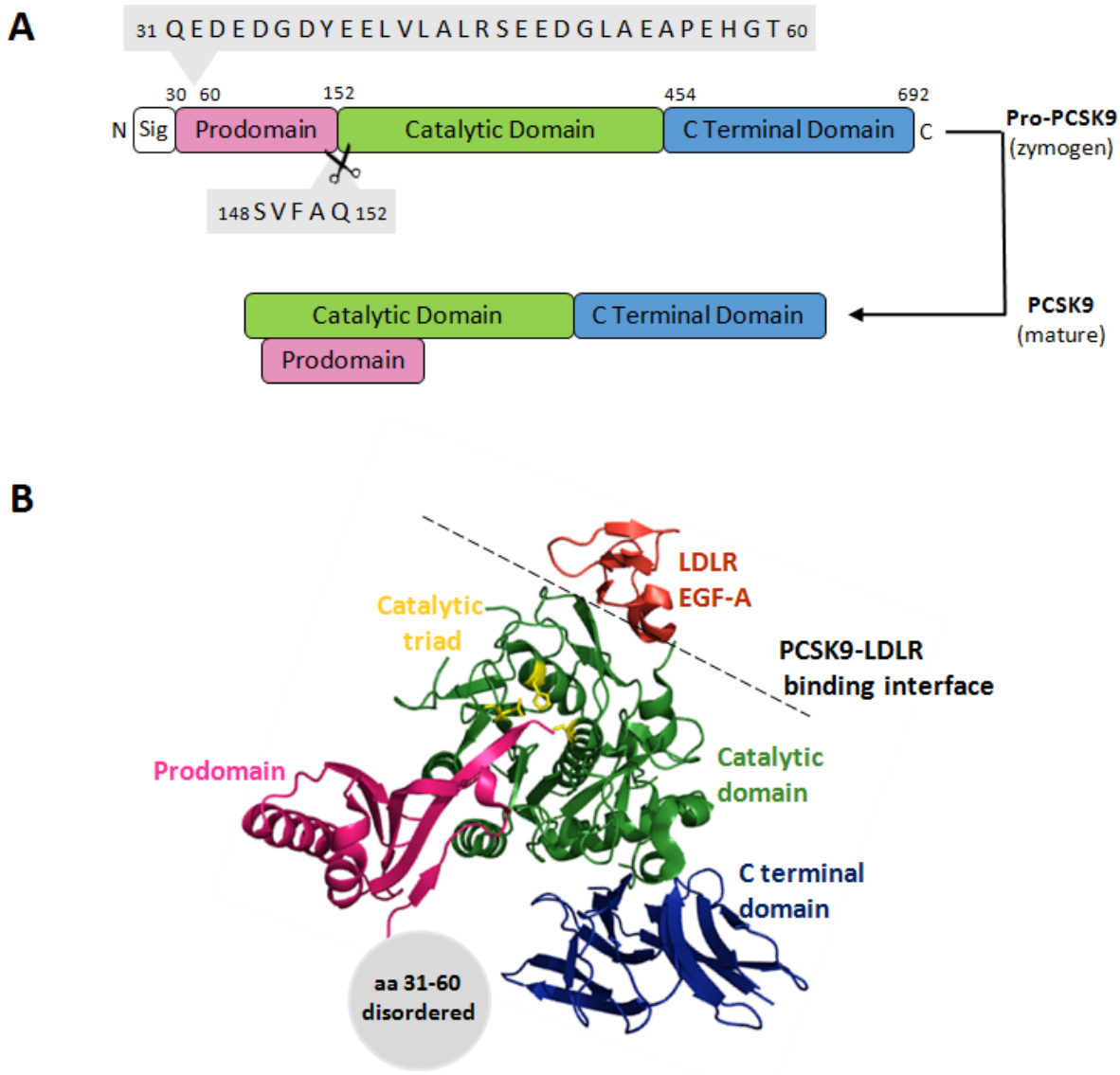

Figure 1: Schematic and structure of PCSK9 (A) Schematic of translated PCSK9, in zymogen form and processed mature form. "Sig" is the signal sequence for secretion, followed by the 3 indicated domains. The amino acid sequence of the disordered region, residues 31-60 in the PCSK9 prodomain are shown as well as the location of the self-cleavage site from residues 148-152. **(B)** The crystal structure of full-length PCSK9 bound to the EGF-A domain of LDLR, as labelled. Residues forming the catalytic triad of PCSK9 are highlighted in yellow. The possible area of occupancy of the 31-60 disordered region is indicated by a grey area at the N-terminus of the prodomain. Panel based on RCSB database structure 3BPS, modified on Pymol software.

proposed that the C-terminal may have a role in binding an as-yet undetermined cell-surface co-receptor[59,69]. The precise mechanism of PCSK9-mediated LDLR degradation remains undetermined, although its independence from the catalytic activity of PCSK9 has been demonstrated. A catalytically dead PCSK9 mutant (S386A) was expressed in HepG2 cells in trans with its prodomain in order to bypass the need for self-processing for secretion. This PCSK9 variant was comparable to wild-type in its ability to direct LDLR degradation[57]. In vitro studies support that PCSK9 may lock internalized LDLR in an open conformation, preventing recycling and targeting the receptor for lysosomal degradation[70].

Interestingly, PCSK9 exhibits tissue-specific activity, preferentially degrading hepatic cell surface LDLRs over LDLRs on non-hepatic cells such as fibroblasts, kidneys and adrenals[16,65,71,72]. Annexin A2 has been suggested as a natural extra-hepatic inhibitor of PCSK9[72]. Studies by Nguyen et al suggest that increased endosomal dissociation of PCSK9 from LDLR in non-hepatic cells may play a role in tissue specificity as well[71]. The sensitivity of hepatic LDLRs to PCSK9 may reflect an evolutionary mechanism to protect the amount of LDL-cholesterol or lipids circulating and being distributed to the periphery, controlling clearance by the liver. The resistance of certain tissues to PCSK9 may also play a role in tissue specific processes, for example promoting cholesterol uptake for steroid hormone production in the adrenals.

1.3.2 PCSK9-LDLR binding. The LDLR is a modular, transmembrane, calcium-dependent receptor 839 residues long. The extracellular N-terminal region contains a ligand-binding domain with seven cysteine-rich repeats, in which lies the Apolipoprotein B100 (apoB100) binding site that allows binding to LDL and other apoB100-containing lipoproteins[73]. Apolipoprotein E (apo E), found on chylomicrons, VLDL, IDL and HDL, is also a ligand for the LDLR[74,75]. This is followed by epidermal-growth-factor-like domains A and B (EGF-A and EGF-B), a β- propeller domain, an EGF-C domain, a section of O-linked glycans, a transmembrane domain, and finally a short, intracellular C-terminal tail required for endocytosis of the protein, in conjunction with the adaptor protein ARH

(autosomal-recessive hypercholesterolemia)[76-78], also known as LDLRAP1. The EGF-A domain is the primary binding site of PCSK9 on LDLR[67]. Each LDLR binds one apoB100 moiety at a time, and the LDLR-LDL complexes formed in cell-surface clathrin-coated pits are endocytosed[79]. In the low-pH and low-calcium environment of the endosomes, the LDLR adopts a "closed" conformation, releasing the lipoprotein. The LDL migrates to the lysosome for further catabolism, while the receptors are recycled back to the cell surface to continue lipoprotein uptake into the cell[80]. The recycling period for an LDLR is about 10min, with a total lifespan of about 20 hours[81].

PCSK9 binds the EGF-A domain of the LDLR in a 1:1 ratio and a calcium dependent manner[56]. Crystal structures show PCSK9 bound to the EGF-A domain through a site on its catalytic domain, primarily by hydrophobic interactions as well as a number of salt bridges and hydrogen bonds which contribute to specificity[67]. The affinity of PCSK9 for the LDLR EGF-A domain increases at endosomal pH[56,82,83]. In an acidic environment, protonation of His-306 in the LDLR EGF-A allows the formation of a salt bridge with Asp-374 of PCSK9. At neutral pH, unprotonated His-306 does not form this hydrogen bond, instead forming an intramolecular hydrogen bond with Ser-305[68]. Increased overall affinity to LDLR at acidic pH may also involve further contacts between the LDLR ligand binding domain and the C-terminal domains of PCSK9[84]. Tighter PCSK9-LDLR binding in the endosomal and lysosomal compartments in cells is presumed to play a role in the ability of PCSK9 to prevent LDLR recycling, mediating its degradation instead. The C-terminal domain of PCSK9 has been shown to be required for LDLR degradation activity[56,85-87], although it remains unknown whether this is through an indirect structural role or through some direct binding interaction, either with the LDLR or to a co-factor[88].

1.4 Regulation of circulating PCSK9 levels

1.4.1 Transcriptional regulation. Like most genes in the cholesterol synthesis pathway, PCSK9 is regulated by the SREBP-2 transcription factor through a sterol regulatory element on its proximal

promoter[89,90]. This creates a seemingly paradoxical situation where SREBP-2 mediated activation simultaneously increases cellular LDLR levels and upregulates PCSK9 secretion, which then leads to degradation of the LDLRs. This problem is also a feature of statin treatment, as the SREBP-2 mediated upregulation of LDLRs in response to HMGCoA inhibition also leads to PCSK9 upregulation[91,92]. It is likely that this "futile cycle" of LDLR production and simultaneous degradation is not the whole picture – that there are instead additional layers of regulation of this dynamic that are as yet unknown. The studies in this dissertation will reveal more about potential post-transcriptional regulators of PCSK9 activity in circulation.

The PCSK9 promoter also contains a functional binding site for the transcription factor HNF1α shortly upstream of the SRE[93]. HNF1α appears to work in concert with SREBP-2 in the activation of PCSK9 transcription. HNF1α is a liver-enriched transcription factor, regulating genes in the liver and intestines, which may help to explain the high expression of PCSK9 in the liver[93]. HNF1α gene targets are also involved in lipid and cholesterol metabolism, as well as acute-phase inflammatory responses, thus possibly forming a connection between PCSK9 and inflammation[94].

1.4.2 Expression Patterns. The Human Protein Atlas[1†] lists high PCSK9 expression in liver, lungs, cerebellum, and in the gastrointestinal tract, particularly small intestines. Upon secretion, PCSK9 circulates in the blood plasma at concentrations that vary widely between individuals, ranging from approximately 30-3000 ng/mL, on average at 500 ng/mL[95]. In circulation, PCSK9 can also be found as a truncated species thought to be cleaved by the PC furin[61]. A study found this cleaved form to have a 2-fold lowered LDLR affinity[96] and is thus considered to be less-active[97]. While this study found the cleaved fragment to remain partially bound, another study reported that furin-cleaved PCSK9 does not retain the cleaved fragment[98]. This would render it unable to bind LDLR as the N-

[1] † Accessible online at https://www.proteinatlas.org

terminal region of the catalytic domain contains several important contact points with the LDLR EGFA domain[67].

PCSK9 levels positively correlate with plasma LDL-cholesterol levels[99-102]. Plasma concentrations of PCSK9 are tied to cholesterol synthesis, since both the PCSK9 gene and the genes in the cholesterol synthesis pathway are transcriptionally regulated by SREBP-2. Consequently, concentrations of plasma PCSK9 have been observed to mirror the cholesterol synthesis marker lathosterol in exhibiting a diurnal rhythm. Both PCSK9 and lathosterol levels peak between midnight and dawn while reaching lows in the late afternoon to evening[103]. Fasting also strongly reduces serum PCSK9 levels, again mirroring lathosterol concentrations[103].

PCSK9 levels differ by gender, being generally higher in women than men[95,104]. Hormonal status appears to affect PCSK9 levels: growth hormone is associated with mediating PCSK9 diurnal rhythm[103], while oestrogen appears to be a negative regulator of PCSK9 in humans[104]. Thyroid hormone appears to down-regulate PCSK9[105]. Glucose homeostasis and diabetes status affects circulating PCSK9 and mRNA, although it appears there may be differential regulation in hyperglycemic vs. hyper-insulinemic conditions[28]. There are many studies using many different animal models that link PCSK9 expression to a great many other things[28], including transcription factors such as farnesoid X receptor (FXR)[106] and liver X receptor (LXR)[107], or drugs such as fenofibrates[108-110] and CETP inhibitors[111,112].

1.5 PCSK9 and lipoproteins

1.5.1 Lipoproteins. Cholesterol and triglycerides are transported in the circulation in macromolecular structures known as lipoproteins. Lipoproteins are structured aggregates of proteins and lipids, facilitating transport of the lipids in the aqueous environment of the circulation. Lipoproteins generally have a hydrophobic core where the lipids are stored as triacylglycerols and cholesteryl esters, and a phospholipid outer layer containing some free cholesterol[113]. Lipoproteins

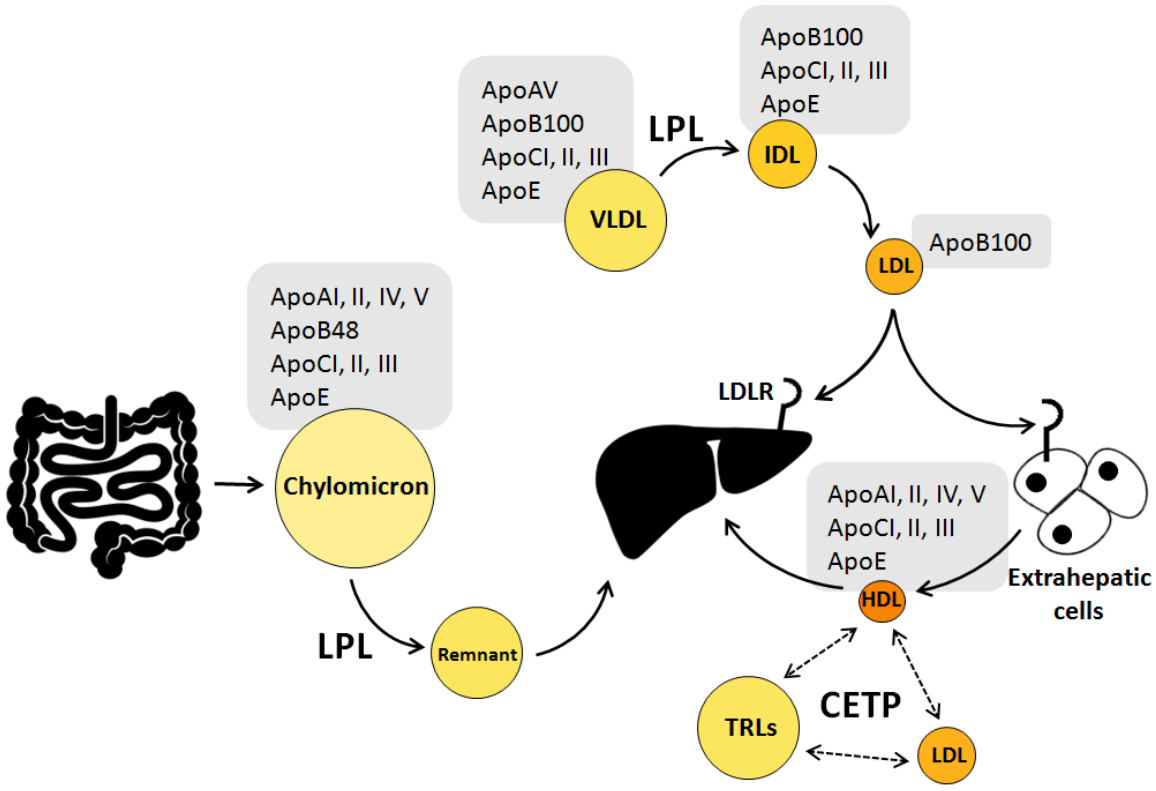

Figure 2: Cholesterol transport in circulation. Circulation and metabolism of lipoproteins. Chylomicrons rich in dietary fat and cholesterol in the form of triglycerides (TG) and cholesteryl esters. Lipoprotein lipase (LPL)- mediated catabolism in the circulation releases free fatty acids to peripheral tissues and forms chylomicron remnants which are taken up by the liver. The liver produces TG-rich very low density lipoproteins (VLDL) which also get catabolized in the circulation by LPL to intermediate and low density lipoproteins (IDL, LDL). Cholesterol-rich LDL is cleared from the circulation by the liver through LDL receptor (LDLR) mediated endocytosis. LDLR also contributes along with other receptors in hepatic clearance of remnant lipoproteins (chylomicron- or VLDL-derived) that have acquired the LDLR ligand apoE. Other tissues expressing LDLRs can also internalize LDL-cholesterol. High density lipoproteins (HDL) are also produced by the liver and are involved in carrying cholesterol from the periphery back to the liver. Cholesteryl ester transfer protein (CETP) exchanges triglycerides and cholesteryl esters between lipoprotein particles. The ranges of apolipoproteins associated with each lipoprotein class are indicated in grey boxes.

can be broadly classified based on size and density into chylomicrons, very low density lipoproteins (VLDL), intermediate density lipoproteins (IDL), low density lipoproteins (LDL) and high density lipoproteins (HDL). Within each class of lipoprotein there exists considerable heterogeneity in terms of size, density and composition. Proteins known as apolipoproteins are embedded on the outer surface of the lipoproteins, some acting as ligands for the respective cell-surface receptors for each class of lipoprotein. They play a major role in determining and stabilizing the size and structure of the lipoprotein particle. In addition to lipid transport, lipoproteins can carry other bioactive molecules such as proteins, vitamins, drugs, etc[114-116].

Chylomicrons are the largest and least dense lipoprotein, produced from the small intestine after dietary fats are absorbed from the gut and containing primarily triglycerides. They are short lived, being catabolized in the circulation within a few hours of secretion[117]. VLDL is produced from the liver, and is the next largest lipoprotein, also primarily carrying triglycerides. VLDL is catabolized in the circulation to smaller, slightly more cholesterol-rich IDL particles. VLDL and IDL particles are eventually catabolized to very small, highly cholesterol rich LDL particles[14]. Lipid-poor HDL particles are also produced by the liver, acting as cholesterol acceptors from the peripheral cells and carrying cholesterol to the liver for excretion through bile[118]. An overview of lipoprotein metabolism can be found in **Figure 2**. This report will deal mainly with the VLDL, IDL and LDL classes of lipoproteins, which are the apoB100-containing lipoproteins.

1.5.2 Apolipoproteins. There are several classes of apolipoproteins, some of which can be exchanged between lipoprotein particles[119]. The major classes are apoA, apoB, apoC and apoE, although there are other minor classes. There are subtypes within each of these classes: apoAI, AII, AIV, AV; apoB100, B48; apoCI, CII, CIII[14]. They vary greatly in size, from 550kDa for apoB100[120] to just over 6kDa for apoCI[14]. Apolipoproteins utilize motifs that form amphipathic helices in proximity to lipid surfaces of certain packing and composition[121], to associate with the lipid portion

of lipoprotein particles[113,122]. These amphipathic helices are lipid-ordered, i.e. their formation is energetically more favorable at the phospholipid surface[123].

Different populations of apolipoproteins are found on different lipoprotein classes[124], each having different functions, such as structural components (e.g. apoB acts as an assembly platform for VLDL and chylomicron synthesis[14,125]), as receptor ligands (e.g. apoB and apoE as ligands for LDLR[73,75]) and as regulators of enzyme activity (apoCII activates lipoprotein lipase, a triglyceride hydrolyzing enzyme, while apoCI and III act as inhibitors of the lipase[14]). Apolipoproteins are often used as markers of lipoprotein identity and classification. The range of apolipoproteins generally found on each lipoprotein type is indicated in **Figure 2**.

1.5.3 Metabolism of ApoB100-containing Lipoproteins. The production of apoB100-containing lipoproteins begins with the synthesis of apoB100 in the liver, a massive 4536 amino acid protein that is largely hydrophobic[120]. ApoB is synthesized at a relatively constant rate, its levels being regulated mainly through degradation[126]. The nascent apoB100 is partially lipidated during translation by MTP (microsomal triglyceride transfer protein) to form a primordial VLDL particle[125]. This lipidation is dependent on triglyceride availability; insufficient triglyceride availability leads to apoB degradation through multiple proteasomal and non-proteasomal pathways[127,128]. The primordial VLDL particle is transported from the ER to the Golgi in specialized VLDL-transport vesicles[129,130]. Posttranslational modifications of apoB occur in the Golgi[131,132]. In the distal Golgi, it is generally agreed that the primordial particles undergo further lipidation from luminal lipid droplets to form full-sized VLDL particles, although some conflicting literature exists on this matter[129]. The fully lipidated VLDL particles are then secreted into the circulation, although the molecular mechanisms of this step have not been fully elucidated[129].

In the circulation, the TG-rich VLDL particles are catabolized by the enzyme lipoprotein lipase on the surface of the vascular endothelium to release fatty acids to peripheral tissues[133]. Hydrolysis of

the triglycerides converts the VLDL to smaller, denser, more cholesterol-rich particles. The metabolism of the apoB100-containing lipoproteins may be thought of in a simplified linear model where the triglyceride-rich lipoproteins are converted progressively from VLDL → IDL → LDL, although kinetic studies indicate some non-linear components in the model, such as direct clearance of VLDL and IDL from circulation, slightly different conversion speeds and paths based on lipid and apolipoprotein heterogeneity within lipoprotein classes, and direct production of LDL- or IDL- range particles from liver [134-136]. LDLRs are the primary form of clearance of these lipoproteins, although different apolipoproteins act as the LDLR ligand at different stages of remodeling (extensive lists of the apolipoprotein content of various lipoprotein classes are found in literature[14]). At the VLDL stage, apolipoprotein E is the ligand that binds LDLR, while on LDL it is the apoB that binds LDLR[73,75]. During conversion of lipoproteins in circulation, the ligand responsible for the binding of the lipoprotein to the LDL receptor switches from apo E to apo B as the particle becomes smaller[137,138]. Lipolysis leads to a conformational change of the apoB100 C-terminus that exposes the LDLR binding epitope[73]. Circulating lipoproteins are also modified by cholesteryl-ester transfer protein (CETP), which transfers cholesteryl esters and triglycerides between lipid-rich VLDLs and lipid poor HDLs[139,140].

It is relevant to the studies in this dissertation to note that as the apoB100-containing lipoproteins undergo remodeling and the particle diameter and lipid composition changes, the conformation and exposure of apoB on the particle surface also changes. Proteolytic accessibility studies and antibody epitope availability studies find different parts of apoB to be available on VLDL vs. LDL particles. The antibody epitope studies found that defined regions in the apoB C-terminus and near the LDLR-binding site were more available in LDL compared to VLDL and IDL[141,142]. Proteolysis studies found more sites on apoB to be protease-susceptible on LDL than VLDL[143], which may be due to smaller particle size leading to increased exposure of apoB. However, changing the core lipid compositions of lipoproteins have also been demonstrated to change apoB conformation[144].

1.5.4 ApoB Editing. While apoB100 is an obligatory structural component of VLDL produced from the human liver, enterocytes produce chylomicrons that contain apoB48, consisting of the N-terminal 48% of the full apoB sequence. This version of apoB results from post-transcriptional editing of the apoB mRNA by the APOB mRNA editing complex (APOBEC1) which creates a stop codon in the transcript[145]. While the editing of apoB is restricted to enterocytes in humans, rodents edit their apoB to B48 in both the liver and intestine, meaning a predominant proportion of rodent TG-rich lipoproteins are B48-containing rather than B100[146]. The B48 lipoproteins do not bind to LDLR through apoB, as the truncated apoB lacks the LDLR binding site in the C-terminus[73]. Instead apoE is the ligand that allows binding of the remnants of these lipoproteins to LDLR and LDLR-related protein (LRP)[147].

1.5.5 LDL. LDL particles are on average 22nm across and are generally defined as being in the density range of 1.019-1.063 g/mL[148]. LDL exists in subclasses ranging from large buoyant (over 26nm diameter, density 1.025-1.035 g/mL) to progressively smaller, denser LDL, with the latter subtype having a higher association with atherosclerosis and myocardial infarction[149-151]. The phospholipid component of LDL is primarily phosphatidylcholine (PC) and sphingomyelin, followed by lyso-PC and phosphatidylethanolamine (PE), in addition to others[148]. Each LDL particle contains one non-exchangeable apoB100 molecule as its only apolipoprotein moiety, acting as the ligand for the LDLR[73,148]. ApoB100 is one of the largest known proteins (4536 residues) and is insoluble, making structural studies of apoB difficult. However, electron microscopy[148,152] and small angle neutron scattering[153] revealed that apoB is wrapped around the LDL particle in a three-dimensional conformation containing kinks and a central cavity. Circular dichroism indicated the presence of alpha helices and beta sheets[153]. Computational analyses led to the picture of a penta-partite model of the apoB100 protein, with three regions of amphipathic alpha helices alternated by two regions of amphipathic beta sheets. The arrangement of these putative regions on the lipoprotein particle surface has been elegantly depicted in visual models by Hevonoja et al[148]. It is the continuous

amphipathic beta sheet regions that are believed to confer the high lipid-affinity and non-exchangeability of the apoB100 on LDL[154,155].

1.5.6 PCSK9-LDL binding. In the past, harsh conditions in high-salt ultracentrifugations would strip lipoproteins of PCSK9, making it difficult to determine if PCSK9 bound to lipoproteins[99]. Indirect evidence of PCSK9 association with lipoproteins began coming out in 2008, from size exclusion chromatography studies where PCSK9 co-migrated with LDL-sized particles[156,157]. Positive identification of PCSK9 binding to LDL in human plasma came from more detailed studies, which utilized density gradient separations to isolate an LDL fraction that was shown to contain PCSK9[64,158]. Importantly, >30% of circulating PCSK9 was found to be associated with LDL in normolipidemic human plasma, suggesting a significant role of LDL association in regulating PCSK9 function[156,158]. Cell culture experiments in our lab have demonstrated that in the presence of physiological concentrations of LDL, PCSK9 exhibits a decreased ability to bind and degrade LDLR[158]. However, it must be noted here that some research groups believe LDL-bound PCSK9 is the more active form due to protection from furin cleavage, based on studies that find more non-LDL-bound PCSK9 to be furin-cleaved[159,160]. Unfortunately, these studies do not address whether furin-cleaved PCSK9 simply has a lower affinity for lipoproteins, thus being found proportionally more in apoB-free fractions. Interestingly, these studies also present data suggesting LDL-bound PCSK9 has a stronger affinity for the LDLR-EGFAB domain, although the method of separation of the LDL-bound PCSK9 and how it was ensured that the PCSK9 did not dissociate from LDL once isolated was not well explained in this report[159].

Co-immunoprecipitation in the presence of lipid solubilizing detergents[158,161] and mammalian two-hybrid assays[162] support that PCSK9-LDL association likely occurs through a protein-protein interaction between PCSK9 and apoB, although a specific binding site on either protein has not yet been established. In vitro assays show that the interaction is a specific, saturable, one-site binding with a K_d of 350 nM[158]. Studies using apoB truncations suggest that PCSK9 can still interact with

apoB within the B18 region (the N-terminal 18% of the apoB sequence)[162], but it should be noted that these studies employed very high (500-fold) over-expression of PCSK9 in cultured cell experiments.

Observations of the interaction with VLDL have been conflicted. One study observed the presence of PCSK9 in highly concentrated and pooled FPLC fractions of transgenic mouse plasma in the VLDL range[162]. However, in vitro studies using isolated human lipoproteins and density-gradient ultracentrifugation did not observe PCSK9 interacting with VLDL[158]. It is possible that the interaction with VLDL is much weaker than the interaction with LDL, thus making it difficult to observe it under all conditions. Additionally, PCSK9 has been observed to associate with Lp(a)[163], which is an atherogenic LDL-like particle containing apolipoprotein (a) linked to apoB through a disulfide bond[164,165]. It appears that PCSK9 does not interact with HDL[158,166]. The interaction of PCSK9 with isolated apoB48-containing chylomicrons in apoB100-free fractions has not been studied yet.

1.6 Study Rationale and Overview

As discussed in section 1.1, alternative methods of PCSK9 inhibition are desirable. If the LDL-binding site on PCSK9 can be found, and the mechanism of how LDL inhibits PCSK9 can be elucidated, then a new target for inhibitor design may be available. Designing inhibitors targeting the PCSK9 prodomain have already been proposed as an idea based on previous structural studies[167], and much of our research has focused on structure-function aspects of the prodomain. The studies described within this dissertation address two broad aspects of the PCSK9-LDL interaction:

1) *What are the structural requirements and consequences of PCSK9 binding to LDL?*

   In chapter 2, it will be shown that an environment-dependent helical shift occurs in the N-terminal of the PCSK9 prodomain, which plays a role in the ability of PCSK9 to bind LDL and is

modulated by the common loss-of-function polymorphism R46L in PCSK9. In addition, data will be presented that indicates a possible intramolecular interaction between the PCSK9 prodomain and C-terminal domain as a result of the helical shift, which holds implications for an allosteric mechanism occurring in PCSK9 upon lipoprotein binding. Chapter 3 will look at a region of clustered sites for natural GOF mutations and their importance in the LDL interaction.

2) *How do changes in lipoprotein populations affect PCSK9 association?*

   There has been some conflict in the published literature about whether or not PCSK9 is able to bind to TG-rich lipoproteins such as VLDL. In chapter 4 we will present data that suggests that PCSK9 can associate with IDL, and to a lesser extent VLDL, suggesting a lipoprotein remodeling-dependent aspect of PCSK9-LDL association. Data from human plasma will be presented that looks into the effects of elevated circulating lipoprotein levels on the lipoprotein-bound pool of PCSK9.

Overall, these studies provide insight into the nature of the interaction of PCSK9 with lipoproteins. They provide a foundation on which to base novel drug design as well as future studies into the physiological role of this interaction.

Chapter 2: A lipid-ordered helix in the PCSK9 prodomain affects PCSK9-LDL binding

2.1 Introduction

An N-terminal region of the PCSK9 prodomain (residues 31-52 following the signal peptide cleavage site) is known to be required for LDL binding[158]. This region is disordered and absent in crystal structures of PCSK9[56,58,59]. Deletion of this same region on PCSK9 increases the affinity of PCSK9 for LDLR by >7-fold, although this region is spatially distant from the primary LDLR binding site on the PCSK9 catalytic domain[67] **(Figure 1)**. Furthermore, removal of a stretch of mainly acidic residues within this N-terminal region (residues 33-40) increases LDLR binding[168,169]. This suggests an allosteric regulatory role for this region. Herein, we identify a short section of this region (residues 37-47) that adopts an amphipathic α-helical structure in the presence of a membrane-mimetic micelle environment. This coil-to-helix transition was further promoted by a PCSK9 LOF mutation associated with an antiatherogenic lipid profile in humans[170]. These studies provide evidence of an alternate structural conformation in the PCSK9 prodomain that favors LDL association, and which may regulate PCSK9 function and LDL-cholesterol levels in humans through a structural role or through direct binding.

2.2 Results

To investigate specific features within the disordered region that may be important for LDL binding, a conserved stretch of mainly acidic residues and an adjacent stretch of hydrophobic residues **(Figure 3A)** were mutated in full length recombinant PCSK9. The acidic stretch (residues 33-40) was deleted, while the hydrophobic stretch and an adjacent arginine residue were replaced with a disordered linker (residues 41-46: LVLALR→GGSGGS). These constructs were transiently expressed in HEK293 cells and conditioned media from these cells was collected, concentrated, and incubated with isolated human LDL in vitro. Relative amounts of PCSK9 in these incubations were

normalized through SDS-PAGE and immunblotting-based detection of PCSK9 in the conditioned media. LDL-PCSK9 binding reactions were then subjected to density gradient ultracentrifugation to separate LDL-PCSK9 complexes from unbound PCSK9 **(Figure 3B)**. Western blot analyses of density gradient fractions show that the acidic stretch deletion abolished LDL binding while hydrophobic stretch disruption decreased LDL binding significantly **(Figure 3C)**, suggesting a role for both these motifs in the LDL interaction. These mutants remained functional in terms of LDLR binding ability, as assessed by cellular uptake of exogenous PCSK9 by LDLR-transfected cells **(Figure 3D).** It is interesting to note that there are trends (though not statistical significance) toward increased LDLR-mediated uptake for both the full disordered region deletion (Δ31-52) and for the acidic stretch deletion (Δ33-40), which corroborates literature[67,168,169].

Secondary structure predictive modelling of this region was done using computational PSIPRED protein sequence analysis[171]. Residues 38-48 were predicted to be helical **(Figure 4A)**. Heliquest modeling[172] predicts the helix to have a hydrophobic face and a relatively polar face, giving it a directional hydrophobic moment **(Figure 4B)**. Since the region is normally disordered, a conformation change from random-coil-to-helix may be triggered by a change in proximal environment, for example a change in hydrophobicity, as may occur in proximity to lipoproteins. Thus, we performed assessments of the secondary structures that this motif can form in aqueous versus hydrophobic environments. Synthesized peptides of this region were dissolved in phosphate buffer or in buffer containing dodecylphosphocholine (DPC) micelles. Circular dichroism spectra of

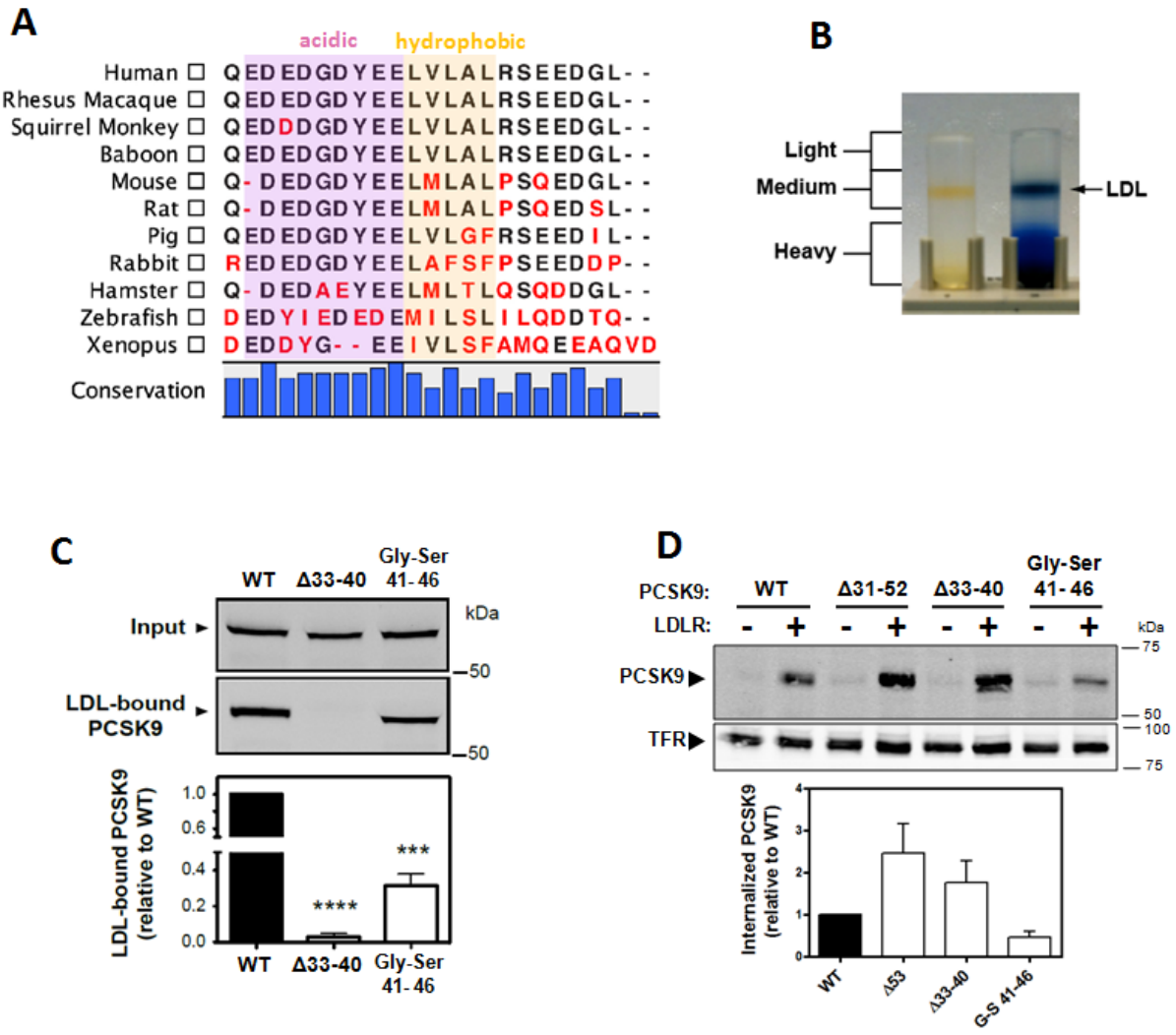

Figure 3: Conserved motifs in the N-terminal region affect LDL-binding ability of PCSK9. (A) Amino acid sequence of residues 31-52 in the PCSK9 prodoman, aligned across species. Blue bars at bottom indicate % conservation. **(B)** Photographic representation of Optiprep density gradients created by ultracentrifugation, where lipoproteins float into discrete bands according to their density (left). An LDL band from a plasma sample is indicated with an arrow in the "medium" density fraction. An identical tube stained with Coomassie Blue (right) demonstrates how proteins associated with LDL are also found in the medium density fraction. **(C)** Representative Western Blot (top) of inputs and LDL-bound fractions of in vitro PCSK9-LDL binding reactions. Probed for FLAG to detect recombinant C-terminally FLAG-tagged PCSK9. Quantification of 3 experiments plotted as mean ± standard error (bottom). Stars indicate statistical difference from wild-type according to on-way ANOVA followed by Dunnet's post-test (*** $p \leq 0.001$, **** $p \leq 0.0001$) **(D)** HEK293 cells transfected or not transfected with human wild-type LDLR were treated with exogenous 10µg/mL wild-type or mutant PCSK9-FLAG from conditioned medium for 2 hours at 37°C. Cells were then lysed and proteins resolved by SDS-PAGE and detected by western blotting. Plotted quantification means from n=3 ± SEM.

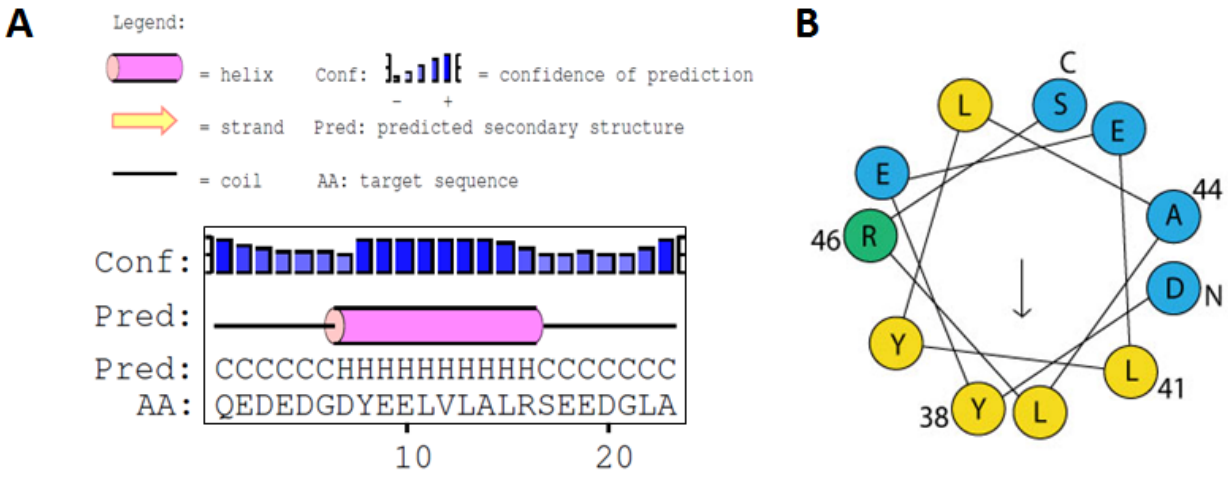

Figure 4: **A motif in the disordered N-terminal of PCSK9 is predicted to be a helix. (A)** PSIPRED[171] results of the disordered sequence (residues 31-52). **(B)** Heliquest software[172] predicts the helical motif to form an amphipathic helix with a hydrophobic moment direction shown by the arrow. Hydrophobic residues are in yellow, polar or charged residues are in blue or green.

these peptides revealed that the motif remained in a random coil conformation in aqueous buffer, but in the presence of micelles adopted a distinctly helical conformation **(Figure 5A)**. Mutant peptides of the region were also observed in buffer vs. micelle environments in order to test the effect of disrupting helix formation. The targeted A44P mutation, which in full-length PCSK9 was previously shown to cause a 90% loss of LDL binding (unpublished, Appendix C, Figure C1), failed to show a shift to helical conformation with micelles **(Figure 5B)**. This supports that a random coil-to-helix conformation change in the N- terminal of PCSK9 occurs in hydrophobic environments. Taken together with previous findings that full-length A44P- or L41P-PCSK9 (both introducing helix-disrupting prolines into the helical motif) dramatically lose LDL binding (unpublished, Appendix C, Figure C1), it indicates that formation of a helix in the N-terminal region plays an important role in PCSK9-LDL binding.

The impact of the putative helical motif on LDL binding was more quantitatively investigated in the context of relative affinity for LDL. Competition binding assays were performed using purified recombinant wild-type, A44P- or Δ31-52-PCSK9 as competitors to Dylight-labelled wild-type PCSK9 in the presence of LDL. It was observed that while A44P-PCSK9 showed a 6-fold decrease in its ability to compete with dye-labelled wild-type PCSK9 for binding to LDL (wild-type inhibitor constant (K_i) $= 102.2 \pm 53.18$ nM; A44P $K_i = 651.1 \pm 79.4$ nM), it was still capable of effective competition at high concentrations **(Figure 5C and D)**. This contrasts with Δ31-52-PCSK9, which is a full deletion of the disordered N-terminal region and which remains unable to compete with labelled wild-type PCSK9 for LDL binding even at high concentrations **(Figure 5C)**. This suggests that while the helical structure plays a role in regulating the PCSK9-LDL interaction, protein-protein binding of PCSK9 to apoB100 is still capable of occurring without its formation.

The natural PCSK9 mutation R46L is commonly found in the Caucasian population and is considered a loss-of function variant that confers protection against CVD[20,173,174]. It is interesting to

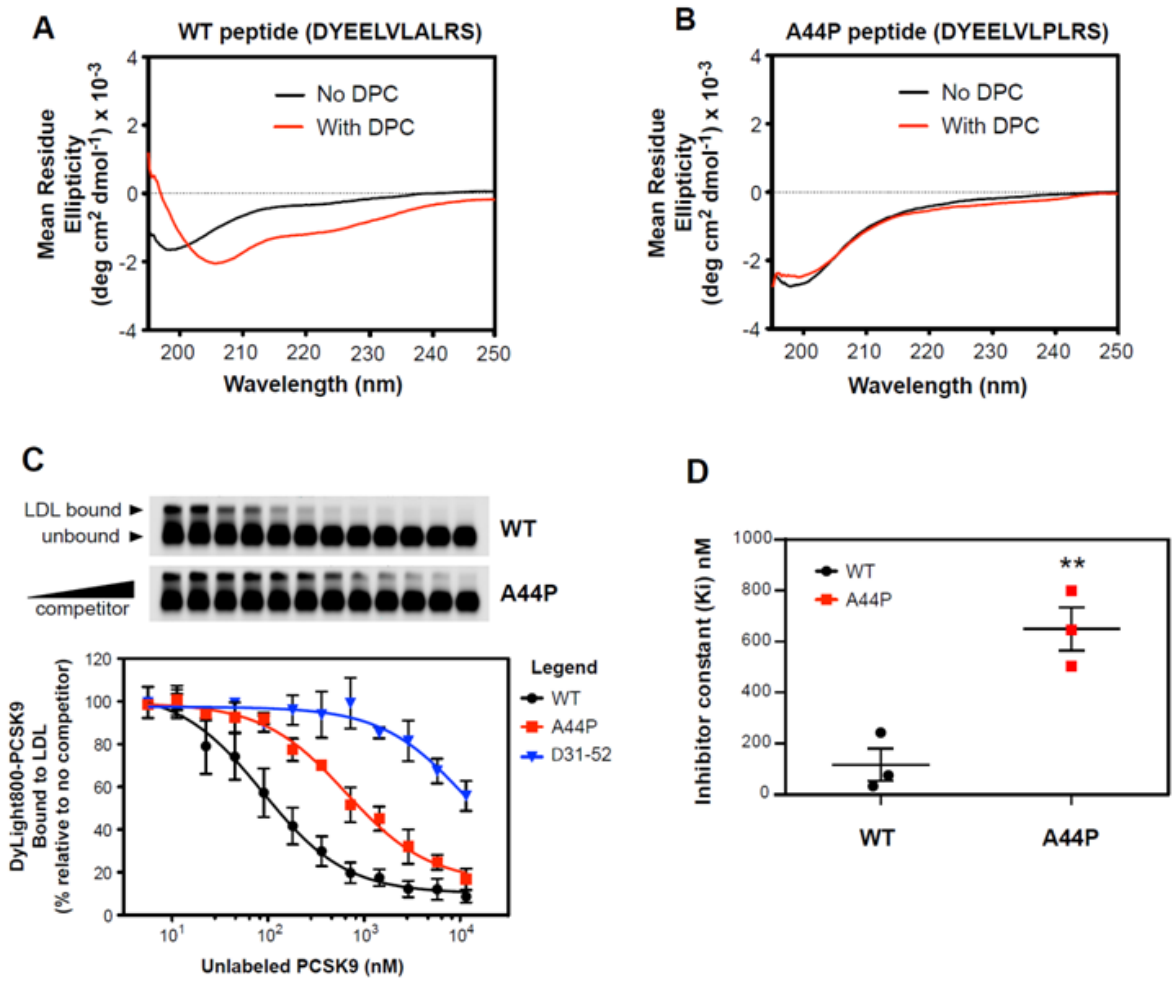

Figure 5: The disordered N-terminal region undergoes a structural transition in response to a hydrophobic environment. (A) and **(B)** Circular dichroism spectra of 31µM prodomain peptide (either wild-type: GDYEELVLALRS, or A44P: GDYEELVLPLRS) in 50mM phosphate buffer containing 2.5% dodecylphosphocholine or buffer only. Spectra shown are representative of three independent experiments. **(C)** In vitro competition curves where 10.8nM infrared dye labelled PCSK9 was incubated with 500µg/mL LDL, in the presence of up to 500-fold excess unlabelled PCSK9, either wild-type or mutant. Bound and free complexes were resolved by electrophoresis on 0.7% agarose gels. Gels were visualized on a LI-COR Odyssey system. Bound labeled PCSK9 was quantified and fit to a one-site binding curve on Prism5 software using non-linear regression. Plotted mean ± standard error (n=3). **(D)** Mean inhibitor constants obtained from experiments in (C) plotted ± standard error (n=3). **p≤0.01.

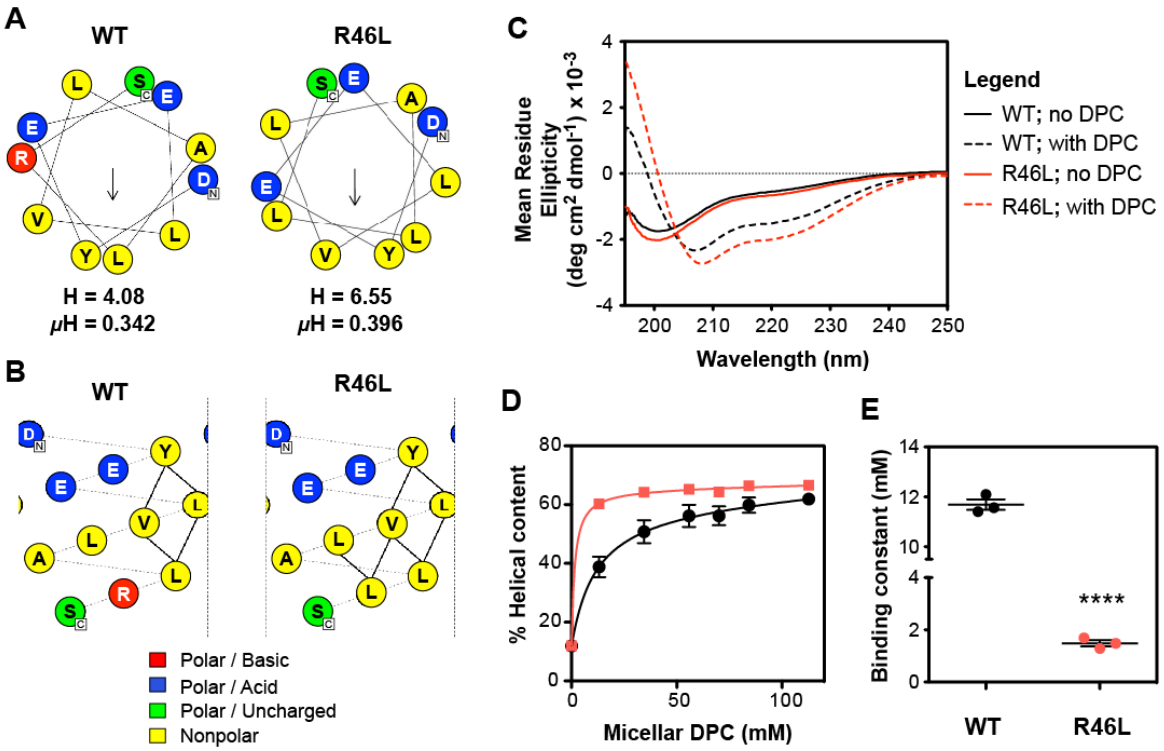

Figure 6: Natural mutation R46L modulates helicity and lipid affinity in the prodomain N-terminal. (A) Mutation of the putative helix from Figure 4 (left) to the R46L variant (right) on HeliQuest, and the resulting effects on the hydrophobic moment (μM). **(B)** Predicted hydrophobic side-chain interactions between residues of the putative N-terminal helix with either arginine or leucine at position 46. Constructed on NetWheels software online (http://lbqp.unb.br/NetWheels/) **(C)** Circular dichroism spectra of 31μM prodomain peptide (wild-type: GDYEELVLALRS, R46L: GDYEELVLALLS) in 50mM phosphate buffer containing 2.5% dodecylphosphocholine or buffer only. Spectra shown are representative of three independent experiments. **(D)** Mean % helical content (n=3) of either the wild-type or the R46L variant peptide as detergent concentration is increased. Secondary structure calculations based on circular dichroism spectra using deconvolution algorithm CONTIN. **(E)** Binding constants obtained from curves in (D) plotted as mean of n=3 ± standard error. ****p ≤ 0.0001.

note that the arginine to leucine substitution would add a hydrophobic residue in proximity to the putative hydrophobic face and increase stabilizing side-chain interactions along the face **(Figure 6)**.

To test whether this extension of the hydrophobic face would affect helical structure in a micelle environment, circular dichroism studies were performed similar to above. It was found that the R46L-containing version of the peptide underwent a much stronger helical shift in a DPC micelle environment than the wt peptide. The percent helicity of the peptide obtained at different DPC micelle concentrations allowed lipid binding curves to be obtained, revealing that the R46L substitution confers a 7.8-fold higher affinity for micelles than the wild-type **(Figure 6E)**. Interestingly, this lipid-affinity effect of R46L was not seen in previously performed competition binding experiments (unpublished, Appendix C, Figure C2), where the K_i of R46L remains comparable to wild-type. It is possible that the competition binding assay is not sensitive enough to reveal the lipid effects of the PCSK9-lipoprotein interaction, and shows only the affinity resulting from the stronger protein-protein interaction.

Collaborative work with Dr. Ariela Vergara-Jaque at the Universidad de Talca in Chile yielded more stringent computational models of the disordered PCSK9 N-terminal region in full-length PCSK9 **(Figure 7)** based on molecular dynamics simulations. These models corroborate experimental findings by predicting a helical motif in the disordered region. Interestingly, as shown in Figure 7, these models also predict a smaller, second helix from residues D50-G59. Not only did these models confirm our existing experimental findings, they generated additional hypotheses to test. The models predict several novel residue interactions between the prodomain and C-terminal domain, notably salt bridges between Y38 (prodomain) and R469 (CTD) and between D35 (prodomain) and R496 (CTD), and potentially t-shaped pi-stacking interactions between Y38 and F515. Such intramolecular interactions could have implications for alternate global conformations of the PCSK9 protein in different conditions, e.g. during LDL binding. Mutagenesis was thus carried out to

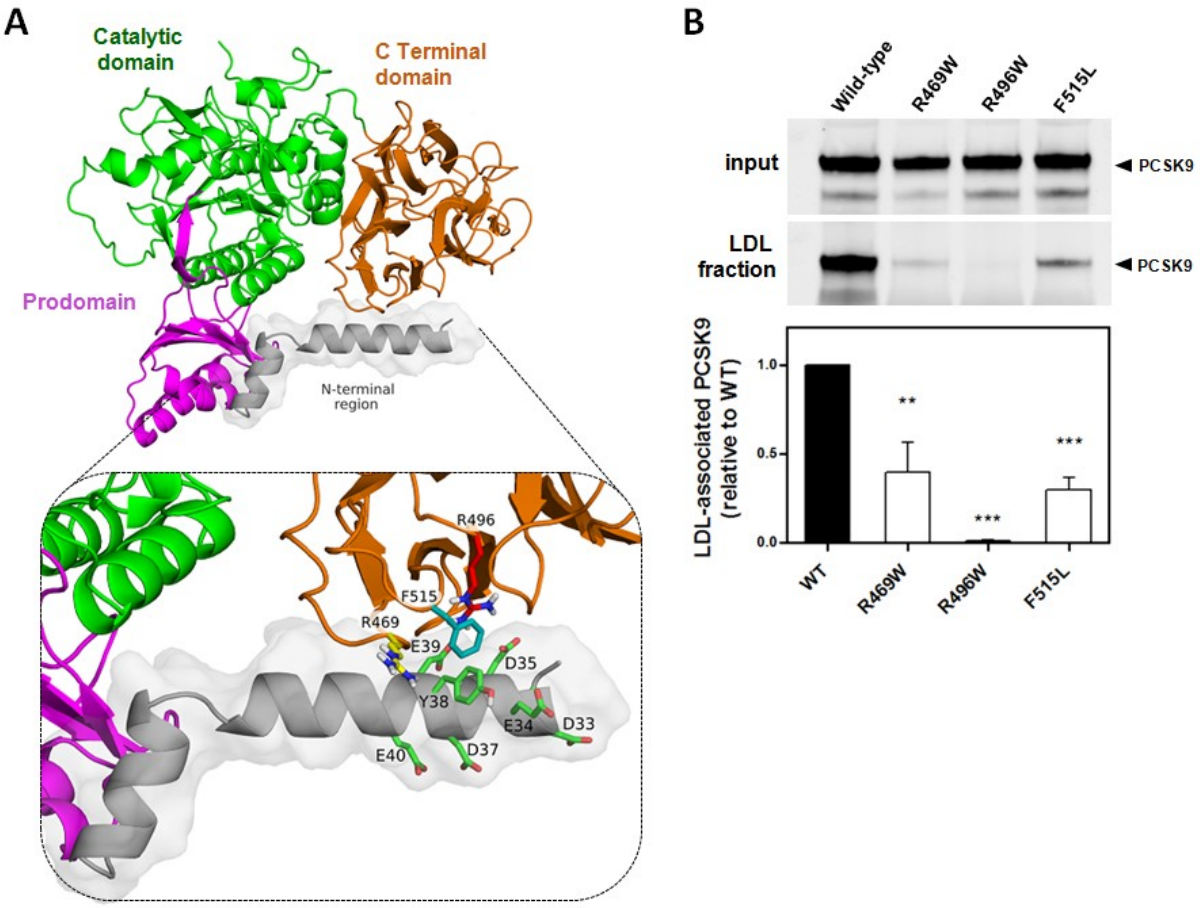

Figure 7: Modeling of the N-terminal portion of the prodomain. (A) Cartoon representation of the full-length PCSK9 structure modeled by Rosetta[175]. The modeled N-terminal prodomain is colored in grey and highlighted by a transparent surface. Key polar residues interacting with the C-terminal domain are displayed as sticks and colored by atom type. The Cα atoms of R469, F515 and R496 are colored in yellow, cyan, and red, respectively. **(B)** In-vitro LDL binding assay done with PCSK9 conditioned media and isolated LDL, using density gradient centrifugation, similar to Figure 3C. Western blot of LDL and input fractions representative of 3 independent experiments. Plotted mean of n=3 ± SEM. Stars indicate statistical difference from wild-type according to on-way ANOVA followed by Dunnet's post-test (** $p \leq 0.01$, *** $p \leq 0.001$)

generate R496W, R469W and F515L, three natural GOF variants that exist in human populations [174,176,177]. In vitro LDL binding assays were carried out to determine if disruption of these residues affected LDL binding. All 3 of these mutations showed loss of LDL binding, with R496W being the most severe. These results confirm the importance of these residues in the LDL interaction further suggest that an intramolecular interaction in PCSK9 could be playing a role in the ability of PCSK9 to bind LDL.

2.3 Discussion

The results in this chapter indicate that the disordered region in the PCSK9 prodomain undergoes a structural shift from a random coil to an alpha helix, ostensibly in response to a change in the hydrophobicity of its environment. The presence of the helical motif affects the ability of PCSK9 to associate with LDL, however whether this is through a structural role or direct binding is yet to be determined. While this region is known to be required for LDL binding, it has not been demonstrated whether this is the site for a protein-protein interaction with apoB. That this region is also autoinhibitory to LDLR binding[67] indicates that this region may play an allosteric role in regulating the interaction with LDL and LDLR. The intramolecular interactions between the prodomain and CTD predicted by the computational models and supported by in vitro data **(Figure 7)** provide a mechanism by which the structural shift in the N-terminal region of the prodomain could induce global conformational changes in PCSK9 that would in turn affect the affinity of the catalytic domain binding site for the EGF-A domain of the LDLR.

The induction of the structural shift through modulating the hydrophobicity of the surrounding environment **(Figure 5)** suggests that the lipid component of LDL may play a role in PCSK9 binding, introducing two layers to the PCSK9-LDL interaction: a protein-protein binding component and a protein-lipid interaction component. This introduces other potential determinants of PCSK9 targeting to lipoprotein surfaces such as composition, lipid packing and surface curvature.

Exchangeable lipoproteins of the major A, E and C classes depend upon lipoprotein surface packing and composition for their amphipathic helices to be targeted to these surfaces[121]. CTP:phosphocholine cytidylyltransferase (CCT) is a rate-determining enzyme in phosphatidylcholine synthesis which forms α-helices in its membrane binding domains only in the presence of anionic lipids[178]. Our CD experiments with protein-free DPC micelles separate the lipid component of the interaction from the apoB-binding component of the interaction, confirming that lipidic environments are capable of regulating the helical shift. We did attempt to investigate possible PCSK9-lipid interactions through in vitro liposome-binding assays (data not shown, preliminary results were presented in Master's thesis). While the results from those experiments initially suggested to us that PCSK9 was capable of associating with liposomes composed of phosphatidylcholine and phosphatidylethanolamine, they were not conclusive. Wild-type PCSK9 showed consistent liposome association, however, similar binding was also often observed with LDL-non-binding mutant A44P-PCSK9. Thus these results became difficult to interpret – they could represent non-specific binding, or suggest an alternative, as-yet unexplored lipid binding motif elsewhere in PCSK9. Extensive investigations into using liposomes of various sizes and lipid compositions did not yield more consistent results, but there is scope for these studies to be expanded (see Chapter 5 for future directions).

However, the short N-terminal helix in question may not represent a lipid-associating motif at all, despite its ability to be structurally influenced by a lipidic environment. We believe this due to the following reasons: Firstly, the residue distribution of the amphipathic helix in question does not entirely fit with the pattern of charge distribution typically observed in other lipid-associating helices - lipid-binding or membrane-binding helices often contain positively charged residues positioned at the interface of their polar and non-polar sides, to facilitate association of the domain with the negatively charged polar head groups of phospholipids[113]. In contrast, the current helix of interest lacks these positive charges at the polar-non-polar interface. The arginine at position 46

represents the only positive charge there, however, as was seen with the R46L mutation, loss of that positive charge did not hinder micelle-induced helix formation, rather it was enhanced **(Figure 6)**. Secondly, previous investigations into the role of a tyrosine at position 38 (located on the hydrophobic face of the helix) through site-directed mutagenesis found that replacing that residue with a negatively charged aspartate residue did not abolish LDL binding (although it was decreased – data not shown, reported previously in Masters' thesis). Additionally, sulfation of the tyrosine-38 still does not abolish LDL binding (Lagace, data not shown). Continued LDL-binding despite negative charges on the hydrophobic face diminishes the possibility that the hydrophobic face of the helix would be inserted into the hydrophobic layer of the lipoprotein exterior. Lastly, PSIPRED modeling predicts the formation of the N-terminal helix even in aqueous environments. Thus the apparently amphipathic pattern of the helix may play less of a lipid-binding role and more of a structural role where it positions certain residues for conformation-dependent interactions. Whether there are other environmental factors, for example pH, that may drive this helix formation aside from lipidic conditions, would be a future area of research. As an additional note, the lipid component of the PCSK9 interaction with lipoproteins would be quite weak compared to the protein-protein component given the short nature of the N-terminal amphipathic helix and the dissociation constants obtained in the micromolar rather than nanomolar range in CD titration experiments **(Figure 6)**.

Based on the inducible nature of the helical shift, and the intermolecular interaction that it likely precipitates, we suggest a two-step process of PCSK9 binding to LDL, where free PCSK9 in the circulation undergoes an environment-dependent helix formation in its prodomain, leading to an intramolecular bridging of the prodomain and catalytic domain that overall results in a conformation amenable to stable lipoprotein binding. It can also be expected that this conformation of PCSK9 would have an allosterically lowered affinity for the LDLR, helping to explain PCSK9 inhibition by LDL as well as the dual importance of the conserved acidic stretch in the prodomain in

regulating both LDL and LDLR binding. This model will be visualized in Chapter 3 (see **Figure 10)**, in combination with additional LDL-binding determinants investigated upstream in the prodomain.

The gain-of-function mutations in the PCSK9 C-terminal domain (R469W, R496W and F515L) caused a loss of LDL binding in vitro **(Figure 7)**, which makes sense in light of the allosteric model presented above. Disruption of the intermolecular prodomain – C-terminal domain interaction would not allow formation of the LDL-binding conformation, thus decreasing the inhibited pool of LDL-bound PCSK9 and increasing LDLR-degrading free PCSK9 in the circulation. Future "switch" mutation analysis where the R496, R469 and F515 residues are mutated to the opposing prodomain residues that they are predicted to interact with (Y38 and D35) would help to confirm these interactions.

The PCSK9-LDL interaction would thus introduce a new layer of reciprocal regulation in the LDL-LDLR-PCSK9 axis, where PCSK9 up-regulates plasma LDL levels through its action on LDLR, and LDL down-regulates PCSK9 activity, allowing itself to be cleared from circulation in a negative feedback loop. PCSK9 itself may be partially cleared as a passive component of LDL in this process, which could in part explain a small but significant decrease in plasma PCSK9 concentration in individuals with the R46L-PCSK9 mutation[95]. Information presented in Chapter 4 will allow speculation that the PCSK9-LDL interaction may be an ancient mechanism by which triglyceride clearance from circulation was controlled by this negative feedback.

2.4 Materials and Methods

Mutagenesis of PCSK9

A modified version of the QuickChange™ site-directed mutagenesis protocol (Stratagene, La Jolla, CA) was used to introduce point mutations or deletions into wild-type PCSK9-FLAG. Forward and reverse primers, both of which carried the desired mutations, were designed according to QuickChangeTM guidelines. Each 50 ul PCR contained 1X Phusion High Fidelity Buffer, 0.3 mM

dNTP mix, 0.3 μM each of both forward and reverse primer, 1 ng/μl of template DNA and 1 unit of Phusion DNA polymerase. Thermocycling was initiated at 98°C for 30 seconds, followed by 25 cycles of amplification. Each cycle consisted of 10 seconds denaturation at 98°C, 30 seconds annealing at 62°C, and 30 seconds / kb of extension at 72°C. A final extension step of 10 minutes at 72°C concluded the reaction. PCR was followed by digestion of original non-mutant template strands with 10 units DpnI enzyme. 3 μl of the DNA was transformed into One Shot Top Ten Chemically Competent E. coli. Bacterial transformant selection was done by plating on Luria Broth (LB) agar plates with ampicillin. Mutations were confirmed by sequencing. Primer design for the Gly-Ser 41-45 mutant was done according to Liu and Naismith, 2008[179]. See appendix for primer sequences.

Cell culture and conditioned media

HEK293 cells were maintained in monolayer cultures in Dulbecco Modified Eagle Medium (DMEM) (4.5g/L glucose) supplemented with 100 units/mL penicillin and 100 μg/mL streptomycin sulfate and 10% fetal bovine serum, at 5% carbon dioxide and 37°C. For transient transfections, cells were grown to ~80% confluency, and then transiently transfected with 1.5 μg of DNA (either wild-type or mutant PCSK9-FLAG construct) and 15 μl of 7.5 mM polyethylenimine (Linear, MW 25,000, purchased from Polysciences) per well in 6-well Corning cell culture dishes. Cells were put in serum free conditions, *i.e.* FBS supplementation was replaced with 1X Insulin-Transferrin-Selenium supplementation (Thermo Fisher Scientific) 18 hours after transfection and allowed to secrete PCSK9 for 48 hours before harvesting the medium. Collected media was centrifuged at 1000xg to pellet cells, and the cell free supernatant transferred to new tubes and stored at 4°C for upto a week. PCSK9 quality and relative quantities in the medium were monitored through SDS-PAGE and western blotting.

LDL isolation

Human LDL was isolated from plasma as described previously[158]. Briefly, blood from healthy, fasted volunteers was collected into commercial lavender-topped evacuated EDTA tubes and plasma separated by low speed centrifugation (2000 x*g* for 20 minutes at 4°C). Protease inhibitors were added to the cleared plasma (1 mM PMSF and 50 units/liter aprotinin). LDL particles (density = 1.019–1.065 g/mL) were isolated from human plasma using sequential potassium bromide flotation ultracentrifugation[180], where light density lipoproteins are first separated from LDL and HDL by adjusting the density of 28-30 mL of plasma to 1.018 g/mL by the addition of solid KBr salt, then overlaying with 1.019 g/mL KBr solution in Beckman quick seal tube and centrifuging for 18 hours at 33,000 rpm in a Ti50.2 rotor. The LDL and HDL in the lower portion of the tube are then separated by slicing at the overlay boundary, collecting the lower portion and adjusting density with solid KBr to 1.063 g/mL. The centrifugation is repeated at 40,000rpm and the upper portion containing LDL is extensively dialyzed against phosphate-buffered saline (PBS) containing 0.25 mM EDTA. Protein concentrations in lipoprotein preparations were determined using a modified Lowry assay[181].

PCSK9 protein purification

Stably transfected HEK293 suspension cell lines expressing wild-type or mutant PCSK9 were seeded in 1.5 L liquid cultures at 100,000 cells/mL in UltraDOMA hybridoma serum-free growth medium (Lonza) supplemented with 10% (v/v) FBS, 10 mM L-Glutamine, 100 units/mL penicillin and 100 µg/mL streptomycin sulfate. Cultures were grown without carbon dioxide at 37°C with stirring at 93 rpm for 7 days. Medium was harvested by pelleting cells at 3700 rpm for 20 minutes and filtering through 0.22 µm Millipore filter units. The pH of the medium was adjusted by addition of 50 mM final concentration Tris-HCL at pH 7 (pH 7.4 at 4°C). FLAG-tagged protein was bound to anti- FLAG M2 affinity columns by gravity flow, washed in TBSC (Tris-Buffered Saline with Calcium: 50 mM Tris-HCl pH 7.4, 150 mM NaCl, 2 mM $CaCl_2$) and eluted with 100 µg/mL FLAG peptide

(Thermo Scientific). The eluted protein was then concentrated 80-fold in Amicon filter units (10 kDa molecular weight cut-off, Millipore) and purified by FPLC on a Superdex 200 column. Final protein was eluted in HBSC (HEPES Buffered Saline with Calcium: 25m M HEPES-KOH, pH 7.4, 150 mM NaCl, 2 mM $CaCl_2$). PCSK9-containing fractions were pooled and concentrated approximately 5-fold. Purity of the protein was assessed by SDS-PAGE and Coomassie Brilliant Blue R-250 staining (Bio-Rad); concentration was estimated by BCA protein assay (Pierce).

In vitro PCSK9-LDL binding assay

Binding reactions (0.4 mL volume) each containing 300 µg LDL (total protein) and 300 µl wild-type or mutant PCSK9 conditioned media with 1% Ovalbumin in low-salt HBSC buffer (25 mM HEPES-KOH, pH 7.4, 75 mM NaCl, 2 mM $CaCl_2$) were incubated at 37°C for 1 hour. LDL-bound and free PCSK9 were then separated by Optiprep (iodixanol) gradient ultracentrifugation according to a modified version of a previously described protocol[182]. Briefly, a 9% Optiprep sample solution was prepared by diluting 0.35 mL of each binding reaction with 0.6 mL of 60% Optiprep and 2 mL of buffer (25 mM HEPES, pH 7.4) in a 3.3 mL Beckman Optiseal tube. The sample was over-layed with 0.3mL 25 mM HEPES, pH 7.4 in a 3.3 mL Beckman Optiseal tube. Tubes were centrifuged in a TLN100 rotor (Beckman Coulter) at 100,000 rpm for 2 hours at 4°C. LDL-containing fractions (300 µl) were collected by puncturing tube walls with a 22G needle and drawing into a 1mL syringe. Equivalent amounts of input (original binding reaction before Optiprep addition) and LDL-fraction were resolved by SDS-PAGE on 8% acrylamide gels, and relative PCSK9 content analyzed and quantified by western blotting.

Western Blotting

Western blot samples were prepared in final 1X loading buffer (50 mM Tris-HCl, pH 6.8; 1% SDS; 5% glycerol; 10 mM EDTA; 0.0032% bromophenol blue) and boiled at 96°C for 5 minutes before loading onto acrylamide gels for resolving by SDS-PAGE. Resolved proteins were transferred to nitrocellulose membranes (BioRad) for immunoblotting. After primary antibody incubation,

secondary infrared dye (IRDye800)-labeled antibodies were used for detection on a LI-COR Odyssey infrared imaging system (LI-COR Biosciences). Band intensity was quantified using Odyssey 2.0 software. The monoclonal antibodies 15A6 & 13D3 recognize the C-terminal domain and the catalytic domain of PCSK9 respectively[15], and were purified from hybridomas in the lab. Secondary IRDye-labeled goat anti-mouse IgG antibodies were purchased from LI-COR Biosciences.

Circular dichroism

Lyophilized synthetic peptides (custom designed, Biomatik) were dissolved in water with 0.1 % ammonium hydroxide (to aid solubility) at stock concentrations in the range of 500 – 2000 □M. Stock solutions of peptide were diluted to make 30μM samples of peptide in buffer (10 mM Tris, 130 mM NaCl, pH 8.5) with or without dodecylphosphocholine (DPC) micelles (ranging from 0-4% DPC w/v in solution) using a Jasco J-815 CD spectropolarimeter at 37°C in a 0.1-cm quartz cuvette. Spectra were acquired from 200 to 250 nm using five accumulations at 20 nm/minute and a data integration time of 8 seconds. Secondary structure deconvolution of spectra was carried out in CDPro software with the CONTIN algorithm and SP43 reference set. To measure the apparent affinity of peptide-lipid interactions, ~30 μM peptide was mixed with increasing concentrations of DPC micelles, and CD spectra were collected after each increment as described above. Errors represent S.E. of at least three independent replicates.

Competition binding assay

Binding reactions containing 0.5 mg/mL of LDL, 10.8 nM DyLight800-labelled wild-type PCSK9 and increasing amounts (upto a 500-fold excess, highest 5000 nM)) of purified unlabelled wild-type or mutant PCSK9 were incubated at 37°C for 1 hour in HBSC (HEPES Buffered Saline-Calcium buffer: 25 mM HEPES-KOH, pH 7.4, 150 mM NaCl, 2 mM CaCl2) and 1% BSA before being resolved on a 0.7% agarose gel (electrode buffer: 90 mM Tris, pH 8.0, 80 mM Borate, 2 mM Calcium lactate) at 40 V for 2 hours. Labelled PCSK9 was then visualized directly in the gel using a LI-COR Odyssey infrared imaging system (LI-COR Biosciences). Intensity data was fit to a sigmoidal one-site binding

curve using non-linear regression in Graphpad Prism 5 software to obtain the inhibitor constant (K_i) for each protein.

Computational modelling

The crystal structure of PCSK9 at 1.9-Å resolution (PDB ID 2QTW)[59] was used to model the missing residues in the N-terminal region of the prodomain. The structure adopted by residues 31 to 60 was constructed using the fragment-based de novo protein structure prediction method in ROSETTA v3.8[183]. In preparation for the modeling, 3-mer and 9-mer fragment library files were created with the ROSETTA server[175], identifying protein-fragment structures in the Protein Data Bank that are compatible with the PCSK9 sequence. Based on these libraries, 180,000 refined PCSK9 models including the N-terminal prodomain were built. The known part of the PCSK9 structure was kept fixed during the conformational search. Analysis of the ROSETTA total score against the Cα RMSD relative to the lowest score model was used to evaluate the modeling convergence. The best full-length PCSK9 model was selected as that with the lowest ROSETTA score. Secondary structure prediction with PSIPRED v3.3[171], as well as protein compactness and local secondary structural features estimated with the "protein meta-structure" approach[184] are consistent with the predicted structure. The final model was analyzed using PyMOL v1.8.4 (Schrödinger, LLC).

Statistical analyses

All statistical analyses were carried out on Graphpad Prism 5 software. All experiments were repeated a minimum of 3 times, and all graphs report mean values with error bars showing standard error of the mean (SEM). Means were compared by paired or un-paired student t-tests as appropriate, or by one-way ANOVA followed by a post-test (Dunnett's test to compare all columns vs. control column, or Bonferroni's test to compare all column pairs).

Chapter 3: The effect of natural mutations on PCSK9-LDL binding.

3.1 Introduction

While the N-terminal disordered region is required for LDL binding as discussed in the previous chapter, there is as of yet no evidence to confirm that it is the site of direct protein-protein interaction with ApoB. Thus other regions of PCSK9 may also act as LDL-binding determinants. Many natural polymorphisms, causing either gains or losses in function, exist in the PCSK9 gene across human populations. Gain-of-function variants in PCSK9 generally have dramatic effects on plasma cholesterol levels, frequently being associated with severe hypercholesterolemia, while reductions in blood cholesterol levels due to loss-of-function PCSK9 polymorphisms tend to be relatively moderate, with lowered CVD risk mostly attributed to the accumulated effect of a lifetime of moderately lower LDL-cholesterol[185]. We hypothesized that GOF mutations would exist that decrease LDL binding, since we have previously observed LDL to inhibit PCSK9 activity[158].Thus we became interested in a surface exposed region of the PCSK9 prodomain, spatially adjacent to the disordered N-terminal region, which contains a cluster of sites known for hypercholesterolemia-associated polymorphisms **(Figure 9A)**. We used mutagenesis and in-vitro LDL binding assays to assess the effects of these mutations on the ability of PCSK9 to bind LDL and found that they all severely disrupt PCSK9-LDL binding. The discussion that follows will analyze what that might mean in terms of functionality.

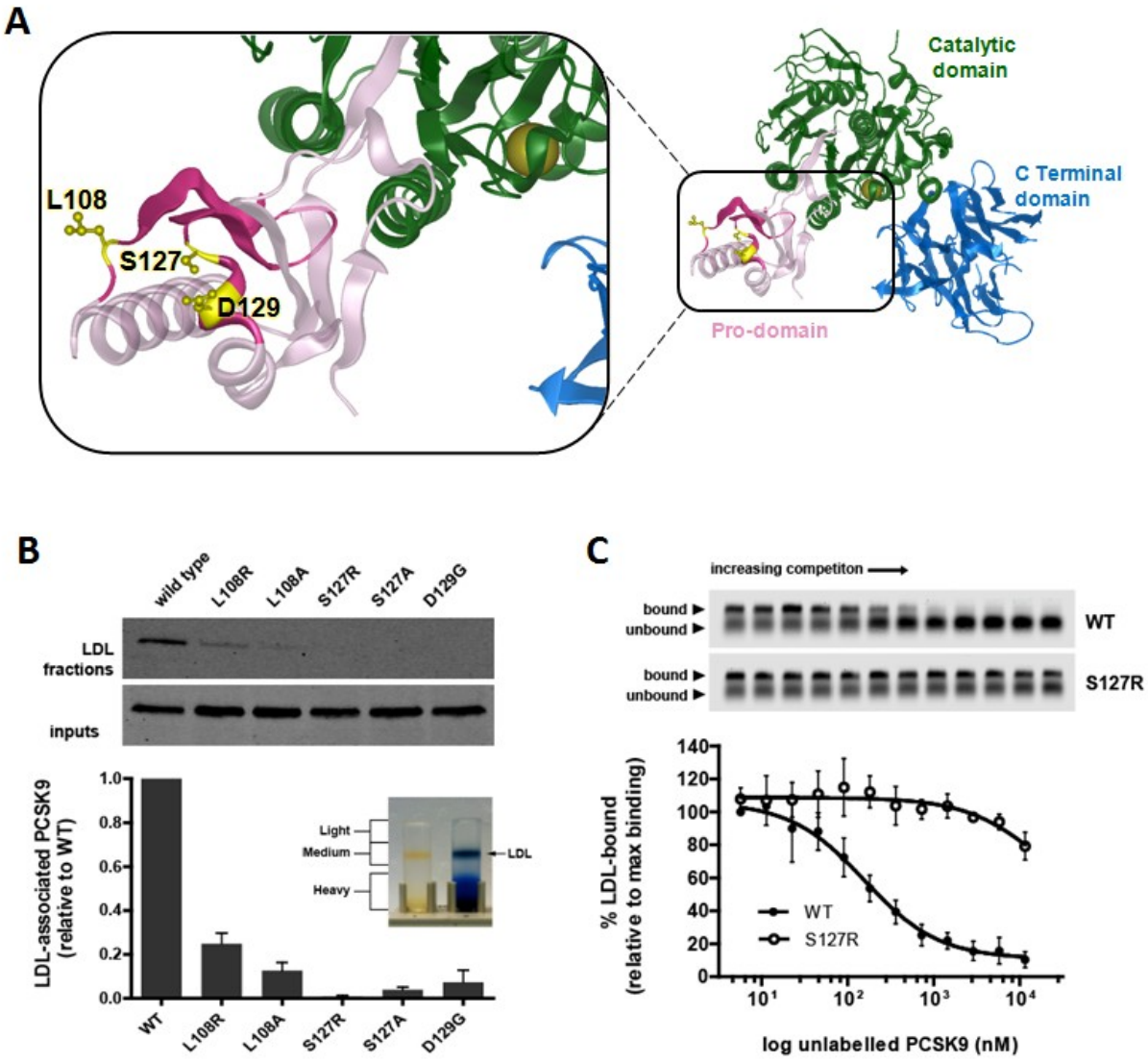

Figure 8: A clustered site for gain-of-function mutations causes defects in PCSK9-LDL binding. (A) Right: The crystal structure of PCSK9, modified from the published PDB structure 2QTW. A relatively unstructured loop bearing the region of interest is highlighted in darker pink. Left: The residues S127, L108 and D129 are highlighted in yellow in the inset, with their side chains depicted in ball-and-stick format. **(B)** In-vitro binding reactions of wild-type or mutant PCSK9 + isolated human LDL were centrifuged in iodixanol gradients to separate LDL-bound and non-bound PCSK9. PCSK9 in the LDL-containing fraction (Medium) was detected by western blotting. Quantification shown in graph, where the mean of n=3 with standard error is plotted. **(C)** In vitro competition curves where 10.8nM infrared dye labelled wild-type PCSK9 was incubated with 500µg/mL LDL, in the presence of up to 500-fold excess unlabelled wild-type or mutant PCSK9. Bound and free complexes were resolved by electrophoresis on 0.7% agarose gels. Gels were visualized on a LI-COR Odyssey system. Bound labeled PCSK9 was quantified and fit to a one-site binding curve on Prism5 software using non-linear regression. Plotted mean ± standard error (n=3). Plotted mean of n=3 ± standard error.

3.2 Results

We investigated the ability of the natural variants L108R[186], S127R[17,187] and D129G[187] to bind LDL in-vitro by incubating conditioned media of wild-type or mutant PCSK9 with LDL (amounts of conditioned media adjusted to have comparable amounts of wild-type and mutant PCSK9) and separating LDL-bound and unbound PCSK9 by density gradient ultracentrifugation. We found that all three variants showed a dramatic loss in LDL binding, with S127R having the most severe effect **(Figure 8B)**. The substitution of S127 and L108 to arginine would introduce positive charges to this region, while the D129G substitution would remove the acidic aspartate residue. In order to investigate whether the LDL binding defect resulted from the change in net charge to this area, we substituted the S127 and L108 with uncharged alanine residues and again assessed in vitro LDL binding. The alanine mutants did not recover LDL binding, indicating that the ability to bind LDL depends on the presence of the native residue at these sites rather than on the charge status of the site **(Figure 8B)**.

Since the S127R variant showed the most severe loss in LDL binding in the ultracentrifugation assay, we tested whether some LDL binding would still be able to occur at high non-physiological concentrations. Competition binding assays similar to those in Chapter 2 were performed with purified recombinant wild-type or S127R-PCSK9 as unlabeled LDL-binding competitors. It was found that similar to the full Δ31-52 deletion, the S127R mutation prevented effective competition even at the highest concentrations tested **(Figure 8C)**. This indicates that the serine at position 127 is highly critical to the LDL interaction, and may be implicated in the protein-protein binding site with apoB.

3.3 Discussion

That all 3 of these natural mutations are both defective in LDL-binding and associated with hypercholesterolemia supports the theory that non-LDL bound PCSK9 would be in a conformation

that has a higher LDLR affinity relative to LDL-bound PCSK9, as explained in Chapter 2. The three natural mutation sites studied appear to show differing importance in requirement for LDL binding, with S127 being the most necessary, and L108 being the least. The S127 and D129 residues are well conserved across species[187], while the L108 is only well conserved among primates[186]. Currently the mechanism of action of these GOF mutations has still not been elucidated. However, our findings allow us to speculate that subjects born with these polymorphisms in PCSK9 would be lacking a form of negative regulation of their PCSK9, i.e. LDL binding, leading to long-term elevated levels of hypercholesterolemia. Indeed, all 3 of these mutants have shown increased affinity for LDLR in vitro or increased degradation of the LDLR in cell culture in various past studies[56,82,186-188].

The surface exposed nature of this gain-of-function mutation-site clustering region (henceforth referred to as the "GOF area") makes it a candidate for a protein-protein interaction with a lipoprotein particle. Our results indicate that the presence of the native residues is what preserves LDL binding rather than non-specific charge preservation of the area. Thus, these residues may be involved in an interaction that requires those side chains to form important salt bridges. The electronegative nature of the head groups of both serine (S127) and aspartate (D129) would fit this idea. The aliphatic nature of the leucine at position 108 does not allow salt bridge formation, but it may play a role in hydrophobic interactions with the apoB binding partner. This hydrophobic interaction may be dependent on the size and shape of the leucine side chain, as a similarly aliphatic and non-polar alanine (L108A) failed to rescue LDL binding. It is interesting to note here that in published structures of PCSK9 bound to full length LDLR, the PCSK9 L108 residue makes hydrophobic contact with the L626 of the LDLR β-propeller domain[167], forming a secondary interface with the LDLR. In fact, all three of these mutation sites are found at this interface with the LDLR β-propeller[167]. Thus, in addition to the N-terminal region studied in Chapter 2, the GOF area also holds dual importance in both LDL and LDLR binding, although it was also found in the same

study that the L108-L626 interaction only marginally contributes to the overall affinity of PCSK9 for LDLR.

Theories to explain the FH-associated phenotypes of these variants have been put forward in previous studies. Investigations of apoB kinetics in ADH subjects with the S127R-PCSK9 polymorphism show an increase in apoB100 production, related to an overproduction of VLDL, IDL and LDL, where conversion of VLDL to IDL and LDL was also decreased[189]. Similar apoB overproduction was seen in rat hepatoma cells[190]. By what mechanism the S127R mutation would be increasing apoB production or affecting VLDL conversion is not clear, but a host of potentially relevant intracellular interactions have turned up in various studies. Most interestingly, yeast two-hybrid assays find PCSK9 interacting with apoB itself intracellularly in hepatocytes[162]. It has been suggested that PCSK9 is somehow involved in posttranslational degradation of apoB within the secretory pathway, and the S127R variant differentially affects this process[191]. The LDLR has been implicated in lowering VLDL secretion by increasing pre-secretory degradation of apoB[192], and there is evidence that PCSK9 interacts with and mediates LDLR degradation intracellularly[193]. Together, these could suggest that intracellular PCSK9-mediated LDLR degradation counterbalances LDLR-mediated apoB pre-secretory degradation. Thus, the increased LDLR degrading activity of S127R-PCSK9[56,187,194] could more strongly prevent pre-secretory apoB degradation. There has been data linking PCSK9 and the S127R variant to ubiquitination pathways[195], and VLDL assembly is also known to be regulated by apoB ubiquitination[196]. Another intracellular factor that links PCSK9 and apoB is the sorting receptor sortilin, overexpression of which increases hepatic secretion of both PCSK9[197] and apoB lipoproteins[198,199]. Increased cell-surface LDLR degradation by S127R may also lower liver triglyceride uptake in the form of apoE-containing chylomicron- and VLDL-remnants, resulting in production of cholesteryl ester-enriched VLDLs that are more resistant to conversion in the circulation. It has also been postulated that cholesterol coming into the cell packaged in remnant lipoproteins is more potent than LDL-C at

suppression of SREBP processing in the liver; thus decreased remnant uptake could result in increased lipogenesis and an indirect metabolic effect on VLDL production[200,201]. Whichever the case, it is likely that a combination of mechanisms lead to S127R-associated hypercholesterolemia: increased lipoprotein production as well as increased LDLR degradation amplified by a lack of negative PCSK9 regulation by LDL binding.

As mentioned above, the L108 residue interacts with L626 in the LDLR β-propeller domain[167]. Abifadel *et al* have postulated that the hypercholesterolemic phenotype of L108R is due to the introduction of the positive charge, proposing that an arginine at 108 would form a new electrostatic interaction with the LDLR glutamic acid at 605 instead of LDLR-L626, thus tightening the LDLR-binding and creating a gain-of function for PCSK9[186]. Our in vitro results where L108A does not rescue LDL-PCSK9 binding indicates that the arginine in L108R would not be the driver of the loss-of LDL binding. Similarly, a mutagenesis study found through modeling that the S127R mutation in PCSK9 could make a salt bridge with the D129 residue[194], but our finding that S127A does not rescue LDL binding excludes that salt bridge from being the reason that S127R would lack LDL-binding.

Finally, we present an integrated model that combines our findings from this chapter and Chapter 2 to demonstrate how PCSK9 may be interacting with lipoprotein particles in **Figure 9**. An intramolecular interaction between the C-terminal domain and the newly modeled N-terminal helix might, in addition to allosterically lowering affinity of the catalytic domain for the LDLR, act to position the GOF area in a way that facilitates apoB binding or lowers affinity of the GOF area for the LDLR β-propeller domain.

3.4 Materials and Methods

See Chapter 2, Section 2.4: Mutagenesis of PCSK9, LDL isolation, PCSK9 conditioned media, In vitro PCSK9-LDL binding assay, Western Blotting, Competition binding assay.

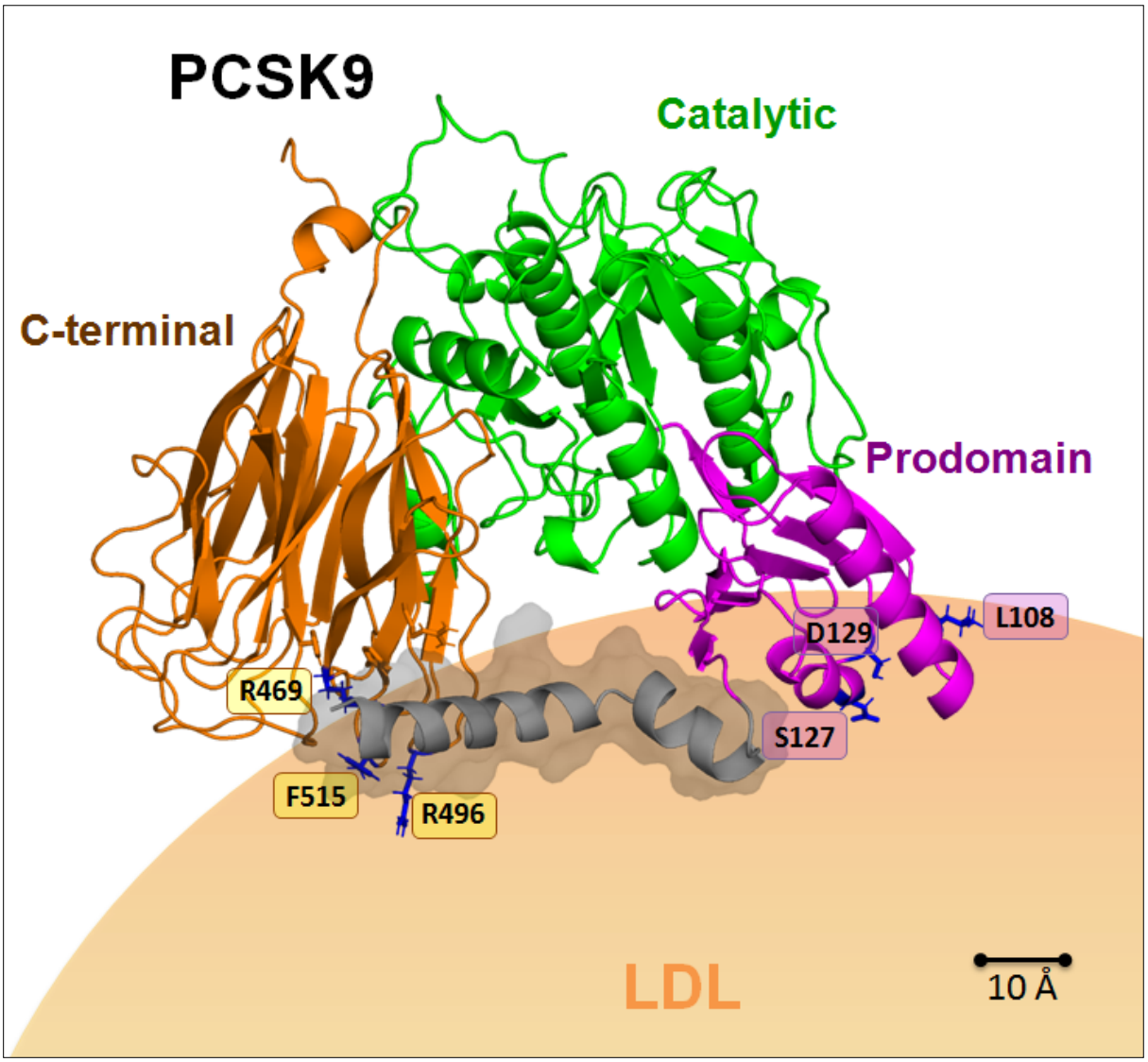

Figure 9: A model for PCSK9 association with LDL. The full-length PCSK9 structure as modeled using Rosetta software[175] is depicted in purple, green and dark orange to denote the 3 domains as labelled, as well as the prodomain N-terminal region in grey. The relative size of an approximately 22 nm diameter LDL particle is shown as a light orange sphere at bottom. PCSK9 is depicted as approaching the LDL in an orientation that would maximize proximity of all the regions of PCSK9 found to affect LDL-binding in our mutagenesis studies to the LDL surface. Residues of importance in both the prodomain and catalytic domain have been labelled. Note the relative positions of the two broad areas of interest in our investigations: the putative intramolecular interaction of the C-terminal domain with the N-terminal of the prodomain (left, yellow residue labels) and the cluster of familial hypercholesterolemia-associated polymorphism sites (right, purple residue labels).

Chapter 4: PCSK9 associates with triglyceride-rich lipoproteins in a remodeling-sensitive manner

4.1 Introduction

While multiple studies have characterized the PCSK9-LDL interaction, whether PCSK9 can bind to apoB-containing lipoproteins other than LDL has not yet been extensively studied. VLDL, which exclusively contains apoB100 in humans, is catabolized and remodeled in the circulation by lipoprotein lipase and CETP to form the short-lived intermediate-density lipoprotein (IDL) and finally to LDL. Intestinal derived chylomicrons contain apoB48, and are metabolized mainly by lipolysis to chylomicron remnant particles. Both VLDL and chylomicron remnant particles, collectively termed TG-rich lipoprotein (TRL) remnants, acquire the LDLR ligand apoE, thus hepatic LDLR participates along with other cell surface receptors in plasma TRL clearance. It is unclear whether PCSK9 can bind to these TRL remnants. In the past we observed that plasma PCSK9 did not associate with VLDL in fasted normolipidemic human samples, and recombinant PCSK9 did not bind isolated VLDL[158]. This suggests that PCSK9 is responsive to the intravascular VLDL→IDL→LDL conversion. However other studies observed low levels of PCSK9 association with VLDL in mice[162]. We hypothesize that PCSK9 may bind to an epitope on apoB that is relatively unavailable on VLDL but becomes readily available on TRL remnants and LDL upon remodeling in the circulation, thus limiting PCSK9's ability to mediate LDLR degradation in the late postprandial stage. This would suggest that PCSK9 could bind to intermediate density lipoproteins (IDL), the intermediate in the catabolism of VLDL to LDL. Data presented in this chapter will provide evidence that PCSK9 does indeed bind IDL with similar affinity to LDL. These results are supported by findings in human hypertriglyceridemic plasma samples containing lipoprotein profiles shifted toward larger TRL populations.

4.2 Results

Lipoproteins isolated from human plasma by the sequential sodium bromide density-gradient ultracentrifugation method[180] are stripped of PCSK9, likely due to conditions of prolonged high-salt and centrifugal force **(Figure 10A)**. Thus, lipoprotein fractions prepared in this manner can be used in binding assays free from interference from endogenous bound PCSK9. To determine which classes of apoB100-containing lipoproteins PCSK9 binds to, gel shift assays were performed by incubating infrared-dye labelled PCSK9 with isolated fractions of human LDL, IDL or VLDL normalized for their apoB content (measured by a commercial apoB ELISA). Reactions were incubated at 37°C and then resolved on an agarose gel. PCSK9 with lower mobility and overlapping with apoB migration indicated that PCSK9 was able to associate strongly with both LDL and IDL. A weak overlap of PCSK9 and apoB was also observed with VLDL, but the vast majority of PCSK9 was in an unbound form following incubation with VLDL **(Figure 10B)**. In vitro PCSK9 association with IDL was also tested using density gradient ultracentrifugation assays. Infrared dye labelled PCSK9 was again incubated with isolated VLDL, IDL or LDL and the binding reactions subjected to density gradient ultracentrifugation, resulting in differential floatation of the different lipoproteins. The gradients were fractionated **(Figure 11A)**, and the fractions analyzed for labelled PCSK9 using SDS-PAGE, and for cholesterol content using enzymatic, colorimetric plate assay to track overlap of PCSK9 and lipoprotein distribution within the gradients (Appendix C, Figure C3). We observed that PCSK9 indeed shows a notable ability to associate with what is likely a small, dense sub-fraction of IDL **(Figure 11B)**, while association with VLDL was very minimal.

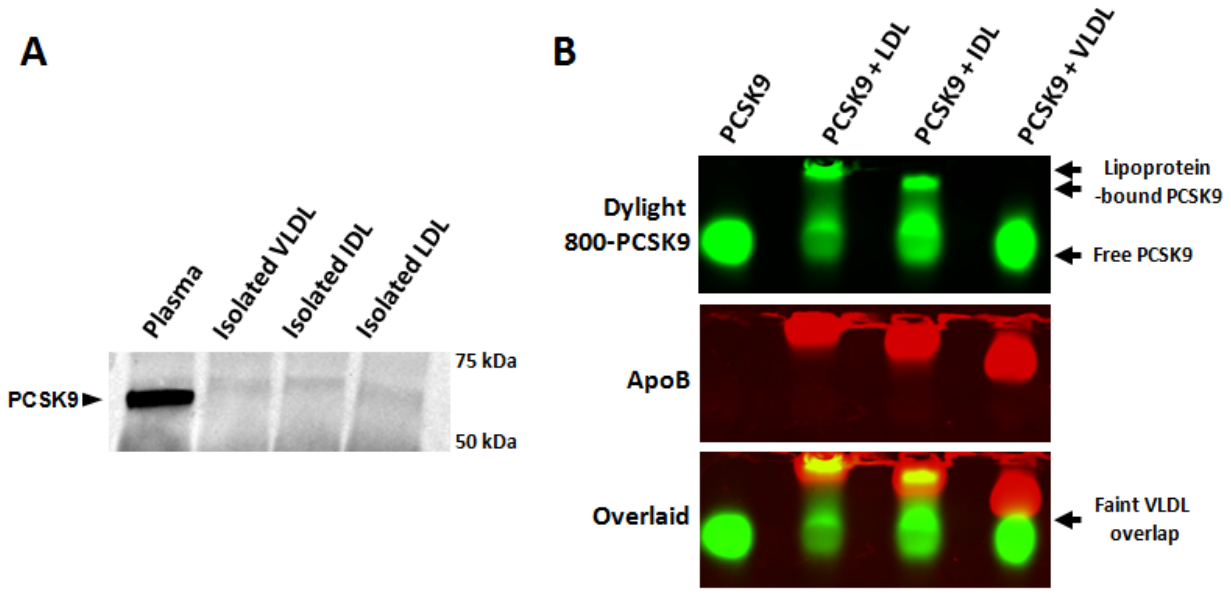

Figure 10: PCSK9 associates strongly with both IDL and LDL. (A) Lipoproteins isolated from human plasma by sodium bromide density-gradient ultracentrifugation are stripped of PCSK9. Equivalent volumes of fasted plasma or isolated lipoproteins were immunoprecipitated with anti-PCSK9 polyclonal antibody. Samples were resolved by SDS-PAGE and immunoblotted for PCSK9. **(B)** Gel shift assay of PCSK9 with isolated lipoproteins. Incubations were carried out for 1 h at 37°C containing combinations of lipoprotein (normalized for apoB content) and Dylight800-labeled wild-type PCSK9. Reaction mixtures were resolved in 0.7% agarose gels and transferred to nitrocellulose. ApoB100 was detected by immunoblotting using a Dylight680-labeled secondary antibody. Blots were scanned using the LI-COR Odyssey infrared imaging system using dual channel detection of dye-labeled proteins.

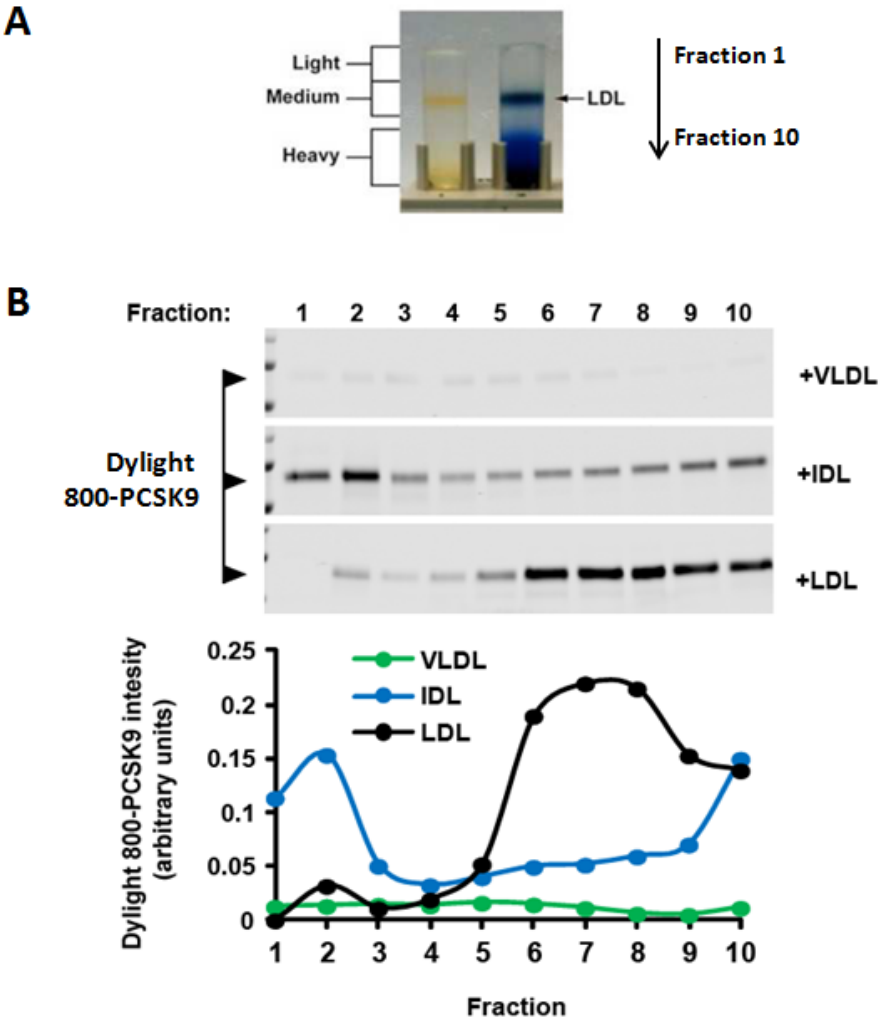

Figure 11: PCSK9 associates with IDL in vitro. (A) Schematic of fractionation. Less dense TG-rich lipoproteins float to the top while LDL floats lower. Gradients were fractionated from top to bottom. (B) In-vitro binding reactions of infrared dye labelled PCSK9 (800-PCSK9) with isolated human VLDL, IDL or LDL were centrifuged in iodixanol density gradients similar to Figure 3B. Portions of each fraction were subjected to SDS-PAGE and gels visualized on a LI-COR Odyssey system. The free unbound PCSK9 is not shown due to interference from high concentrations of Optiprep at the bottom of the tubes. Results shown are for one experiment representative of 3 independent experiments.

To more quantitatively assess the IDL interaction relative to the LDL interaction, competition binding analysis was performed. Infrared-dye labelled PCSK9 was incubated with either IDL or LDL (amounts normalized for apoB) in the presence of increasing concentrations of unlabeled recombinant PCSK9 as competitor. Lipoprotein-bound and unbound labelled PCSK9 was assessed by resolving on agarose gels and the bound bands were quantified and fit to a one-site binding curve using non-linear regression. The inhibition constants (K_i) obtained from both the LDL and IDL curves (LDL $K_i = 152.4 \pm 97.3$ nM; IDL $K_i = 99.4 \pm 99.4$ nM) were not statistically different from each other **(Figure 12)**.

Hyper-triglyceridemic patients exhibit plasma lipoprotein profiles with higher proportions and concentrations of TRLs in the VLDL and IDL category due either to increased production from the liver and intestine or through decreased peripheral catabolism[202]. Since PCSK9 associated with IDL in-vitro, we wanted to observe whether PCSK9 was also able to associate with more TG-rich lipoproteins in plasma. Fasted plasma samples from 4 hyper-triglyceridemic patients with plasma triglycerides in the 95th percentile range were subjected to density ultracentrifugation and fractionated similar to the in vitro experiments. Fractions were analyzed for endogenous PCSK9 content using ELISA and for cholesterol and triglyceride content using enzymatic, colorimetric assay. It was found that, relative to normolipidemic plasma, the lipoprotein-bound PCSK9 in the hyper-triglyceridemic subjects consistently showed a shift toward a more triglyceride-rich lipoprotein population, as assessed by a change in PCSK9-containing fractions **(Figure 13)**. This result is reflective of the in vitro IDL binding experiments and supports that PCSK9 can also bind to TRL remnants in human plasma.

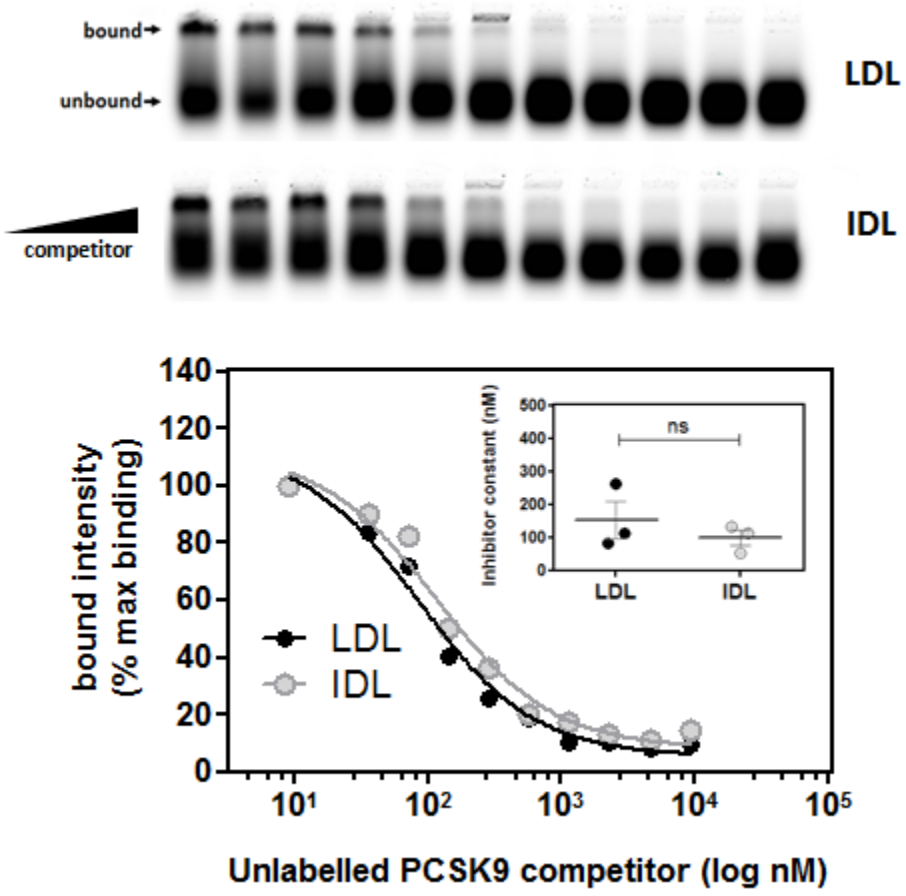

Figure 12: PCSK9 associates with IDL and LDL with similar affinity. In vitro competition curves where 21nM infrared dye labelled wild-type PCSK9 was incubated with 0.2 µg/µl of LDL-apoB or IDL-apoB in the presence of 450-fold excess unlabelled wild-type PCSK9. Lipoprotein-bound and free PCSK9 were resolved by electrophoresis on 0.7% agarose gels. Gels were visualized on a LI-COR Odyssey system. Bound labeled PCSK9 was quantified and fit to a one-site binding curve on Prism5 software using non-linear regression. Data shown is one representative experiment of 3 independent experiments.

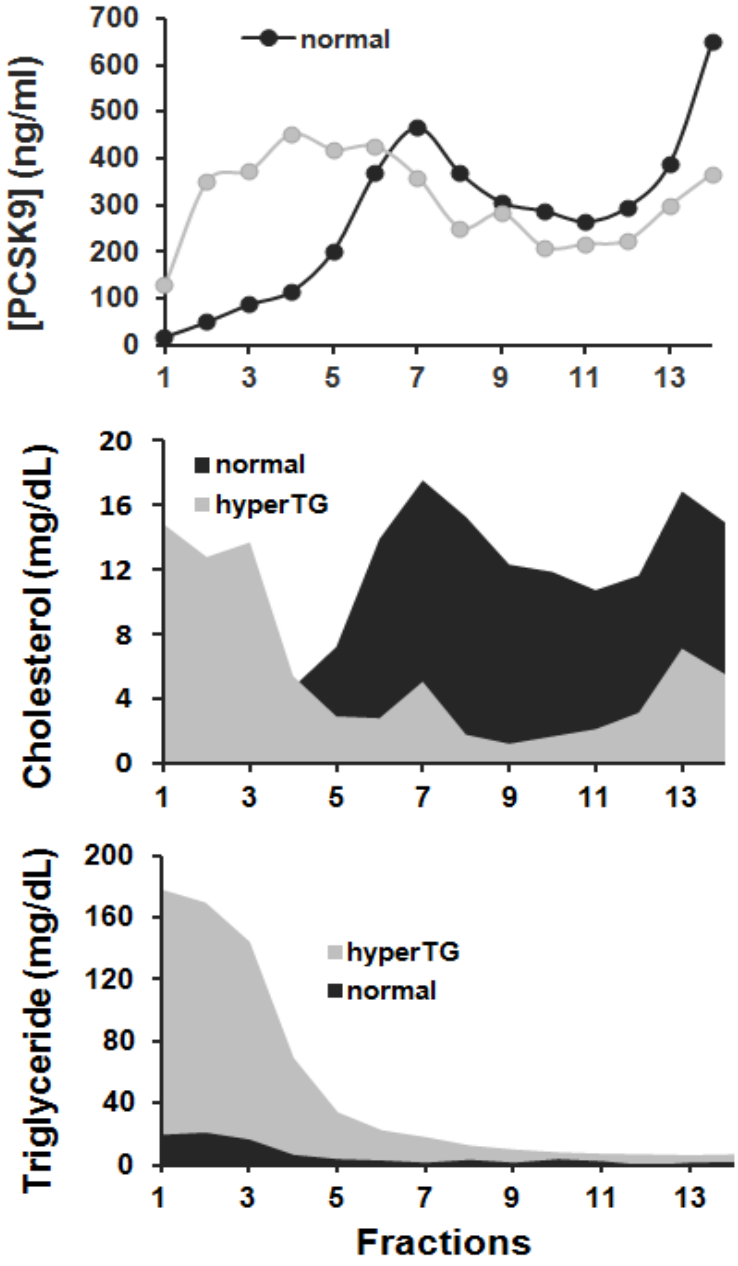

Figure 13: Lipoprotein-bound PCSK9 shifts to a more triglyceride-rich lipoprotein population in hypertriglyceridemic plasma. Fasted normolipidemic or hypertriglyceridemic plasma were incubated at 37 °C for 15 minutes before being subjected to density gradient ultracentrifugation. Resulting density gradients were fractionated from lowest to highest density. PCSK9 content of each fraction was assessed by ELISA, while cholesterol and triglyceride content of each fraction was measured by colorimetric, enzymatic plate assay.

If PCSK9 is responsive to changes in plasma LDL concentrations, there should be proportionally more PCSK9 bound to LDL in subjects with hypercholesterolemia, which typically is due to increased LDL-C. Therefore, we hypothesized that PCSK9 distribution may be influenced by the concentration of circulating LDL particles. To test this hypothesis, we studied plasma samples from hypercholesterolemic (n=41; LDL-C $>$ 4.9 mM) subjects compared to normolipidemic controls (n=40; LDL-C $<$ 3 mM). Total PCSK9 concentrations in the plasma were measured by ELISA. The control group had a mean plasma PCSK9 of 295.1 $\pm$ 15.1 ng/mL, while the hypercholesterolemic group had a mean plasma PCSK9 of 335.0 $\pm$ 17.3 ng/mL **(Figure 14A)**. This trend toward higher PCSK9 levels in hypercholesterolemia agrees with previous studies that find PCSK9 levels to be elevated in hypercholesterolemia[92,203], although our difference did not become statistically significant. These plasma samples were then resolved by density gradient centrifugation and the PCSK9 in the LDL-containing fractions and in the non-LDL fractions again quantified by ELISA. We found that the proportion of LDL-bound PCSK9 increased modestly from 26% in the normolipidemic group to 29% in the hypercholesterolemic group (p=0.04, **Figure 14B)**. We also conducted a sub-analysis of 10 individuals from each group, 10 with the lowest LDL-C in the control group and 10 with the highest LDL-C in the hypercholesterolemic group. This time the plasma PCSK9 concentration went from 286.3 $\pm$ 32.5 ng/mL in the control group to 352.0 $\pm$ 49.3 ng/mL in the hypercholesterolemic group **(Figure 14C)**, although this difference still did not reach statistical significance. The difference between the proportion of LDL-bound PCSK9 also became more apparent, going from 21.6% in the control group to 30.8% in the hypercholesterolemic group (p=0.003, **Figure 14D)**.

4.3 Discussion

The differential association of PCSK9 observed in vitro with VLDL, IDL and LDL suggest that the ability of PCSK9 to associate with apoB100-containing lipoproteins is dependent on the remodeling

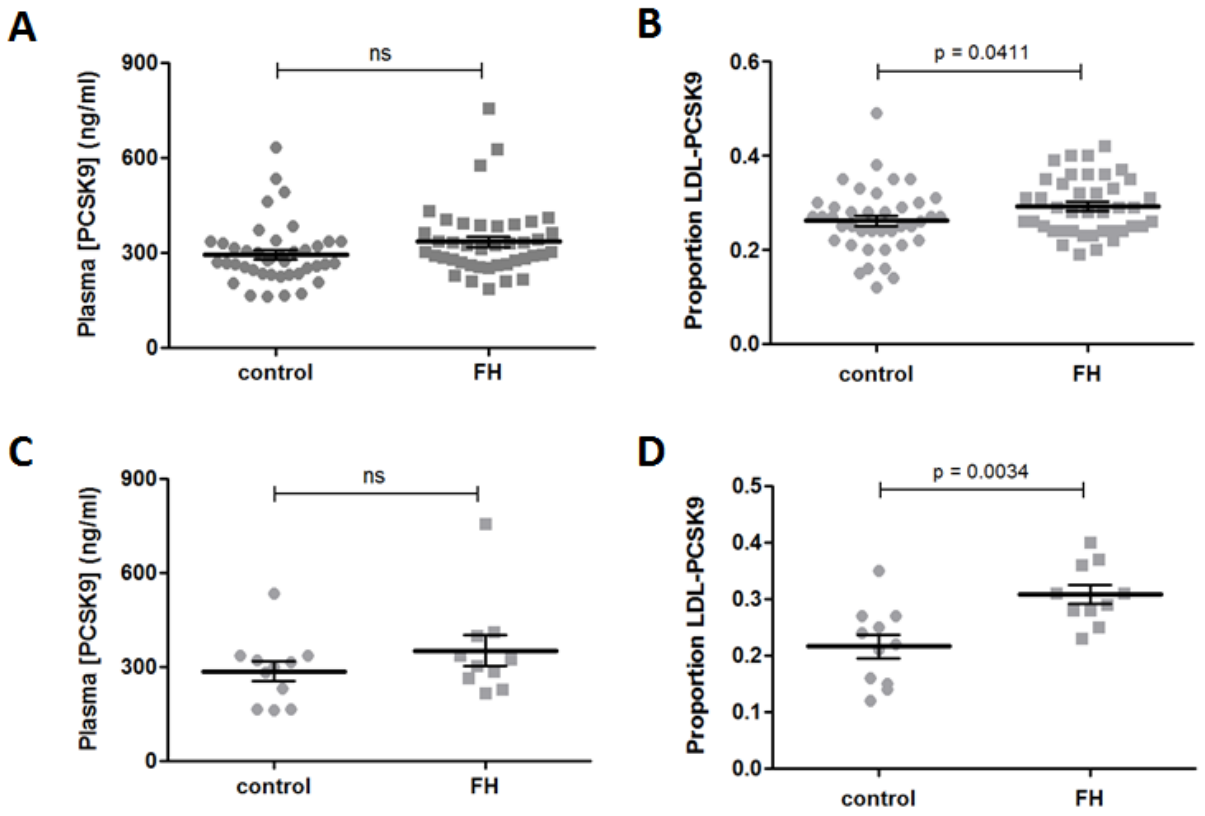

Figure 14: More PCSK9 is LDL-bound in hypercholesterolemic subjects. (A) Fasted normolipidemic (n=41) or hypercholesterolemic (n=41) plasma was measured for PCSK9 concentration by ELISA. **(B)** The same plasma samples as in (A) were incubated at 37 °C for 15 minutes before being subjected to density gradient ultracentrifugation. A light-density fraction containing the apoB100-lipoproteins was collected and PCSK9 content measured by ELISA. **(C)** and **(D)** are the results of a subanalysis of the data set in (A) and (B) where plasma PCSK9 and LDL-PCSK9 are compared between the 10 individuals with the lowest LDL-C in the control group with the 10 highest LDL-C in the hypercholesterolemia group.

status of the lipoprotein. PCSK9 seems able to associate strongly and comparably with both IDL and LDL, while only very weakly, if at all, with VLDL. These results raise two immediate questions - What could mediate the differential recognition of lipoproteins by PCSK9? What could be the functional significance of this in circulation?

To answer the first question it must be considered what is different between the lipoprotein classes structurally and chemically. These differences include size and shape, lipid content, and differences in both protein content and conformation. Although heterogeneity exists in each class of lipoprotein, it can be broadly said that the diameter of VLDL > IDL > LDL[204]. Thus, surface curvature and surface lipid packing may play a role in PCSK9 affinity for the lipoprotein particle, particularly if any lipid interactions are involved. Particle size may also affect surface electrostatics: core lipids have been seen to extrude to the surface in smaller HDL particles[205], although similar investigations have not been done with apoB100 lipoproteins. Lipid content and composition also varies between the lipoprotein classes, progressing from more triglyceride-rich VLDL to more cholesterol-rich LDL, in addition to variations in individual lipid species[206,207]. Biophysical studies have manipulated the ability of apolipoproteins to bind lipoprotein mimetic particles by changing core lipid content from triglyceride-rich to cholesteryl ester-rich and modulating surface free cholesterol content[119,208].

Protein factors that could differentiate PCSK9 binding could involve features of the apoB100 moiety, or even presence or absence of other protein factors, such as other apolipoproteins. The conformation and surface exposure of apoB changes throughout the lipoprotein remodeling process, as discussed in the introductory chapter (see Section 1.5). Thus it may be that the PCSK9 binding epitope on apoB only becomes available after remodeling of VLDL in circulation has progressed to a certain stage in the IDL / LDL spectrum. We did not find the affinity of PCSK9 for IDL and LDL to be significantly different **(Figure 12)**, suggesting that a difference in epitope exposure rather than a difference in epitope conformation is the reason for differential association.

Additionally, it is possible that other apolipoproteins present on the particles can act as determinants of PCSK9 binding. VLDL and IDL particles contain ApoE and apoCI, II and III[14]. By the time the particle has been converted to LDL, these apolipoproteins have been lost and apoB100 remains as the only apolipoprotein. Proteins associated with lipoprotein surfaces can displace each other[209,210]. It is possible that somewhere along the conversion process, the loss of one of these apolipoproteins allows PCSK9 binding.

A relevant parallel for lipoprotein-remodeling dependent binding is the interaction of LDLR with apoB100 only in the later stages of VLDL remodeling, i.e. in the late IDL – LDL stages. The more triglyceride-rich VLDL particles do not have the epitope for the LDLR binding repeats available until lipolysis leads to a conformational change of the apoB100 C-terminus[73]. ApoE, the alternate LDLR ligand, is present on chylomicron and VLDL remnants, but is absent on LDL particles. Thus, mechanisms regulating lipoprotein metabolism in circulation exist that depend on the stage of lipoprotein conversion to exert regulatory influence on clearance.

The functional significance of conversion-dependent association of PCSK9 with LDL may similarly be in regulating LDL clearance. It is unknown whether the LDLR binding site and the PCSK9 binding site on apoB100 would overlap or lead to competitive binding. However, circulating LDL particles typically outnumber circulating PCSK9 molecules by a 200:1 ratio; thus even if competitive binding were the case, this would be unlikely for PCSK9 to exert a direct regulatory effect on LDL levels[94]. The reverse is more likely, where lipoprotein interaction regulates PCSK9 activity based on changes in the circulating lipoprotein population. Keeping in mind evidence that lipoprotein binding inhibits PCSK9[158], we propose that lipoprotein conversion-sensing plays a role in negative regulation of PCSK9 activity: it may promote PCSK9-mediated degradation of LDLR when the circulating lipoprotein population is more VLDL-like, while suppressing PCSK9 activity when the lipoprotein

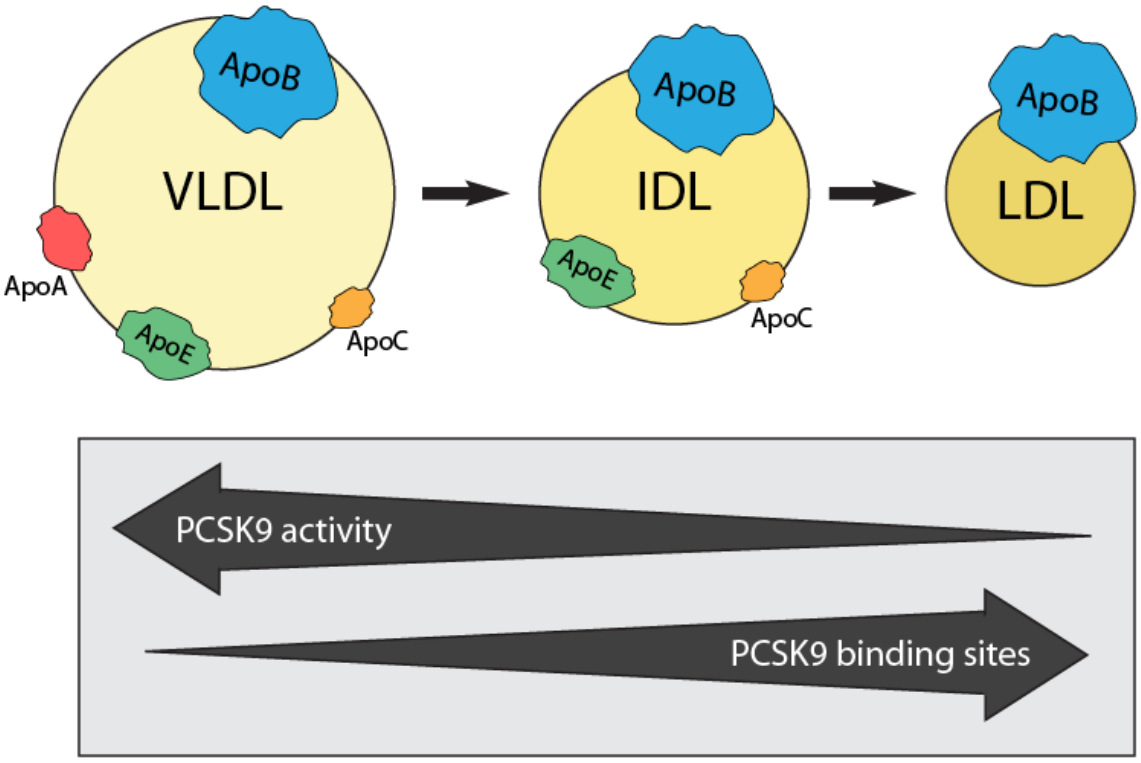

Figure 15: A model for the regulation of PCSK9 activity by lipoprotein binding. When the population of circulating lipoproteins is mostly made up of very low-density lipoproteins (VLDL), less PCSK9 is in the lipoprotein-bound inactive state, leading to LDL receptor down-regulation and slow lipoprotein clearance from blood. However when the VLDLs are remodeled to intermediate, then low density lipoproteins (IDL, LDL), PCSK9 is able to bind more lipoproteins. Thus more PCSK9 is sequestered in an inactive pool, leading to up-regulated LDL receptor protein and efficient lipoprotein clearance by the liver. Four broad aspects of lipoprotein remodeling may govern PCSK9 affinity: (1) lipoprotein size and shape (2) lipid content and composition (3) the apolipoprotein population found on the particle (4) apoB100 conformation or surface exposure.

population is more LDL-like **(Figure 15)**. For example, post-prandially, when most circulating lipoproteins are triglyceride-rich, less PCSK9 may be sequestered in a lipoprotein-bound, inactive state, leading to the down-regulation of LDLRs, which in turn inhibits clearance of the TG-rich lipoproteins from the circulation and extends their excursion time. Once these lipoproteins have been remodeled in the circulation through the action of lipoprotein lipase, more PCSK9 binds lipoproteins and enters the inactive pool. This in turn upregulates LDLR expression, enhancing clearance of IDL and LDL from circulation. This theory is supported by the observation that PCSK9 inhibition lowers IDL and LDL production rates, indicating increased VLDL remnant clearance[211]. An evolutionary role for this mechanism may be envisioned during times of food scarcity, when it may have been advantageous to extend the circulation time of TG-rich lipoproteins to maximize distribution of energy-rich fatty acids to peripheral tissues before clearing the lipoproteins away through the liver. Plasma PCSK9 levels do positively correlate with fasting plasma triglyceride levels[95,102,212,213] and TRL concentrations[214,215]. Our data in human hypertriglyceridemic plasma (PCSK9 shifted to TRL association, **Figure 13**) and hypercholesterolemic plasma (increase in proportion of LDL-associated PCSK9, **Figure 14**) show that the distribution of lipoprotein-bound PCSK9 is sensitive to changes in plasma lipoprotein profiles in circulation. In other words, the affinity of the PCSK9-lipoprotein interaction is such that it allows PCSK9 to respond to changes in plasma IDL/LDL-cholesterol levels. If the affinity was too weak, we would expect that changes in PCSK9 distribution would not be observed.

If the above model is true, it may be asked why hyperlipidemic subjects are not protected from the actions of PCSK9 – their increased concentrations of lipoprotein remnants should sequester more of their PCSK9 in the non-active pool. Lagace posits that this may be explained by the above mechanism being disrupted by a modern diet and constant feeding[94]. Circulating PCSK9 is higher postprandially[103,216], thus constant and easy access to food would lead to chronically elevated PCSK9 levels. PCSK9 levels are also found to be higher in hypercholesterolemia in literature[92],

although the difference between the two groups in our cohort did not become statistically significant. It is difficult to explain why we do not see the expected significant difference in PCSK9 levels. Most of the samples in our hypercholesterolemic group came from individuals with elevated LDL-C, but not yet considered diseased and not on lipid-lowering medication. Thus, they may not exhibit the elevated PCSK9 to the same extent as the previous studies have found.

The interaction with IDL observed in these studies indicate that the downregulation of PCSK9 activity begins in the IDL phase of lipoprotein conversion. Studies in which correlations are found between plasma PCSK9 levels and plasma TRL concentrations also find in sub-analyses that this correlation is specifically with the IDL component of lipoproteins[215], concluding that PCSK9 influences triglyceride levels via effects on IDL metabolism. Indeed, kinetics studies on lipoprotein metabolism report that treatment with PCSK9 inhibitors Alirocumab[217] and Evolocumab[211] increased the fractional clearance rate of VLDL and IDL in addition to increased LDL clearance, contributing to a lower LDL production rate. These effects are likely through PCSK9 effects on the LDLR.

The utility of PCSK9 prolonging the excursion of TRLs in a remodeling-dependent manner may not be limited to fatty acid distribution during starvation; it may even play a role in delivering extra cholesterol to tissues generating steroid hormones, such as the adrenals. In addition, lipoproteins function in innate immune responses to infection, sequestering pathogen-derived toxins such as lipopolysaccharides (LPS). LPS administration increases VLDL and LDL levels[218]. In serum, LPS binds to VLDL and LDL and becomes inactivated[219,220]. PCSK9 has already been linked to innate immunity and sepsis outcomes, where it has been observed to interfere with pathogenic lipid clearance in human cells and in mice in an LDLR-dependent manner[221,222] . PCSK9-mediated control of the population of lipoprotein subclasses in circulation could influence these immune-related functions, e.g. by changing the LPS carrying capacity of the circulating lipoprotein population, or controlling uptake of toxin-carrying lipoproteins into the liver or other tissues.

4.4 Materials and Methods

Lipoprotein isolation

See Chapter 2, section 2.4 – "Lipoprotein isolation" for full procedure. VLDL ($d < 1.006$ g/mL), IDL ($d = 1.006–1.019$ g/mL), LDL ($d = 1.019–1.065$ g/mL) were isolated. Total protein concentrations in lipoprotein preparations were determined using a modified Lowry assay[181], while apoB concentration was determined using a human apoB ELISA specific for apoB100 (Mabtech).

Gel shift of PCSK9 with VLDL, IDL and LDL

3.3 ng/µl of Dylight800 labelled wild-type PCSK9 were incubated with 0.15 µg/µl LDL in 30 µl reactions in low-salt HBSC buffer (25 mM HEPES-KOH, pH 7.4, 75 mM NaCl, 2m M CaCl2) with 1% (w/v) bovine serum albumin for blocking. Binding was allowed to occur at 37°C for 1 hour, after which 18 µl of 4X Ficoll loading dye (10% (w/v) Ficoll400, 0.02% (w/v) bromophenol blue, 90 mM Tris, pH 8.0, 80 mM Borate, 2 mM Calcium lactate) was added to each reaction. 20 µl of each was resolved on a 0.7% agarose gel as described above. Proteins were transferred onto nitrocellulose membranes using a 1 hour upward capillary transfer, and proteins then visualized. Labelled PCSK9 was visualized directly using a LI-COR Odyssey infrared imaging system (LI-COR Biosciences), while apoB was detected by immunoblotting before being detected on the LI-COR scanner.

In vitro ultracentrifugation of PCSK9 with VLDL, IDL and LDL

1 µg of Dylight800 labelled wild-type PCSK9 was incubated with 0.15 µg/µl apoB of VLDL, IDL or LDL, in 0.5 mL reactions with 1% Ovalbumin for blocking, in HBSC (HEPES Buffered Saline-Calcium buffer: 25 mM M HEPES-KOH, pH 7.4, 150 mM NaCl, 2 mM $CaCl_2$). Binding was allowed to occur at 37°C for 1 hour. Lipoproteins and associated PCSK9 were then resolved by Optiprep (iodixanol) gradient ultracentrifugation similar to a modified version of a previously described protocol[182]. Briefly, a 7% Optiprep sample solution was prepared by diluting 0.45 mL of each binding reaction with 0.35 mL of 60% Optiprep and 2.2 mL of buffer (25 mM HEPES, pH 7.4) in a 3.3 mL Beckman Optiseal tube. The sample was overlayed with 0.3 mL 25mM HEPES, pH 7.4. Tubes were centrifuged

in a TLN100 rotor (Beckman Coulter) at 100,000 rpm for 2 hours at 4°C. The gradients were fractionated from top to bottom into 300 µl fractions on a Gilson FC-204 fraction collector, using Fluorinert FC-40 (Sigma) injected into the bottom of the tube to push tube contents up into the fractionator without disturbing the gradient. 20 µl samples of each fraction were resolved on 8% acrylamide by SDS-PAGE and Dylight800 labelled PCSK9 visualized directly in the gel using a LI-COR Odyssey infrared imaging system (LI-COR Biosciences). Cholesterol and triglyceride content of each fraction was measured using the colorimetric, enzymatic plate assay reagents provided in the Cholesterol E kit and the LabAssay Triglyceride kit (Wako Diagnostics).

Human plasma density gradient ultracentrifugation

0.4 mL of plasma was incubated at 37°C for 15 mins, then diluted in 0.35mL 60% Optiprep and 2.4 mL 25 mM HEPES, pH 7.4 (final 7% Optiprep) in a 3.3mL Beckman Optiseal tube and overlayed with 0.3 mL 25 mM HEPES, pH 7.4. Centrifugation and fractionation of gradients were then carried out similar to above. PCSK9 content of each faction was measured by an in-house PCSK9 ELISA using the antibodies 13D3, which recognizes an epitope in the catalytic domain, and 15A6, which recognizes an epitope in the C-terminal, domain as coating to capture PCSK9[15]. Cholesterol and triglyceride content of each fraction was measured using the colorimetric, enzymatic plate assay reagents provided in the Cholesterol E kit and the LabAssay Triglyceride kit (Wako Diagnostics).

Competition binding assay

Binding reactions containing 0.2 µg/µl of LDL-apoB or IDL-apoB, and 20 nM DyLight800-labelled wild-type PCSK9 competed with increasing amounts (upto a 450-fold nM excess) of purified unlabelled wild-type PCSK9 were incubated at 37°C for 1 hour in HBSC (HEPES Buffered Saline-Calcium buffer: 25 mM HEPES-KOH, pH 7.4, 150 mM NaCl, 2 mM CaCl2) and 1% BSA before being resolved on a 0.7% agarose gel (electrode buffer: 90 mM Tris, pH 8.0, 80 mM Borate, 2 mM Calcium lactate) at 40 V for 2 hours. Labelled PCSK9 was then visualized directly in the gel using a LI-COR Odyssey infrared imaging system (LI-COR Biosciences). Intensity data was fit to a sigmoidal one-

site binding curve using Graphpad Prism 5 software to obtain the inhibitor constant (K_i) for each lipoprotein.

Western Blotting

Proteins from agarose gels were transferred to nitrocellulose membranes (BioRad) using upward capillary transfer. Membranes were then immunoblotted for apoB using the primary mouse antibody 1D1. Secondary infrared dye (IRDye800)-labeled antibodies were used for detection on a LI-COR Odyssey infrared imaging system (LI-COR Biosciences).

PCSK9 ELISA

In-house ELISA. PCSK9 was captured using a mixture of two mouse antihuman monoclonal antibodies: 13D3, which recognizes the catalytic domain, and 15A6, which recognizes the carboxyl terminus of PCSK9[15]. Each antibody was diluted in coating buffer (20 mM NaPO4 (pH 7.5), 100 mM NaCl) to a final concentration of 10 μg/mL and attached to Nunc Maxisorp plates overnight at 4°C. Wells were washed three times with PBS containing 0.08% Tween 20 (pH 7.4) (PBST), blocked with 0.5% BSA for 1–2 hours, and then washed again three times with PBST. Density gradient fractions samples were diluted 1:5 and 100 μl added to each well. At the end of the incubation, the wells were washed three times in PBST. The biotinylated in-house polyclonal antibody 1697, raised against full-length PCSK9, was used as detection antibody (10 μg/mL), followed by horseradish peroxidase-conjugated avidin and then 100 μl per well of Thermo Scientific Pierce 1-Step Ultra TMB ELISA Substrate. Reactions were stopped with 1 M sulfuric acid and absorbances read at 450 nm.

Circulex human PCSK9 ELISA. Commercial kit available from MBL International. Plasma samples were thawed at room temperature and used at a 1:100 dilution (100 μl / well).

Chapter 5: Tools for future in vivo studies: preliminary tests

5.1 Introduction

The next natural step to follow our in vitro work in the previous chapters is to make observations in vivo on whether LDL-binding would negatively regulate PCSK9-mediated LDLR degradation in the circulation. In the future, we hope to be able to utilize animal models to study both the long-term ("knock-in models of non-LDL binding PCSK9) and short-term (acute PCSK9 injection or infusion) effects of PCSK9-lipoprotein association in vivo (more details in Chapter 6). While mice have very different natural lipoprotein profiles from humans, genetically engineered mouse models would be a convenient starting point for such studies. Described in this chapter are some preliminary tests that were carried out towards validating tools that would be suitable for these studies. An important feature of these experiments will need to be the use of functional variants of PCSK9 that lack LDL binding but can still mediate normal degradation of LDLR as controls. These controls will allow correct interpretation of LDL-mediated effects vs. LDLR-mediated effects on PCSK9. Since such non-LDL binding human PCSK9 variants have already been characterized for normal LDLR binding in our lab, we decided to test the ability of our purified recombinant human PCSK9 to bind endogenous lipoproteins in mouse plasma. If the hPCSK9 can associate with the lipoproteins in mouse plasma similar to what we see in human plasma, then our purified recombinant hPCSK9 may be used in future acute injection studies. The results of these tests are presented in the chapter.

Non-LDL binding mouse PCSK9 variants will still need to be characterized for long-term knock-in model creations, and even ideally for injection or infusion in acute studies. Since mice are the most common and available study tool of choice, it would also be interesting to characterize parallels in structure-function features between human and mouse PCSK9. This chapter will present mutagenesis and in-vivo LDL-binding results that will explore this as well.

5.2 Results

In order to test binding of our purified recombinant human PCSK9 with endogenous mouse lipoproteins, plasma from 9 week-old female mice, either chow-fed wild-type or 4-weeks western diet-fed *apoE-/-*, was incubated with infrared dye-labelled recombinant human PCSK9, and then subjected to density gradient centrifugation. Gradients were fractionated from lightest to heaviest densities and presence of PCSK9 in each fraction detected by SDS-PAGE and in-gel IR-dye detection on a Licor scanner. A modestly higher amount of PCSK9 was present in lighter-density fractions for *apoE-/-* plasma than for wild type, indicating increased floatation of PCSK9 into fractions with more triglyceride-rich lipoproteins **(Figure 16A)**. The PCSK9 distribution somewhat mirrored the cholesterol distribution in the gradient, which in turn is indicative of the lipoprotein distribution.

Similar incubations of hyperlipidemic *apoE-/-* plasma were carried out with non-labelled recombinant human wild-type or A44P-mutant PCSK9, which was previously found to be defective for human LDL binding, but normally mediated LDLR degradation (unpublished, see Appendix C, Figure C1 and Figure C4). After density gradient ultracentrifugation and fractionation, human PCSK9 present in fractions was detected by an in-house human-specific ELISA. More wild-type PCSK9 than A44P-PCSK9 was present in lighter fractions, indicating specificity in the floatation of PCSK9 with the increased lipoprotein containing fractions **(Figure 16B)**. The pattern of wild-type PCSK9 flotation again mirrored the floatation pattern of cholesterol in the gradient, measured to monitor lipoprotein distribution.

The above results seem to indicate that in hyperlipidemic *apoE-/-* plasma, some association of hPCSK9 can occur. Thus in hypercholesterolemic plasma where PCSK9-LDL association would be

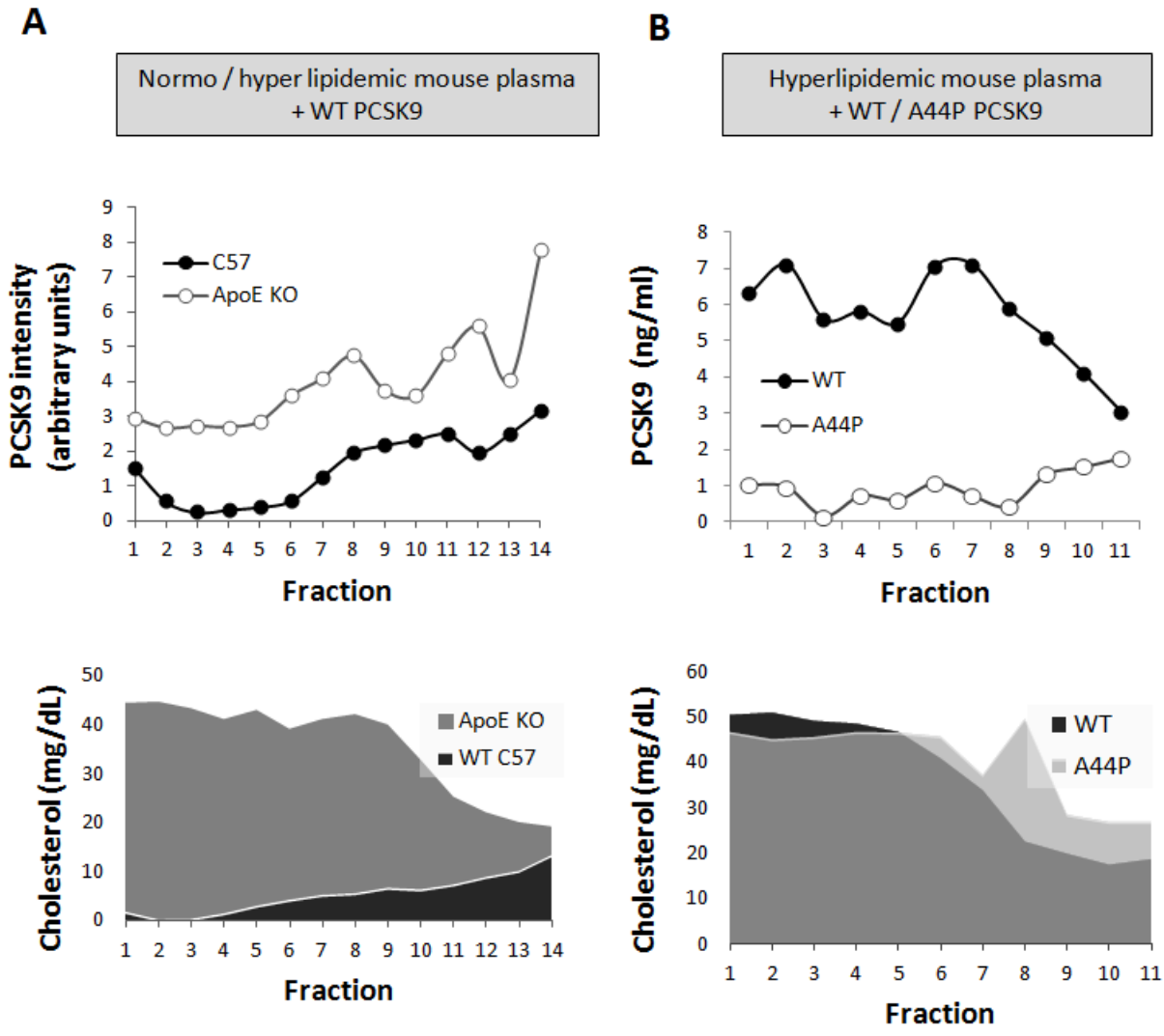

Figure 16: Test for recombinant human PCSK9 associating with mouse lipoproteins. (A) Plasma from chow fed wild-type C57 mice or from western-diet fed *apoE-/-* mice was incubated with IR-dye labelled purified recombinant human PCSK9, then subjected to density gradient centrifugation. Gradient fractions analyzed for PCSK9 content using SDS-PAGE and detection on a Licor scanner, while fractions were analyzed for cholesterol content by enzymatic colorimetric plate assay. **(B)** Western diet-fed *apoE-/-* mouse plasma was incubated with either purified recombinant wild-type PCSK9 or LDL-non-binding A44P-PCSK9, and then subjected to density gradient centrifugation. Gradient fractions analyzed for PCSK9 content by ELISA, and for cholesterol content by enzymatic colorimetric plate assay.

high, it would be expected that differences may be observed in the rate of acute LDLR-mediated clearance of PCSK9 due to LDL binding. Specifically, since we hypothesize from Chapter 2 that LDL-bound PCSK9 would have a lower affinity for LDLR, we would expect lower LDLR-mediated acute PCSK9 clearance from blood. Circulating PCSK9 has a fast LDLR-dependent clearance phase with a half-life of ~5 minutes, and previous studies have shown >90% removal of a 4 μg injection of purified human PCSK9 into mouse circulation[16]. However, in a small pilot test where we retro-orbitally injected one mouse each (either 4 weeks western diet-fed *apoE-/-* or chow-fed wild-type C57BL/6), with 4 μg exogenous purified wild-type or A44P-hPCSK9, we observed no difference in their acute clearance from circulation over a 20 minute time-course either between wild-type or mutant PCSK9, or between normo- or hyperlipidemic plasma **(Figure 17)**.

Equivalents of non-LDL binding mutations in humans were also created in mouse PCSK9 by site-directed mutagenesis. These were tested for binding to isolated human LDL in vitro. Previously, our lab had tested the binding of purified recombinant wild-type mouse PCSK9 to human LDL in vitro (unpublished, presented previously in Master's thesis) and found that it bound comparably to wild-type human PCSK9. Thus, the mouse-PCSK9 – human LDL interaction may be used as a valid in vitro assay of relative LDL binding. The mutations made in mouse PCSK9 (mA47P, mL44P, mS130R and mD132G; suffix "m" for mouse) were chosen based on the observed regional requirements of human PCSK9 binding to LDL, i.e., the N-terminal region from Chapter 2 and the "GOF region" from Chapter 3. Thus, mA47P, the sequence equivalent of human A44P, and mL44P, the sequence equivalent of human L41P, both non-LDL binding mutants (unpublished, presented previously in Master's thesis), would represent helix-disrupting proline residues in the N-terminal disordered region of the prodomain. Similarly, mS130R and mD132G would be the equivalents of human S127R and D129G, both natural variants associated with severe hypercholesterolemia in human subjects. These mutant constructs were expressed in HEK293 cells and the conditioned media used in in vitro density gradient centrifugation LDL-binding assays. It was found that similar to the

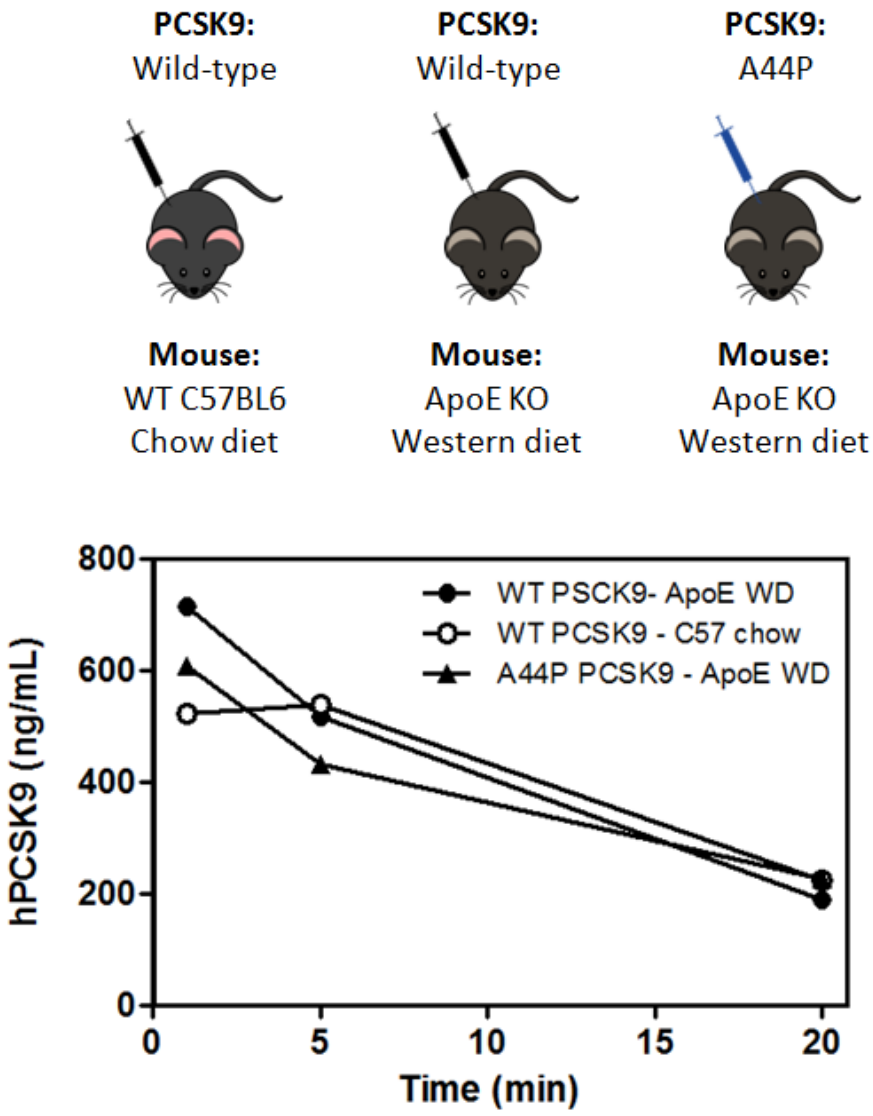

Figure 17: Pilot test of mice injected with exogenous PCSK9 to observe lipoprotein-mediated differences in acute PCSK9 clearance. One mouse each was injected with 4µg purified recombinant human wild-type or A44P-PCSK9 as indicated in the schematic above. Blood samples were collected at indicated time-points after injection (injection = 0 minutes) by submandibular lancet punctures, and PCSK9 in the plasma detected by ELISA. WD = Western Diet.

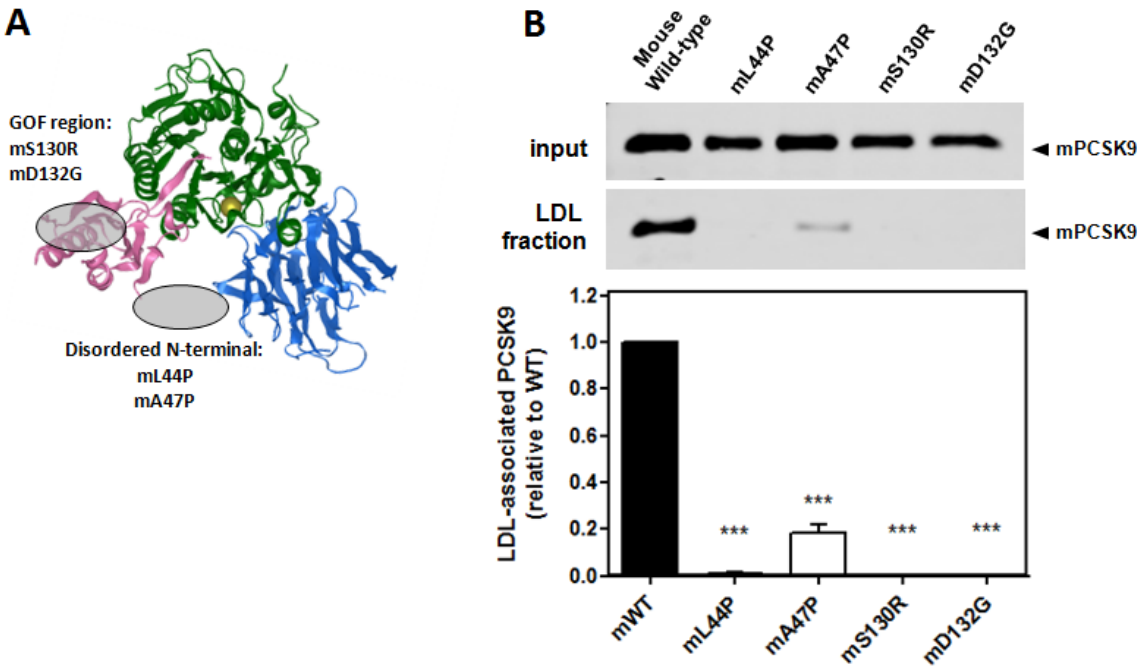

Figure 18: Mutations in mouse PCSK9 which parallel mutations in human PCSK9 also cause loss of LDL binding. (A) Crystal structure of human PCSK9 where prodomain is pink, catalytic domain is green, and C-terminal domain is blue. Greyed areas indicate regions of importance in human LDL binding where the parallel mutations in mouse PCSK9 would also be located. **(B)** In-vitro binding reactions of wild-type or mutant mouse PCSK9 + isolated human LDL were centrifuged in iodixanol gradients to separate LDL-bound and non-bound PCSK9. PCSK9 in the LDL-containing fraction was detected by western blotting. Quantification shown in graph, where the mean of n=3 with standard error is plotted. ***p≤0.001 by one way ANOVA followed by Dunnet's post test.

equivalent human mutants, these mutations in mouse PCSK9 abolished LDL binding, although the mA47P did not lose LDL binding as fully as the others, which again parallels results in human PCSK9 **(Figure 18)**.

5.3 Discussion

The experiments in this chapter set out to evaluate a model system to study the PCSK9-LDL interaction in vivo. This system consisted of injecting human PCSK9 into hyperlipidemic *apoE-/-* mice. We chose this system for initial tests because we already have in our lab characterized non-LDL binding human PCSK9 point mutants for their LDLR binding and degradation, and can thus use them as important negative controls. Also, *apoE-/-* mice are commonly used as models for hypercholesterolemia and atherosclerosis. Hypercholesterolemia is easily induced in these mice when fed an atherogenic diet, leading to large increases in plasma cholesterol, increases in VLDL and LDL, and decreases in HDL[223].

However, the above hPCSK9-*apoE-/-* mouse system is not exactly ideal for several reasons. The biochemistry of hPCSK9 interacting with mouse lipoproteins is not characterized, although both PCSK9 and apoB100 do share high sequence similarity between mouse and human. It is also not known if PCSK9 binds to apoB48. Mice secrete both apoB48 and apoB100 in liver, in contrast to humans, where apoB editing to B48 is limited to the intestine[224]. Such metabolic discrepancies would need to be addressed with transgenic mouse models that have liver-specific apoB100 expression or are apobec-1 knock-outs. Additionally, *apoE-/-* mice on an atherogenic diet experience greatest increases in the VLDL fraction of their lipoproteins, with lower increases in their IDL and LDL fractions[223]. As seen in Chapter 4, PCSK9 association mainly occurs with IDL and LDL, not with VLDL. Thus, a VLDL-enriched circulating lipoprotein population is not ideal to observe LDL-mediated PCSK9 regulation. In using this mouse model, it was hoped that the induced increases in IDL and LDL would be sufficient to mediate physiologically relevant PCSK9-lipoprotein

interaction. While our initial results in vitro suggested that this may be the case **(Figure 16)**, these results were not borne out on a small scale in vivo **(Figure 17)**.

The negative results of the pilot injection experiment underscore the importance of considering several factors in study design. As already discussed, this was not overall an ideal study system, and the hPCSK9-LDL interaction may not have been robust or prevalent enough to mediate observable differences in PCSK9 clearance. Although the human PCSK9 interaction with the mouse LDLR has also not been characterized, previous studies have observed normal clearance of exogenously administered human PCSK9 from mouse circulation[15,16]. As well, a time-point between 5 and 20 minutes may have allowed better resolution of small differences in clearance before reaching the end of the fast clearance phase. Overall, this was a very preliminary experiment done on a very small scale to indicate whether it was possible to use this system for our purposes, and the indication obtained was that it is not.

Thus, the move to a more ideal study system should be made for future studies. Transgenic mouse models that express both human CETP and human apoB100 would most closely mimic human lipoprotein profiles[225] and ensure comparable interactions with exogenously administered human PCSK9. Additionally, for long term studies where life-long effects of non-LDL binding PCSK9 would be observed in transgenic mice, non-LDL binding mutants in mPCSK9 must be made. To this end, we tested the LDL binding capacity of several mPCSK9 mutants that represent equivalent non-LDL binding mutants in human PCSK9. Not surprisingly, these mouse PCSK9 mutants mirror the human PCSK9 versions in their capacity to bind LDL **(Figure 18)**. This serves as evidence for parallels in the structure-function features of mouse and human PCSK9, supporting the use of mouse models for the study of PCSK9 physiology. More specifically, it indicates that regions important to hPCSK9-LDL binding function similarly in mPCSK9, i.e. the helix-forming N-terminal from Chapter 2 and the "GOF region" from Chapter 3 play roles in mouse PCSK9 binding to LDL as well. This makes for interesting speculation on the physiological and evolutionary role of PCSK9 in animals such as mice,

which do not naturally carry much of their blood cholesterol in LDL, and would thus probably lack any significant LDL-mediated feedback regulation of PCSK9 activity. The PCSK9 function suggested in Chapter 4, where PCSK9 down-regulates LDLRs to extend TRL excursion and maximize peripheral fatty acid distribution, may still hold in these animals.

More importantly, these non-LDL binding mouse PCSK9 mutants can now be further characterized for their LDLR binding and degradation in hepatic mouse cell lines, for future use as negative controls in in vivo studies.

5.4 Materials and Methods

Density gradient ultracentrifugation of mouse plasma

Plasma from wild-type C57BL/6 or *apoE-/-* mice was previously collected by cardiac puncture and stored at -80 °C. This plasma was thawed at room temperature, then 0.4 mL incubated with 1 μg purified recombinant human PCSK9 (1 μl of purified protein spiked directly into the plasma) at 37°C for 1 hour. The incubations were then diluted then diluted in 0.35 mL of 60% Optiprep and 2.4 mL of 25 mM HEPES, pH 7.4 (final 7% Optiprep) in a 3.3 mL Beckman Optiseal tube and overlayed with 0.3 mL 25 mM HEPES, pH 7.4. Tubes were centrifuged in a TLN100 rotor (Beckman Coulter) at 100,000 rpm for 2 hours at 4°C. The gradients were fractionated from top to bottom into 300 μl fractions on a Gilson FC-204 fraction collector, using Fluorinert FC-40 (Sigma) injected into the bottom of the tube to gently push tube contents up into the fractionator without disturbing the gradient. Cholesterol content of each fraction was measured using the colorimetric, enzymatic plate assay reagents provided in the Cholesterol E kit and the LabAssay Triglyceride kit (Wako Diagnostics). PCSK9 content in fraction was determined either by ELISA of by SDS-PAGE, where 23 μl of each fraction was resolved on an acrylamide gel and Dylight 800-labeled PCSK9 was detected directly in the gel on a Licor scanner and quantified using Odyssey software.

PCSK9 injections in mice

Female wild-type C57BL/6 mice (Charles River) were fed chow diets or *apoE-/-* mice were fed a western diet (Envigo TD.88137, Teklad) for 4 weeks prior to the experiment. At 12 weeks age, the mice anaesthetized under isofluorane and were then retro-orbitally injected[226] with either 100 µl phosphate buffered saline or 4 µg purified recombinant human PCSK9-FLAG protein, either wild-type or A44P mutant, diluted in final 100 µl phosphate buffered saline. Mice were then allowed to regain consciousness and the method of submandibular bleeding using lancet punctures[227] was used to collect blood into Microvette CB 300 µl K2 EDTA tubes (Sarstedt) at 1, 5 and 20 minute time-points after injection at 0 minutes. Collected blood samples were kept on ice until the end of the time-course, at which point they were centrifuged at 4°C at 3500 x g for 20 minutes to obtain cleared plasma. Plasma was collected and stored at -80 °C until thawed for human PCSK9 detection by ELISA.

PCSK9 ELISA

See "*In-house ELISA"* in Chapter 4, Section 4.4.

In vitro PCSK9-LDL binding assay

See "In vitro PCSK9-LDL binding assay" in Chapter 2, Section 2.4.

Chapter 6: Conclusions and Future Study Directions

This dissertation set out to shed light on two broad aspects of the PCSK9 interaction with lipoproteins: the structural details of the physical interaction, and the functional effects that this interaction may have on PCSK9 in the circulation. Elucidation of the exact PCSK9-LDL binding site and the full regulating mechanism that it triggers still require further studies. However, from the current studies, some interesting information can be extracted on the following topics:

6.1 An allosteric mechanism for the regulation of PCSK9 by LDL

Chapter 2 describes the discovery that PCSK9 can undergo an environment-dependent structural shift in its N-terminus, and discusses how this may trigger global structural shifts in the PCSK9 protein that alter its affinity for the LDLR EGF-A domain. Evidence in cell culture suggests that LDL binding keeps PCSK9 in an inactive state[158]. Thus the idea that an inducible conformation change in the prodomain could mimic the inhibitory effects on PCSK9 presents the possibility of a new target on PCSK9 to design cholesterol-lowering drugs. Elucidation of the structure-function role of LDL-binding will provide us with more knowledge of the different active or inactive states of PCSK9, and which target to design small molecules against to favor an inhibited conformation of PCSK9. Future structural studies using techniques such as nuclear magnetic resonance (NMR) and X-ray crystallography are needed to definitively observe these alternate conformations. Desirable experiments to perform would be NMR of the entire disordered region or the entire prodomain of PCSK9 in the presence and absence of micelles or LDL. It would be ideal to obtain complete X-ray crystal structures of PCSK9 in the presence of lipoproteins or lipid mimetics, to compare with existing structures of PCSK9 crystallized in aqueous conditions and bound to the LDLR EGF-A domain[56,58,59].

6.2 The protein-protein binding interface between PCSK9 and apoB

While much attention in this dissertation focuses on the PCSK9 prodomain N-terminal and how it modulates LDL-binding, no evidence to date confirms that that is the site of physical binding between PCSK9 and the apoB moiety on lipoproteins. Chapter 3 investigated an alternate candidate for an apoB binding site, referred to herein as the "GOF region", also located on the prodomain and implicated in hereditary hypercholesterolemia. This site proved to be highly sensitive to mutations of any kind, either charge-disrupting or changing the side-chain size, indicating that the native residues in that area fulfill some critical role in LDL-binding. The GOF region is located on a loop within a section of the PCSK9 prodomain which is not normally present in other PCs due to the second cleavage event that occurs in the maturation process of most PCs. It is due to this region that PCSK9 retains its prodomain in its mature form. It is interesting that this section is preserved on PCSK9 alone. Its importance in LDL binding adds a further functional significance to it.

However, there is still no proof to definitively show the GOF region is the site of interaction with apoB. Such proof will need to come from cross-linking experiments followed by mass-spectrometry to identify the sequence of amino acids that interact on each protein. These experiments have been difficult to perform given the difficult nature of the apoB100 protein in terms of its very large size and high hydrophobicity. Attempts at these experiments in our own lab have encountered problems with obtaining specific PCSK9-apoB cross-linking in comparison to non-LDL binding controls and minimizing apoB cross-linking within itself. Another approach may be to generate PCSK9 engineered to contain unnatural amino acids that form covalent bonds to other proteins in proximity under triggering conditions such as exposure to UV light.

Elucidation of the binding site will provide additional information as to which conformation or exposure level of apoB on different classes of lipoproteins lead to sequestering PCSK9 in lipoprotein-bound pools. Additionally, it will further inform development of new PCSK9 inhibitors.

6.3 PCSK9-lipid interactions

We showed in Chapter 2 that lipidic environments modulate the structural change in the PCSK9 N-terminal domain. However, we were not able to obtain a clear answer as to whether PCSK9 binds to lipid structures or is merely induced to conformationally change in proximity to lipids. Future studies may wish to examine this, as well as whether different lipid species or ratios, free cholesterol content or surface curvature affects PCSK9-lipoprotein interactions. Several methods exist to study lipid-protein binding, including lipid affinity bead pulldown[228,229], lipid overlay assays[230], liposome binding assays[231,232] and surface plasmon resonance. SPR would be especially suitable for obtaining quantitative binding affinity data using immobilized liposomes or micelles. Liposome binding assays employing simple pelleting of the liposomes by centrifugation, along with bound proteins[232], are the simplest and quickest way of assessing lipid association. However, our work using this technique did encounter problems assessing specificity of the interaction, as discussed in Section 2.3. Thus, it may be desirable to try different methods. Another interesting approach may be to assess PCSK9-lipoprotein binding with lipoproteins treated with Methyl-β-cyclodextrins[233] to deplete cholesterol content, or lipoproteins treated with lipoprotein lipase to modulate core triglyceride content.

6.4 A negative feedback loop to regulate PCSK9 activity in circulation

As demonstrated in Chapter 4, PCSK9 can bind not only to LDL but also to more TG-rich lipoproteins in the IDL range, while binding to VLDL is barely detectable. This remodeling-dependent association of PCSK9 with lipoproteins affects lipoprotein-bound pools of PCSK9 in the circulation, and may act as a negative feedback mechanism that limited PCSK9 activity only in late postprandial stages in an evolutionary setting of low-nutrient periods of starvation. This feedback control of PCSK9 activity could even serve to monitor lipolysis or lipid transfer of apoB100-containing lipoproteins. However, in humans, modern dietary conditions potentially create a situation where plasma LDL levels are determined more by hepatic clearance than by generation

from dietary input. In this case, PCSK9 function promotes an expanded LDL pool size that contributes to coronary heart disease in the expanded lifespan of modern humans. The physiological significance of the PCSK9-lipoprotein interaction could be investigated in future studies by comparing lipoprotein-bound PCSK9 distribution in fasted vs. postprandial plasma samples, and in long-term animal models. Understanding how lipoproteins regulate and modulate PCSK9 activity in circulation will hold implications both for PCSK9-inhibiting drug design as well as for personalized medicine – individuals with differing PCSK9 activities due to differing lipoprotein profiles may benefit from more tailored therapeutic prescriptions for hypercholesterolemia.

6.5 In vivo studies of the PCSK9-lipoprotein interaction

No studies have been done in vivo to specifically study the physiological effects of the PCSK9 interaction with LDL. Thus, important future studies to undertake are the evaluation of acute and long term effects of the PCSK9-LDL interaction on PCSK9 clearance and hepatic LDLR expression, most probably in mice. Specifically, injection or infusion studies delivering an acute bolus of PCSK9 into hypercholesterolemic circulation would allow measurement of the rate of PCSK9 clearance as well as the extent of hepatic LDLR degradation in the presence of elevated LDL in the short term. These studies must be controlled with non-LDL binding PCSK9 which remains functional in terms of LDLR degradation, to separate the effects of the LDLR interaction on PCSK9. As well, the creation of genetically modified "knock-in" mice endogenously expressing such non-LDL binding PCSK9 would allow the study of life-long effects of the absence of PCSK9 regulation by circulating lipoproteins. Various parameters in these animals could be measured to assess the long-term physiological consequences of non-LDL regulated PCSK9, such as circulating PCSK9 and lipoprotein levels, hepatic LDLR, and histological comparisons of atherosclerotic development on chow vs. atherogenic diet. Our preliminary tests using *apoE-/-* mice in Chapter 4 indicate that choice of mouse model should be taken into careful consideration, to maximize the human

representativeness of the lipoprotein profile. As well, the biochemistry of human PCSK9 interacting with mouse lipoproteins must be taken into further account.

While evaluating different mouse models for use in these studies, it may be investigated whether mice are the best animal model to use at all. Two important aspects to consider are: (1) whether the lipoprotein profiles and metabolism of that model are comparable to humans, and (2) whether PCSK9 sequence, structure and function shows significant homology to humans in that model. Past knock-down and knock-out studies in zebrafish and mice suggest that PCSK9 may function differently in mammals vs. non-mammals[234]. Mice are the most common animal model used to study mammalian biology. However, the lipoprotein profiles of mice differ fundamentally from humans. Mice produce apoB48-lipoproteins from both liver and intestine, in contrast to humans where apoB editing to produce B48 is restricted to the intestine[224]. Mice also lack CETP, thus they normally have HDL as the predominant circulating lipoprotein[235], in contrast to humans that predominantly have LDL. Primate models such as African green monkeys and rhesus monkeys have the most human-representative lipoprotein profiles[236]. However, more appropriate for preliminary pre-clinical studies would be small animals such as hamster or rabbit on high cholesterol diet, which show significant proportions of LDL in their circulating lipoproteins[236]. Hamsters are considered useful hypercholesterolemia models because they have CETP activity, the majority of their LDL-C is cleared through the LDLR, and apoB48 is produced from the intestine, while the liver produces B100[237]. More recently there have been suggestions that hamsters are not good at developing atherosclerotic lesions[237], however, for preliminary PCSK9-LDL interaction studies, the development of an appropriately atherogenic lipoprotein profile should be sufficient. Rabbits are considered appropriate hypercholesterolemia models for reasons similar to hamsters[238]. Rabbits also have specifically apoB100-producing livers[239]. Transgenic rabbit models expressing human apoB100 exist[240]. Guinea pigs are also a good candidate, as they carry the majority of their cholesterol in LDL and have CETP and LP activity, resulting in lipoprotein delipidation cascades

similar to humans[241]. Pigs are another animal model used for atherosclerotic research. However, these would be larger animal models and may be more useful in lesion-observing studies where anatomical similarities to humans in terms of size and vasculature may be more important. A summary of sequence similarity between PCSK9 and apoB100 of these species of interest is presented in Table 1.

Table 1: Sequence identity matching of human PCSK9 and apoB100 protein sequences to various species

	PCSK9		ApoB	
	Uniprot ID	**% human sequence identity**	**Uniprot ID**	**% human sequence identity**
Rhesus Monkey	A8T666	96.4	G7N9H7	85.1
Pig	13LGB2	79.7	F1SCV9	76.6
Rat	P59996	77.3	F1M6Z1	69.2
Mouse	Q80W65	77.0	E9Q414	69.7
Guinea pig	G3GTK5	74.9	H0V4A3	70.4
Chinese hamster	H0VTV9	75.9	G3GZQ0	68.1

6.6 Conclusion

The PCSK9-LDL interaction is still a relatively unexplored aspect of lipoprotein biology. It holds great potential for development of hypercholesterolemia therapeutics. It may also hold the key to answering basic questions about PCSK9 biology, such as why SREBP2-mediated up-regulation of both LDLR and PCSK9 appears to make a futile cycle of LDLR production and degradation, and whether there is more to the picture. Thus, this area calls for further study and understanding.

This thesis has provided new molecular detail on the PCSK9–LDL interaction, providing evidence through gain-of-function mutation studies that it is inhibitory and sensitive to lipoprotein remodeling in the post-prandial period, suggesting an evolutionary role. While this mechanism may be dysregulated in a modern diet, further understanding of the mechanism whereby LDL inhibits PCSK9 activity could lead to novel small molecule therapeutic approaches.

References

1. Seidah NG, Benjannet S, Wickham L, Marcinkiewicz J, Jasmin SB, Stifani S, Basak A, Prat A, Chretien M. The secretory proprotein convertase neural apoptosis-regulated convertase 1 (NARC-1): liver regeneration and neuronal differentiation. Proceedings of the National Academy of Sciences of the United States of America 2003;100(3):928-933.
2. Sabatine MS, Giugliano RP, Keech AC, Honarpour N, Wiviott SD, Murphy SA, Kuder JF, Wang H, Liu T, Wasserman SM and others. Evolocumab and Clinical Outcomes in Patients with Cardiovascular Disease. N Engl J Med 2017;376(18):1713-1722.
3. Schwartz GG, Steg PG, Szarek M, Bhatt DL, Bittner VA, Diaz R, Edelberg JM, Goodman SG, Hanotin C, Harrington RA and others. Alirocumab and Cardiovascular Outcomes after Acute Coronary Syndrome. N Engl J Med 2018;379(22):2097-2107.
4. Tabas I, Williams KJ, Boren J. Subendothelial lipoprotein retention as the initiating process in atherosclerosis: update and therapeutic implications. Circulation 2007;116(16):1832-1844.
5. Schwenke DC, Carew TE. Initiation of atherosclerotic lesions in cholesterol-fed rabbits. II. Selective retention of LDL vs. selective increases in LDL permeability in susceptible sites of arteries. Arteriosclerosis 1989;9(6):908-18.
6. Mundi S, Massaro M, Scoditti E, Carluccio MA, van Hinsbergh VWM, Iruela-Arispe ML, De Caterina R. Endothelial permeability, LDL deposition, and cardiovascular risk factors-a review. Cardiovasc Res 2018;114(1):35-52.
7. Boren J, Olin K, Lee I, Chait A, Wight TN, Innerarity TL. Identification of the principal proteoglycan-binding site in LDL. A single-point mutation in apo-B100 severely affects proteoglycan interaction without affecting LDL receptor binding. J Clin Invest 1998;101(12):2658-64.
8. Flood C, Gustafsson M, Richardson PE, Harvey SC, Segrest JP, Boren J. Identification of the proteoglycan binding site in apolipoprotein B48. J Biol Chem 2002;277(35):32228-33.
9. Williams KJ, Tabas I. The response-to-retention hypothesis of early atherogenesis. Arteriosclerosis, Thrombosis, and Vascular Biology 1995;15(5):551-561.
10. Williams KJ, Tabas I. The response-to-retention hypothesis of atherogenesis reinforced. Current opinion in lipidology 1998;9(5):471-474.
11. Berberich AJ, Hegele RA. The complex molecular genetics of familial hypercholesterolaemia. Nat Rev Cardiol 2019;16(1):9-20.
12. Harada-Shiba M, Takagi A, Miyamoto Y, Tsushima M, Ikeda Y, Yokoyama S, Yamamoto A. Clinical features and genetic analysis of autosomal recessive hypercholesterolemia. J Clin Endocrinol Metab 2003;88(6):2541-7.
13. Goldstein JL, Brown MS. The LDL receptor. Arteriosclerosis, Thrombosis, and Vascular Biology 2009;29(4):431-438.
14. Ramasamy I. Recent advances in physiological lipoprotein metabolism. Clinical chemistry and laboratory medicine : CCLM / FESCC 2014;52(12):1695-1727.
15. Lagace TA, Curtis DE, Garuti R, McNutt MC, Park SW, Prather HB, Anderson NN, Ho YK, Hammer RE, Horton JD. Secreted PCSK9 decreases the number of LDL receptors in hepatocytes and in livers of parabiotic mice. The Journal of clinical investigation 2006;116(11):2995-3005.
16. Grefhorst A, McNutt MC, Lagace TA, Horton JD. Plasma PCSK9 preferentially reduces liver LDL receptors in mice. Journal of lipid research 2008;49(6):1303-1311.
17. Benjannet S, Rhainds D, Essalmani R, Mayne J, Wickham L, Jin W, Asselin MC, Hamelin J, Varret M, Allard D and others. NARC-1/PCSK9 and its natural mutants: zymogen cleavage

and effects on the low density lipoprotein (LDL) receptor and LDL cholesterol. The Journal of biological chemistry 2004;279(47):48865-48875.
18. Abifadel M, Rabes JP, Devillers M, Munnich A, Erlich D, Junien C, Varret M, Boileau C. Mutations and polymorphisms in the proprotein convertase subtilisin kexin 9 (PCSK9) gene in cholesterol metabolism and disease. Hum Mutat 2009;30(4):520-9.
19. Cohen J, PertsemLidis A, Kotowski IK, Graham R, Garcia CK, Hobbs HH. Low LDL cholesterol in individuals of African descent resulting from frequent nonsense mutations in PCSK9. Nature genetics 2005;37(2):161-165.
20. Cohen JC, Boerwinkle E, Mosley TH, Hobbs HH. Sequence Variations in PCSK9, Low LDL, and Protection against Coronary Heart Disease. N Engl J Med 2006;354(12):1264-1272.
21. Zhao Z, Tuakli-Wosornu Y, Lagace TA, Kinch L, Grishin NV, Horton JD, Cohen JC, Hobbs HH. Molecular characterization of loss-of-function mutations in PCSK9 and identification of a compound heterozygote. American Journal of Human Genetics 2006;79(3):514-523.
22. Hooper AJ, Marais AD, Tanyanyiwa DM, Burnett JR. The C679X mutation in PCSK9 is present and lowers blood cholesterol in a Southern African population. Atherosclerosis 2007;193(2):445-448.
23. Sirtori CR. The pharmacology of statins. Pharmacol Res 2014;88:3-11.
24. Elley CR. ACP Journal Club. Review: Statins reduce mortality and major vascular events in patients with no history of CV disease. Ann Intern Med 2013;159(2):Jc2.
25. Taylor F, Huffman MD, Macedo AF, Moore TH, Burke M, Davey Smith G, Ward K, Ebrahim S. Statins for the primary prevention of cardiovascular disease. Cochrane Database Syst Rev 2013(1):Cd004816.
26. Ridker PM, Pradhan A, MacFadyen JG, Libby P, Glynn RJ. Cardiovascular benefits and diabetes risks of statin therapy in primary prevention: an analysis from the JUPITER trial. Lancet 2012;380(9841):565-71.
27. Reiner Z. Resistance and intolerance to statins. Nutr Metab Cardiovasc Dis 2014;24(10):1057-66.
28. Melendez QM, Krishnaji ST, Wooten CJ, Lopez D. Hypercholesterolemia: The role of PCSK9. Arch Biochem Biophys 2017;625-626:39-53.
29. Yadav K, Sharma M, Ferdinand KC. Proprotein convertase subtilisin/kexin type 9 (PCSK9) inhibitors: Present perspectives and future horizons. Nutr Metab Cardiovasc Dis 2016;26(10):853-62.
30. Robinson JG, Farnier M, Krempf M, Bergeron J, Luc G, Averna M, Stroes ES, Langslet G, Raal FJ, El Shahawy M and others. Efficacy and safety of alirocumab in reducing lipids and cardiovascular events. N Engl J Med 2015;372(16):1489-99.
31. Kazi DS, Moran AE, Coxson PG, Penko J, Ollendorf DA, Pearson SD, Tice JA, Guzman D, Bibbins-Domingo K. Cost-effectiveness of PCSK9 Inhibitor Therapy in Patients With Heterozygous Familial Hypercholesterolemia or Atherosclerotic Cardiovascular Disease. Jama 2016;316(7):743-53.
32. Glassman PM, Abuqayyas L, Balthasar JP. Assessments of antibody biodistribution. J Clin Pharmacol 2015;55 Suppl 3:S29-38.
33. Weider E, Susan-Resiga D, Essalmani R, Hamelin J, Asselin MC, Nimesh S, Ashraf Y, Wycoff KL, Zhang J, Prat A and others. Proprotein Convertase Subtilisin/Kexin Type 9 (PCSK9) Single Domain Antibodies Are Potent Inhibitors of Low Density Lipoprotein Receptor Degradation. J Biol Chem 2016;291(32):16659-71.
34. Fitzgerald K, White S, Borodovsky A, Bettencourt BR, Strahs A, Clausen V, Wijngaard P, Horton JD, Taubel J, Brooks A and others. A Highly Durable RNAi Therapeutic Inhibitor of PCSK9. N Engl J Med 2017;376(1):41-51.

35. Ray KK, Landmesser U, Leiter LA, Kallend D, Dufour R, Karakas M, Hall T, Troquay RP, Turner T, Visseren FL and others. Inclisiran in Patients at High Cardiovascular Risk with Elevated LDL Cholesterol. N Engl J Med 2017;376(15):1430-1440.
36. Stein EA, Kasichayanula S, Turner T, Kranz T, Arumugam U, Biernat L, Lee J. LDL CHOLESTEROL REDUCTION WITH BMS-962476, AN ADNECTIN INHIBITOR OF PCSK9: RESULTS OF A SINGLE ASCENDING DOSE STUDY. Journal of the American College of Cardiology 2014;63(12, Supplement):A1372.
37. Schulz R, Schlüter K-D. PCSK9 targets important for lipid metabolism. Clinical Research in Cardiology Supplements 2017;12(Suppl 1):2-11.
38. Landlinger C, Pouwer MG, Juno C, van der Hoorn JWA, Pieterman EJ, Jukema JW, Staffler G, Princen HMG, Galabova G. The AT04A vaccine against proprotein convertase subtilisin/kexin type 9 reduces total cholesterol, vascular inflammation, and atherosclerosis in APOE*3Leiden.CETP mice. Eur Heart J 2017;38(32):2499-2507.
39. Pan Y, Zhou Y, Wu H, Chen X, Hu X, Zhang H, Zhou Z, Qiu Z, Liao Y. A Therapeutic Peptide Vaccine Against PCSK9. Sci Rep 2017;7(1):12534.
40. Petersen DN, Hawkins J, Ruangsiriluk W, Stevens KA, Maguire BA, O'Connell TN, Rocke BN, Boehm M, Ruggeri RB, Rolph T and others. A Small-Molecule Anti-secretagogue of PCSK9 Targets the 80S Ribosome to Inhibit PCSK9 Protein Translation. Cell Chem Biol 2016;23(11):1362-1371.
41. Lintner NG, McClure KF, Petersen D, Londregan AT, Piotrowski DW, Wei L, Xiao J, Bolt M, Loria PM, Maguire B and others. Selective stalling of human translation through small-molecule engagement of the ribosome nascent chain. PLoS Biol 2017;15(3):e2001882.
42. McClure KF, Piotrowski DW, Petersen D, Wei L, Xiao J, Londregan AT, KamLet AS, Dechert-Schmitt AM, Raymer B, Ruggeri RB and others. Liver-Targeted Small-Molecule Inhibitors of Proprotein Convertase Subtilisin/Kexin Type 9 Synthesis. Angew Chem Int Ed Engl 2017;56(51):16218-16222.
43. Gustafsen C, Olsen D, Vilstrup J, Lund S, Reinhardt A, Wellner N, Larsen T, Andersen CBF, Weyer K, Li JP and others. Heparan sulfate proteoglycans present PCSK9 to the LDL receptor. Nat Commun 2017;8(1):503.
44. Basak A, Toure BB, Lazure C, Mbikay M, Chretien M, Seidah NG. Enzymic characterization in vitro of recombinant proprotein convertase PC4. Biochem J 1999;343 Pt 1:29-37.
45. Benjannet S, Rondeau N, Day R, Chretien M, Seidah NG. PC1 and PC2 are proprotein convertases capable of cleaving proopiomelanocortin at distinct pairs of basic residues. Proc Natl Acad Sci U S A 1991;88(9):3564-8.
46. Guillemot J, Canuel M, Essalmani R, Prat A, Seidah NG. Implication of the proprotein convertases in iron homeostasis: proprotein convertase 7 sheds human transferrin receptor 1 and furin activates hepcidin. Hepatology 2013;57(6):2514-24.
47. Van de Ven WJ, Creemers JW, Roebroek AJ. Furin: the prototype mammalian subtilisin-like proprotein-processing enzyme. Endoproteolytic cleavage at paired basic residues of proproteins of the eukaryotic secretory pathway. Enzyme 1991;45(5-6):257-70.
48. Duncan EA, Brown MS, Goldstein JL, Sakai J. Cleavage site for sterol-regulated protease localized to a leu-Ser bond in the lumenal loop of sterol regulatory element-binding protein-2. J Biol Chem 1997;272(19):12778-85.
49. Seidah NG, Prat A. The biology and therapeutic targeting of the proprotein convertases. Nature reviews.Drug discovery 2012;11(5):367-383.
50. Henrich S, Lindberg I, Bode W, Than ME. Proprotein convertase models based on the crystal structures of furin and kexin: explanation of their specificity. Journal of Molecular Biology 2005;345(2):211-227.

51. Molloy SS, Thomas L, VanSlyke JK, Stenberg PE, Thomas G. Intracellular trafficking and activation of the furin proprotein convertase: localization to the TGN and recycling from the cell surface. Embo j 1994;13(1):18-33.
52. Ikemura H, Inouye M. In vitro processing of pro-subtilisin produced in Escherichia coli. J Biol Chem 1988;263(26):12959-63.
53. Power SD, Adams RM, Wells JA. Secretion and autoproteolytic maturation of subtilisin. Proc Natl Acad Sci U S A 1986;83(10):3096-100.
54. Anderson ED, VanSlyke JK, Thulin CD, Jean F, Thomas G. Activation of the furin endoprotease is a multiple-step process: requirements for acidification and internal propeptide cleavage. Embo j 1997;16(7):1508-18.
55. Creemers JW, Siezen RJ, Roebroek AJ, Ayoubi TA, Huylebroeck D, Van de Ven WJ. Modulation of furin-mediated proprotein processing activity by site-directed mutagenesis. J Biol Chem 1993;268(29):21826-34.
56. Cunningham D, Danley DE, Geoghegan KF, Griffor MC, Hawkins JL, Subashi TA, Varghese AH, Ammirati MJ, Culp JS, Hoth LR and others. Structural and biophysical studies of PCSK9 and its mutants linked to familial hypercholesterolemia. Nature structural & molecular biology 2007;14(5):413-419.
57. McNutt MC, Lagace TA, Horton JD. Catalytic activity is not required for secreted PCSK9 to reduce low density lipoprotein receptors in HepG2 cells. The Journal of biological chemistry 2007;282(29):20799-20803.
58. Piper DE, Jackson S, Liu Q, Romanow WG, Shetterly S, Thibault ST, Shan B, Walker NPC. The Crystal Structure of PCSK9: A Regulator of Plasma LDL-Cholesterol. Structure 2007;15(5):545-552.
59. Hampton EN, Knuth MW, Li J, Harris JL, Lesley SA, Spraggon G. The self-inhibited structure of full-length PCSK9 at 1.9 A reveals structural homology with resistin within the C-terminal domain. Proceedings of the National Academy of Sciences of the United States of America 2007;104(37):14604-14609.
60. Dewpura T, Raymond A, Hamelin J, Seidah NG, Mbikay M, Chretien M, Mayne J. PCSK9 is phosphorylated by a Golgi casein kinase-like kinase ex vivo and circulates as a phosphoprotein in humans. The FEBS journal 2008;275(13):3480-3493.
61. Benjannet S, Rhainds D, Hamelin J, Nassoury N, Seidah NG. The proprotein convertase (PC) PCSK9 is inactivated by furin and/or PC5/6A: functional consequences of natural mutations and post-translational modifications. J Biol Chem 2006;281(41):30561-72.
62. Brown MS, Goldstein JL. A receptor-mediated pathway for cholesterol homeostasis. Science 1986;232(4746):34-47.
63. Goldstein JL, Brown MS. Regulation of low-density lipoprotein receptors: implications for pathogenesis and therapy of hypercholesterolemia and atherosclerosis. Circulation 1987;76(3):504-7.
64. Tavori H, Fan D, Blakemore JL, Yancey PG, Ding L, Linton MF, Fazio S. Serum proprotein convertase subtilisin/kexin type 9 and cell surface low-density lipoprotein receptor: evidence for a reciprocal regulation. Circulation 2013;127(24):2403-2413.
65. Park SW, Moon YA, Horton JD. Post-transcriptional regulation of low density lipoprotein receptor protein by proprotein convertase subtilisin/kexin type 9a in mouse liver. The Journal of biological chemistry 2004;279(48):50630-50638.
66. Maxwell KN, Breslow JL. Adenoviral-mediated expression of Pcsk9 in mice results in a low-density lipoprotein receptor knockout phenotype. Proceedings of the National Academy of Sciences of the United States of America 2004;101(18):7100-7105.
67. Kwon HJ, Lagace TA, McNutt MC, Horton JD, Deisenhofer J. Molecular basis for LDL receptor recognition by PCSK9. Proceedings of the National Academy of Sciences of the United States of America 2008;105(6):1820-1825.

68. McNutt MC, Kwon HJ, Chen C, Chen JR, Horton JD, Lagace TA. Antagonism of secreted PCSK9 increases low density lipoprotein receptor expression in HepG2 cells. The Journal of biological chemistry 2009;284(16):10561-10570.
69. Ni YG, Condra JH, Orsatti L, Shen X, Di Marco S, Pandit S, BottomLey MJ, Ruggeri L, Cummings RT, Cubbon RM and others. A proprotein convertase subtilisin-like/kexin type 9 (PCSK9) C-terminal domain antibody antigen-binding fragment inhibits PCSK9 internalization and restores low density lipoprotein uptake. J Biol Chem 2010;285(17):12882-91.
70. Leren TP. Sorting an LDL receptor with bound PCSK9 to intracellular degradation. Atherosclerosis 2014;237(1):76-81.
71. Nguyen MA, Kosenko T, Lagace TA. Internalized PCSK9 dissociates from recycling LDL receptors in PCSK9-resistant SV-589 fibroblasts. Journal of lipid research 2014;55(2):266-275.
72. Seidah NG, Poirier S, Denis M, Parker R, Miao B, Mapelli C, Prat A, Wassef H, Davignon J, Hajjar KA and others. Annexin A2 Is a Natural Extrahepatic Inhibitor of the PCSK9-Induced LDL Receptor Degradation. PLoS ONE 2012;7(7):. doi:10.1371/journal.pone.0041865.
73. Boren J, Lee I, Zhu W, Arnold K, Taylor S, Innerarity TL. Identification of the low density lipoprotein receptor-binding site in apolipoprotein B100 and the modulation of its binding activity by the carboxyl terminus in familial defective apo-B100. The Journal of clinical investigation 1998;101(5):1084-1093.
74. Mahley RW. Apolipoprotein E: cholesterol transport protein with expanding role in cell biology. Science 1988;240(4852):622-30.
75. Bradley WA, Gianturco SH. ApoE is necessary and sufficient for the binding of large triglyceride-rich lipoproteins to the LDL receptor; apoB is unnecessary. J Lipid Res 1986;27(1):40-8.
76. He G, Gupta S, Yi M, Michaely P, Hobbs HH, Cohen JC. ARH is a modular adaptor protein that interacts with the LDL receptor, clathrin, and AP-2. The Journal of biological chemistry 2002;277(46):44044-44049.
77. Davis CG, van Driel IR, Russell DW, Brown MS, Goldstein JL. The low density lipoprotein receptor. Identification of amino acids in cytoplasmic domain required for rapid endocytosis. The Journal of biological chemistry 1987;262(9):4075-4082.
78. Gent J, Braakman I. Low-density lipoprotein receptor structure and folding. Cellular and molecular life sciences : CMLS 2004;61(19-20):2461-2470.
79. Anderson RGW, Brown MS, Goldstein JL. Role of the coated endocytic vesicle in the uptake of receptor-bound low density lipoprotein in human fibroblasts. Cell 1977;10(3):351-364.
80. Brown MS, Kovanen PT, Goldstein JL. Regulation of plasma cholesterol by lipoprotein receptors. Science (New York, N.Y.) 1981;212(4495):628-635.
81. Brown MS, Anderson RG, Goldstein JL. Recycling receptors: the round-trip itinerary of migrant membrane proteins. Cell 1983;32(3):663-667.
82. Fisher TS, Lo Surdo P, Pandit S, Mattu M, Santoro JC, Wisniewski D, Cummings RT, Calzetta A, Cubbon RM, Fischer PA and others. Effects of pH and low density lipoprotein (LDL) on PCSK9-dependent LDL receptor regulation. The Journal of biological chemistry 2007;282(28):20502-20512.
83. Zhang DW, Lagace TA, Garuti R, Zhao Z, McDonald M, Horton JD, Cohen JC, Hobbs HH. Binding of proprotein convertase subtilisin/kexin type 9 to epidermal growth factor-like repeat A of low density lipoprotein receptor decreases receptor recycling and increases degradation. The Journal of biological chemistry 2007;282(25):18602-18612.
84. Tveten K, Holla OL, Cameron J, Strom TB, Berge KE, Laerdahl JK, Leren TP. Interaction between the ligand-binding domain of the LDL receptor and the C-terminal domain of

PCSK9 is required for PCSK9 to remain bound to the LDL receptor during endosomal acidification. Hum Mol Genet 2012;21(6):1402-9.
85. Zhang DW, Garuti R, Tang WJ, Cohen JC, Hobbs HH. Structural requirements for PCSK9-mediated degradation of the low-density lipoprotein receptor. Proceedings of the National Academy of Sciences of the United States of America 2008;105(35):13045-13050.
86. Holla OL, Cameron J, Tveten K, Strom TB, Berge KE, Laerdahl JK, Leren TP. Role of the C-terminal domain of PCSK9 in degradation of the LDL receptors. J Lipid Res 2011;52(10):1787-94.
87. Ni YG, Di Marco S, Condra JH, Peterson LB, Wang W, Wang F, Pandit S, Hammond HA, Rosa R, Cummings RT and others. A PCSK9-binding antibody that structurally mimics the EGF(A) domain of LDL-receptor reduces LDL cholesterol in vivo. J Lipid Res 2011;52(1):78-86.
88. Saavedra YG, Day R, Seidah NG. The M2 module of the Cys-His-rich domain (CHRD) of PCSK9 protein is needed for the extracellular low-density lipoprotein receptor (LDLR) degradation pathway. J Biol Chem 2012;287(52):43492-501.
89. Horton JD, Shah NA, Warrington JA, Anderson NN, Park SW, Brown MS, Goldstein JL. Combined analysis of oligonucleotide microarray data from transgenic and knockout mice identifies direct SREBP target genes. Proc Natl Acad Sci U S A 2003;100(21):12027-32.
90. Maxwell KN, Soccio RE, Duncan EM, Sehayek E, Breslow JL. Novel putative SREBP and LXR target genes identified by microarray analysis in liver of cholesterol-fed mice. J Lipid Res 2003;44(11):2109-19.
91. Dubuc G, Chamberland A, Wassef H, Davignon J, Seidah NG, Bernier L, Prat A. Statins upregulate PCSK9, the gene encoding the proprotein convertase neural apoptosis-regulated convertase-1 implicated in familial hypercholesterolemia. Arteriosclerosis, Thrombosis, and Vascular Biology 2004;24(8):1454-1459.
92. Careskey HE, Davis RA, Alborn WE, Troutt JS, Cao G, Konrad RJ. Atorvastatin increases human serum levels of proprotein convertase subtilisin/kexin type 9. J Lipid Res 2008;49(2):394-8.
93. Li H, Dong B, Park SW, Lee HS, Chen W, Liu J. Hepatocyte nuclear factor 1alpha plays a critical role in PCSK9 gene transcription and regulation by the natural hypocholesterolemic compound berberine. The Journal of biological chemistry 2009;284(42):28885-28895.
94. Lagace TA. PCSK9 and LDLR degradation: regulatory mechanisms in circulation and in cells. Current opinion in lipidology 2014;25(5):387-393.
95. Lakoski SG, Lagace TA, Cohen JC, Horton JD, Hobbs HH. Genetic and Metabolic Determinants of Plasma PCSK9 Levels. The Journal of clinical endocrinology and metabolism 2009;94(7):2537-2543.
96. Lipari MT, Li W, Moran P, Kong-Beltran M, Sai T, Lai J, Lin SJ, Kolumam G, Zavala-Solorio J, Izrael-Tomasevic A and others. Furin-cleaved proprotein convertase subtilisin/kexin type 9 (PCSK9) is active and modulates low density lipoprotein receptor and serum cholesterol levels. J Biol Chem 2012;287(52):43482-91.
97. Essalmani R, Susan-Resiga D, Chamberland A, Abifadel M, Creemers JW, Boileau C, Seidah NG, Prat A. In vivo evidence that furin from hepatocytes inactivates PCSK9. J Biol Chem 2011;286(6):4257-63.
98. Han B, Eacho PI, Knierman MD, Troutt JS, Konrad RJ, Yu X, Schroeder KM. Isolation and characterization of the circulating truncated form of PCSK9. J Lipid Res 2014;55(7):1505-14.
99. Alborn WE, Cao G, Careskey HE, Qian YW, Subramaniam DR, Davies J, Conner EM, Konrad RJ. Serum proprotein convertase subtilisin kexin type 9 is correlated directly with serum LDL cholesterol. Clin Chem 2007;53(10):1814-9.

100. Mayne J, Raymond A, Chaplin A, Cousins M, Kaefer N, Gyamera-Acheampong C, Seidah NG, Mbikay M, Chretien M, Ooi TC. Plasma PCSK9 levels correlate with cholesterol in men but not in women. Biochem Biophys Res Commun 2007;361(2):451-6.
101. Lambert G, Ancellin N, Charlton F, Comas D, Pilot J, Keech A, Patel S, Sullivan DR, Cohn JS, Rye KA and others. Plasma PCSK9 concentrations correlate with LDL and total cholesterol in diabetic patients and are decreased by fenofibrate treatment. Clin Chem 2008;54(6):1038-45.
102. Cui Q, Ju X, Yang T, Zhang M, Tang W, Chen Q, Hu Y, Haas JV, Troutt JS, Pickard RT and others. Serum PCSK9 is associated with multiple metabolic factors in a large Han Chinese population. Atherosclerosis 2010;213(2):632-6.
103. Persson L, Cao G, Stahle L, Sjoberg BG, Troutt JS, Konrad RJ, Galman C, Wallen H, Eriksson M, Hafstrom I and others. Circulating proprotein convertase subtilisin kexin type 9 has a diurnal rhythm synchronous with cholesterol synthesis and is reduced by fasting in humans. Arterioscler Thromb Vasc Biol 2010;30(12):2666-72.
104. Ghosh M, Galman C, Rudling M, Angelin B. Influence of physiological changes in endogenous estrogen on circulating PCSK9 and LDL cholesterol. J Lipid Res 2015;56(2):463-9.
105. Bonde Y, Breuer O, Lutjohann D, Sjoberg S, Angelin B, Rudling M. Thyroid hormone reduces PCSK9 and stimulates bile acid synthesis in humans. J Lipid Res 2014;55(11):2408-15.
106. Langhi C, Le May C, Kourimate S, Caron S, Staels B, Krempf M, Costet P, Cariou B. Activation of the farnesoid X receptor represses PCSK9 expression in human hepatocytes. FEBS Lett 2008;582(6):949-55.
107. Costet P, Cariou B, Lambert G, Lalanne F, Lardeux B, Jarnoux AL, Grefhorst A, Staels B, Krempf M. Hepatic PCSK9 expression is regulated by nutritional status via insulin and sterol regulatory element-binding protein 1c. J Biol Chem 2006;281(10):6211-8.
108. Khera AV, Qamar A, Reilly MP, Dunbar RL, Rader DJ. Effects of niacin, statin, and fenofibrate on circulating proprotein convertase subtilisin/kexin type 9 levels in patients with dyslipidemia. Am J Cardiol 2015;115(2):178-82.
109. Costet P, Hoffmann MM, Cariou B, Guyomarc'h Delasalle B, Konrad T, Winkler K. Plasma PCSK9 is increased by fenofibrate and atorvastatin in a non-additive fashion in diabetic patients. Atherosclerosis 2010;212(1):246-51.
110. Troutt JS, Alborn WE, Cao G, Konrad RJ. Fenofibrate treatment increases human serum proprotein convertase subtilisin kexin type 9 levels. J Lipid Res 2010;51(2):345-51.
111. Miyosawa K, Watanabe Y, Murakami K, Murakami T, Shibata H, Iwashita M, Yamazaki H, Yamazaki K, Ohgiya T, Shibuya K and others. New CETP inhibitor K-312 reduces PCSK9 expression: a potential effect on LDL cholesterol metabolism. Am J Physiol Endocrinol Metab 2015;309(2):E177-90.
112. Dong B, Singh AB, Fung C, Kan K, Liu J. CETP inhibitors downregulate hepatic LDL receptor and PCSK9 expression in vitro and in vivo through a SREBP2 dependent mechanism. Atherosclerosis 2014;235(2):449-62.
113. Segrest JP, Garber DW, Brouillette CG, Harvey SC, Anantharamaiah GM. The amphipathic alpha helix: a multifunctional structural motif in plasma apolipoproteins. Adv Protein Chem 1994;45:303-69.
114. Lamon-Fava S, Sadowski JA, Davidson KW, O'Brien ME, McNamara JR, Schaefer EJ. Plasma lipoproteins as carriers of phylloquinone (vitamin K1) in humans. Am J Clin Nutr 1998;67(6):1226-31.
115. Seki J, Okita A, Watanabe M, Nakagawa T, Honda K, Tatewaki N, Sugiyama M. Plasma lipoproteins as drug carriers: pharmacological activity and disposition of the complex of beta-sitosteryl-beta-D-glucopyranoside with plasma lipoproteins. J Pharm Sci 1985;74(12):1259-64.

116. Roy G, Placzek E, Scanlan TS. ApoB-100-containing lipoproteins are major carriers of 3-iodothyronamine in circulation. J Biol Chem 2012;287(3):1790-800.
117. Cortner JA, Coates PM, Le NA, Cryer DR, Ragni MC, Faulkner A, Langer T. Kinetics of chylomicron remnant clearance in normal and in hyperlipoproteinemic subjects. J Lipid Res 1987;28(2):195-206.
118. Sviridov D, Nestel P. Dynamics of reverse cholesterol transport: protection against atherosclerosis. Atherosclerosis 2002;161(2):245-54.
119. Saito H, Lund-Katz S, Phillips MC. Contributions of domain structure and lipid interaction to the functionality of exchangeable human apolipoproteins. Prog Lipid Res 2004;43(4):350-80.
120. Cladaras C, Hadzopoulou-Cladaras M, Nolte RT, Atkinson D, Zannis VI. The complete sequence and structural analysis of human apolipoprotein B-100: relationship between apoB-100 and apoB-48 forms. The EMBO Journal 1986;5(13):3495-3507.
121. Thiam AR, Farese RV, Jr., Walther TC. The biophysics and cell biology of lipid droplets. Nature reviews.Molecular cell biology 2013;14(12):775-786.
122. Gangabadage CS, Zdunek J, Tessari M, Nilsson S, Olivecrona G, Wijmenga SS. Structure and dynamics of human apolipoprotein CIII. J Biol Chem 2008;283(25):17416-27.
123. Drin G, Antonny B. Amphipathic helices and membrane curvature. FEBS Lett 2010;584(9):1840-7.
124. Mahley RW, Innerarity TL, Rall SC, Jr., Weisgraber KH. Plasma lipoproteins: apolipoprotein structure and function. J Lipid Res 1984;25(12):1277-94.
125. Hussain MM, Shi J, Dreizen P. Microsomal triglyceride transfer protein and its role in apoB-lipoprotein assembly. J Lipid Res 2003;44(1):22-32.
126. Olofsson SO, Boren J. Apolipoprotein B secretory regulation by degradation. Arterioscler Thromb Vasc Biol 2012;32(6):1334-8.
127. Fisher EA, Pan M, Chen X, Wu X, Wang H, Jamil H, Sparks JD, Williams KJ. The triple threat to nascent apolipoprotein B. Evidence for multiple, distinct degradative pathways. J Biol Chem 2001;276(30):27855-63.
128. Yao Z, Tran K, McLeod RS. Intracellular degradation of newly synthesized apolipoprotein B. J Lipid Res 1997;38(10):1937-53.
129. Tiwari S, Siddiqi SA. Intracellular trafficking and secretion of VLDL. Arterioscler Thromb Vasc Biol 2012;32(5):1079-86.
130. Siddiqi SA. VLDL exits from the endoplasmic reticulum in a specialized vesicle, the VLDL transport vesicle, in rat primary hepatocytes. Biochem J 2008;413(2):333-42.
131. Tran K, Thorne-Tjomsland G, DeLong CJ, Cui Z, Shan J, Burton L, Jamieson JC, Yao Z. Intracellular assembly of very low density lipoproteins containing apolipoprotein B100 in rat hepatoma McA-RH7777 cells. J Biol Chem 2002;277(34):31187-200.
132. Swift LL. Role of the Golgi apparatus in the phosphorylation of apolipoprotein B. J Biol Chem 1996;271(49):31491-5.
133. Mead JR, Irvine SA, Ramji DP. Lipoprotein lipase: structure, function, regulation, and role in disease. J Mol Med (Berl) 2002;80(12):753-69.
134. Beltz WF, Kesaniemi YA, Howard BV, Grundy SM. Development of an integrated model for analysis of the kinetics of apolipoprotein B in plasma very low density lipoproteins, intermediate density lipoproteins, and low density lipoproteins. J Clin Invest 1985;76(2):575-85.
135. Schreier L, Berg G, Zago V, Gonzalez AI, Wikinski R. Kinetics of in vitro lipolysis of human very low-density lipoprotein by lipoprotein lipase. Nutr Metab Cardiovasc Dis 2002;12(1):13-8.
136. Packard CJ, Shepherd J. Lipoprotein heterogeneity and apolipoprotein B metabolism. Arterioscler Thromb Vasc Biol 1997;17(12):3542-56.

137. Krul ES, Tikkanen MJ, Cole TG, Davie JM, Schonfeld G. Roles of apolipoproteins B and E in the cellular binding of very low density lipoproteins. J Clin Invest 1985;75(2):361-9.
138. Gianturco SH, Brown FB, Gotto AM, Jr., Bradley WA. Receptor-mediated uptake of hypertriglyceridemic very low density lipoproteins by normal human fibroblasts. J Lipid Res 1982;23(7):984-93.
139. Swenson TL, Brocia RW, Tall AR. Plasma cholesteryl ester transfer protein has binding sites for neutral lipids and phospholipids. J Biol Chem 1988;263(11):5150-7.
140. Morton RE, Izem L. Cholesteryl ester transfer proteins from different species do not have equivalent activities. J Lipid Res 2014;55(2):258-65.
141. Marcel YL, Hogue M, Weech PK, Davignon J, Milne RW. Expression of apolipoprotein B epitopes in lipoproteins. Relationship to conformation and function. Arteriosclerosis 1988;8(6):832-44.
142. Wang X, Pease R, Bertinato J, Milne RW. Well-defined regions of apolipoprotein B-100 undergo conformational change during its intravascular metabolism. Arteriosclerosis, Thrombosis, and Vascular Biology 2000;20(5):1301-1308.
143. Chen GC, Zhu S, Hardman DA, Schilling JW, Lau K, Kane JP. Structural domains of human apolipoprotein B-100. Differential accessibility to limited proteolysis of B-100 in low density and very low density lipoproteins. J Biol Chem 1989;264(24):14369-75.
144. Kinoshita M, Krul ES, Schonfeld G. Modification of the core lipids of low density lipoproteins produces selective alterations in the expression of apoB-100 epitopes. J Lipid Res 1990;31(4):701-8.
145. Chan L, Chang BH, Nakamuta M, Li WH, Smith LC. Apobec-1 and apolipoprotein B mRNA editing. Biochim Biophys Acta 1997;1345(1):11-26.
146. Higuchi K, Kitagawa K, Kogishi K, Takeda T. Developmental and age-related changes in apolipoprotein B mRNA editing in mice. J Lipid Res 1992;33(12):1753-64.
147. Martins IJ, Hone E, Chi C, Seydel U, Martins RN, Redgrave TG. Relative roles of LDLr and LRP in the metabolism of chylomicron remnants in genetically manipulated mice. J Lipid Res 2000;41(2):205-13.
148. Hevonoja T, Pentikainen MO, Hyvonen MT, Kovanen PT, Ala-Korpela M. Structure of low density lipoprotein (LDL) particles: basis for understanding molecular changes in modified LDL. Biochimica et biophysica acta 2000;1488(3):189-210.
149. Krauss RM, Burke DJ. Identification of multiple subclasses of plasma low density lipoproteins in normal humans. Journal of lipid research 1982;23(1):97-104.
150. Otvos JD, Jeyarajah EJ, Cromwell WC. Measurement issues related to lipoprotein heterogeneity. The American Journal of Cardiology 2002;90(8, Supplement):22-29.
151. Austin MA, Breslow JL, Hennekens CH, Buring JE, Willett WC, Krauss RM. Low-density lipoprotein subclass patterns and risk of myocardial infarction. Jama 1988;260(13):1917-1921.
152. Ren G, Rudenko G, Ludtke SJ, Deisenhofer J, Chiu W, Pownall HJ. Model of human low-density lipoprotein and bound receptor based on cryoEM. Proc Natl Acad Sci U S A 2010;107(3):1059-64.
153. Johs A, Hammel M, Waldner I, May RP, Laggner P, Prassl R. Modular structure of solubilized human apolipoprotein B-100. Low resolution model revealed by small angle neutron scattering. J Biol Chem 2006;281(28):19732-9.
154. Segrest JP, Jones MK, Mishra VK, Anantharamaiah GM, Garber DW. apoB-100 has a pentapartite structure composed of three amphipathic alpha-helical domains alternating with two amphipathic beta-strand domains. Detection by the computer program LOCATE. Arteriosclerosis and Thrombosis : A Journal of Vascular Biology / American Heart Association 1994;14(10):1674-1685.

155. Segrest JP, Jones MK, De Loof H, Dashti N. Structure of apolipoprotein B-100 in low density lipoproteins. Journal of lipid research 2001;42(9):1346-1367.
156. Fan D, Yancey PG, Qiu S, Ding L, Weeber EJ, Linton MF, Fazio S. Self-association of human PCSK9 correlates with its LDLR-degrading activity. Biochemistry 2008;47(6):1631-1639.
157. Luo Y, Warren L, Xia D, Jensen H, Sand T, Petras S, Qin W, Miller KS, Hawkins J. Function and distribution of circulating human PCSK9 expressed extrahepatically in transgenic mice. Journal of lipid research 2009;50(8):1581-1588.
158. Kosenko T, Golder M, Leblond G, Weng W, Lagace TA. Low density lipoprotein binds to proprotein convertase subtilisin/kexin type-9 (PCSK9) in human plasma and inhibits PCSK9-mediated low density lipoprotein receptor degradation. The Journal of biological chemistry 2013;288(12):8279-8288.
159. Fazio S, Minnier J, Shapiro MD, Tsimikas S, Tarugi P, Averna MR, Arca M, Tavori H. Threshold Effects of Circulating Angiopoietin-Like 3 Levels on Plasma Lipoproteins. J Clin Endocrinol Metab 2017;102(9):3340-3348.
160. Tavori H, Giunzioni I, Linton MF, Fazio S. Loss of plasma proprotein convertase subtilisin/kexin 9 (PCSK9) after lipoprotein apheresis. Circ Res 2013;113(12):1290-5.
161. Hori M, Ishihara M, Yuasa Y, Makino H, Yanagi K, Tamanaha T, Kishimoto I, Kujiraoka T, Hattori H, Harada-Shiba M. Removal of plasma mature and furin-cleaved proprotein convertase subtilisin/kexin 9 by low-density lipoprotein-apheresis in familial hypercholesterolemia: development and application of a new assay for PCSK9. J Clin Endocrinol Metab 2015;100(1):E41-9.
162. Sun H, Samarghandi A, Zhang N, Yao Z, Xiong M, Teng BB. Proprotein convertase subtilisin/kexin type 9 interacts with apolipoprotein B and prevents its intracellular degradation, irrespective of the low-density lipoprotein receptor. Arteriosclerosis, Thrombosis, and Vascular Biology 2012;32(7):1585-1595.
163. Tavori H, Christian D, Minnier J, Plubell D, Shapiro MD, Yeang C, Giunzioni I, Croyal M, Duell PB, Lambert G and others. PCSK9 Association With Lipoprotein(a). Circ Res 2016;119(1):29-35.
164. Gurdasani D, Sjouke B, Tsimikas S, Hovingh GK, Luben RN, Wainwright NW, Pomilla C, Wareham NJ, Khaw KT, Boekholdt SM and others. Lipoprotein(a) and risk of coronary, cerebrovascular, and peripheral artery disease: the EPIC-Norfolk prospective population study. Arterioscler Thromb Vasc Biol 2012;32(12):3058-65.
165. Holmes DT, Schick BA, Humphries KH, Frohlich J. Lipoprotein(a) is an independent risk factor for cardiovascular disease in heterozygous familial hypercholesterolemia. Clin Chem 2005;51(11):2067-73.
166. Brown AJ, Sun L, Feramisco JD, Brown MS, Goldstein JL. Cholesterol addition to ER membranes alters conformation of SCAP, the SREBP escort protein that regulates cholesterol metabolism. Molecular cell 2002;10(2):237-245.
167. Lo Surdo P, BottomLey MJ, Calzetta A, Settembre EC, Cirillo A, Pandit S, Ni YG, Hubbard B, Sitlani A, Carfi A. Mechanistic implications for LDL receptor degradation from the PCSK9/LDLR structure at neutral pH. EMBO Rep 2011;12(12):1300-5.
168. Holla OL, Laerdahl JK, Strom TB, Tveten K, Cameron J, Berge KE, Leren TP. Removal of acidic residues of the prodomain of PCSK9 increases its activity towards the LDL receptor. Biochemical and biophysical research communications 2011;406(2):234-238.
169. Benjannet S, Saavedra YG, Hamelin J, Asselin MC, Essalmani R, Pasquato A, Lemaire P, Duke G, Miao B, Duclos F and others. Effects of the prosegment and pH on the activity of PCSK9: evidence for additional processing events. The Journal of biological chemistry 2010;285(52):40965-40978.
170. Verbeek R, Boyer M, Boekholdt SM, Hovingh GK, Kastelein JJ, Wareham N, Khaw KT, Arsenault BJ. Carriers of the PCSK9 R46L Variant Are Characterized by an Antiatherogenic

Lipoprotein Profile Assessed by Nuclear Magnetic Resonance Spectroscopy-Brief Report. Arterioscler Thromb Vasc Biol 2017;37(1):43-48.
171. Buchan DWA, Minneci F, Nugent TCO, Bryson K, Jones DT. Scalable web services for the PSIPRED Protein Analysis Workbench. Nucleic Acids Research 2013;41(Web Server issue):W349-W357.
172. Gautier R, Douguet D, Antonny B, Drin G. HELIQUEST: a web server to screen sequences with specific alpha-helical properties. Bioinformatics 2008;24(18):2101-2.
173. Humphries SE, Neely RD, Whittall RA, Troutt JS, Konrad RJ, Scartezini M, Li KW, Cooper JA, Acharya J, Neil A. Healthy individuals carrying the PCSK9 p.R46L variant and familial hypercholesterolemia patients carrying PCSK9 p.D374Y exhibit lower plasma concentrations of PCSK9. Clinical chemistry 2009;55(12):2153-2161.
174. Kotowski IK, PertsemLidis A, Luke A, Cooper RS, Vega GL, Cohen JC, Hobbs HH. A spectrum of PCSK9 alleles contributes to plasma levels of low-density lipoprotein cholesterol. American Journal of Human Genetics 2006;78(3):410-422.
175. Kim DE, Chivian D, Baker D. Protein structure prediction and analysis using the Robetta server. Nucleic Acids Research 2004;32(Web Server issue):W526-W531.
176. Allard D, Amsellem S, Abifadel M, Trillard M, Devillers M, Luc G, Krempf M, Reznik Y, Girardet JP, Fredenrich A and others. Novel mutations of the PCSK9 gene cause variable phenotype of autosomal dominant hypercholesterolemia. Hum Mutat 2005;26(5):497.
177. Pisciotta L, Priore Oliva C, Cefalu AB, Noto D, Bellocchio A, Fresa R, Cantafora A, Patel D, Averna M, Tarugi P and others. Additive effect of mutations in LDLR and PCSK9 genes on the phenotype of familial hypercholesterolemia. Atherosclerosis 2006;186(2):433-40.
178. Johnson JE, Cornell RB. Membrane-binding amphipathic alpha-helical peptide derived from CTP:phosphocholine cytidylyltransferase. Biochemistry 1994;33(14):4327-4335.
179. Liu H, Naismith JH. An efficient one-step site-directed deletion, insertion, single and multiple-site plasmid mutagenesis protocol. BMC Biotechnol 2008;8:91.
180. Havel RJ, Eder HA, Bragdon JH. The distribution and chemical composition of ultracentrifugally separated lipoproteins in human serum. The Journal of clinical investigation 1955;34(9):1345-1353.
181. Peterson GL. A simplification of the protein assay method of Lowry et al. which is more generally applicable. Analytical Biochemistry 1977;83(2):346-356.
182. Yee MS, Pavitt DV, Tan T, Venkatesan S, Godsland IF, Richmond W, Johnston DG. Lipoprotein separation in a novel iodixanol density gradient, for composition, density, and phenotype analysis. Journal of lipid research 2008;49(6):1364-1371.
183. Rohl CA, Strauss CE, Misura KM, Baker D. Protein structure prediction using Rosetta. Methods Enzymol 2004;383:66-93.
184. Konrat R. The protein meta-structure: a novel concept for chemical and molecular biology. Cell Mol Life Sci 2009;66(22):3625-39.
185. Davignon J, Dubuc G, Seidah NG. The influence of PCSK9 polymorphisms on serum low-density lipoprotein cholesterol and risk of atherosclerosis. Curr Atheroscler Rep 2010;12(5):308-15.
186. Abifadel M, Guerin M, Benjannet S, Rabes JP, Le Goff W, Julia Z, Hamelin J, Carreau V, Varret M, Bruckert E and others. Identification and characterization of new gain-of-function mutations in the PCSK9 gene responsible for autosomal dominant hypercholesterolemia. Atherosclerosis 2012;223(2):394-400.
187. Homer VM, Marais AD, Charlton F, Laurie AD, Hurndell N, Scott R, Mangili F, Sullivan DR, Barter PJ, Rye KA and others. Identification and characterization of two non-secreted PCSK9 mutants associated with familial hypercholesterolemia in cohorts from New Zealand and South Africa. Atherosclerosis 2008;196(2):659-666.

188. Pandit S, Wisniewski D, Santoro JC, Ha S, Ramakrishnan V, Cubbon RM, Cummings RT, Wright SD, Sparrow CP, Sitlani A and others. Functional analysis of sites within PCSK9 responsible for hypercholesterolemia. J Lipid Res 2008;49(6):1333-43.
189. Ouguerram K, Chetiveaux M, Zair Y, Costet P, Abifadel M, Varret M, Boileau C, Magot T, Krempf M. Apolipoprotein B100 metabolism in autosomal-dominant hypercholesterolemia related to mutations in PCSK9. Arteriosclerosis, Thrombosis, and Vascular Biology 2004;24(8):1448-1453.
190. Sun XM, Eden ER, Tosi I, Neuwirth CK, Wile D, Naoumova RP, Soutar AK. Evidence for effect of mutant PCSK9 on apolipoprotein B secretion as the cause of unusually severe dominant hypercholesterolaemia. Human molecular genetics 2005;14(9):1161-1169.
191. Jirholt P, Adiels M, Boren J. How does mutant proprotein convertase neural apoptosis-regulated convertase 1 induce autosomal dominant hypercholesterolemia? Arterioscler Thromb Vasc Biol. Volume 24. United States2004. p 1334-6.
192. Twisk J, Gillian-Daniel DL, Tebon A, Wang L, Barrett PH, Attie AD. The role of the LDL receptor in apolipoprotein B secretion. J Clin Invest 2000;105(4):521-32.
193. Poirier S, Mayer G, Poupon V, McPherson PS, Desjardins R, Ly K, Asselin MC, Day R, Duclos FJ, Witmer M and others. Dissection of the endogenous cellular pathways of PCSK9-induced low density lipoprotein receptor degradation: evidence for an intracellular route. J Biol Chem 2009;284(42):28856-64.
194. Pandit S, Wisniewski D Fau - Santoro JC, Santoro Jc Fau - Ha S, Ha S Fau - Ramakrishnan V, Ramakrishnan V Fau - Cubbon RM, Cubbon Rm Fau - Cummings RT, Cummings Rt Fau - Wright SD, Wright Sd Fau - Sparrow CP, Sparrow Cp Fau - Sitlani A, Sitlani A Fau - Fisher TS and others. Functional analysis of sites within PCSK9 responsible for hypercholesterolemia. 2008(0022-2275 (Print)).
195. Xu W, Liu L, Hornby D. c-IAP1 binds and processes PCSK9 protein: linking the c-IAP1 in a TNF-alpha pathway to PCSK9-mediated LDLR degradation pathway. Molecules 2012;17(10):12086-101.
196. Fisher EA, Khanna NA, McLeod RS. Ubiquitination regulates the assembly of VLDL in HepG2 cells and is the committing step of the apoB-100 ERAD pathway. J Lipid Res 2011;52(6):1170-80.
197. Gustafsen C, Kjolby M, Nyegaard M, Mattheisen M, Lundhede J, Buttenschon H, Mors O, Bentzon JF, Madsen P, Nykjaer A and others. The hypercholesterolemia-risk gene SORT1 facilitates PCSK9 secretion. Cell Metab 2014;19(2):310-8.
198. Kjolby M, Andersen OM, Breiderhoff T, Fjorback AW, Pedersen KM, Madsen P, Jansen P, Heeren J, Willnow TE, Nykjaer A. Sort1, encoded by the cardiovascular risk locus 1p13.3, is a regulator of hepatic lipoprotein export. Cell Metab 2010;12(3):213-23.
199. Strong A, Ding Q, Edmondson AC, Millar JS, Sachs KV, Li X, Kumaravel A, Wang MY, Ai D, Guo L and others. Hepatic sortilin regulates both apolipoprotein B secretion and LDL catabolism. J Clin Invest 2012;122(8):2807-16.
200. Sniderman AD, Qi Y, Ma CI, Wang RH, Naples M, Baker C, Zhang J, Adeli K, Kiss RS. Hepatic cholesterol homeostasis: is the low-density lipoprotein pathway a regulatory or a shunt pathway? Arterioscler Thromb Vasc Biol 2013;33(11):2481-90.
201. Sniderman AD, Kiss RS, Reid T, Thanassoulis G, Watts GF. Statins, PCSK9 inhibitors and cholesterol homeostasis: a view from within the hepatocyte. Clin Sci (Lond). Volume 131. England: (c) 2017 The Author(s); published by Portland Press Limited on behalf of the Biochemical Society.; 2017. p 791-797.
202. Yuan G, Al-Shali KZ, Hegele RA. Hypertriglyceridemia: its etiology, effects and treatment. Cmaj 2007;176(8):1113-20.

203. Dubuc G, Tremblay M, Pare G, Jacques H, Hamelin J, Benjannet S, Boulet L, Genest J, Bernier L, Seidah NG and others. A new method for measurement of total plasma PCSK9: clinical applications. J Lipid Res 2010;51(1):140-9.
204. Rader D, Hobbs H. Disorders of Lipoprotein Metabolism. In: Hill M, editor. Harrison's Principles of Internal Medicine2005.
205. Amigo N, Mallol R, Heras M, Martinez-Hervas S, Blanco Vaca F, Escola-Gil JC, Plana N, Yanes O, Masana L, Correig X. Lipoprotein hydrophobic core lipids are partially extruded to surface in smaller HDL: "Herniated" HDL, a common feature in diabetes. Sci Rep 2016;6:19249.
206. Christinat N, Masoodi M. Comprehensive Lipoprotein Characterization Using Lipidomics Analysis of Human Plasma. J Proteome Res 2017;16(8):2947-2953.
207. Skipski VP, Barclay M, Barclay RK, Fetzer VA, Good JJ, Archibald FM. Lipid composition of human serum lipoproteins. Biochem J 1967;104(2):340-52.
208. Saito H, Minamida T, Arimoto I, Handa T, Miyajima K. Physical states of surface and core lipids in lipid emulsions and apolipoprotein binding to the emulsion surface. J Biol Chem 1996;271(26):15515-20.
209. Huang Y, Ji ZS, Brecht WJ, Rall SC, Jr., Taylor JM, Mahley RW. Overexpression of apolipoprotein E3 in transgenic rabbits causes combined hyperlipidemia by stimulating hepatic VLDL production and impairing VLDL lipolysis. Arterioscler Thromb Vasc Biol 1999;19(12):2952-9.
210. Larsson M, Vorrsjo E, Talmud P, Lookene A, Olivecrona G. Apolipoproteins C-I and C-III inhibit lipoprotein lipase activity by displacement of the enzyme from lipid droplets. J Biol Chem 2013;288(47):33997-4008.
211. Watts GF, Chan DC, Dent R, Somaratne R, Wasserman SM, Scott R, Burrows S, PH RB. Factorial Effects of Evolocumab and Atorvastatin on Lipoprotein Metabolism. Circulation 2017;135(4):338-351.
212. Baass A, Dubuc G, Tremblay M, Delvin EE, O'Loughlin J, Levy E, Davignon J, Lambert M. Plasma PCSK9 is associated with age, sex, and multiple metabolic markers in a population-based sample of children and adolescents. Clin Chem 2009;55(9):1637-45.
213. Brouwers MC, van Greevenbroek MM, Konrad RJ, Troutt JS, Schaper NC, Stehouwer CD. Circulating PCSK9 is a strong determinant of plasma triacylglycerols and total cholesterol in homozygous carriers of apolipoprotein epsilon2. Clin Sci (Lond) 2014;126(9):679-84.
214. Guardiola M, Plana N, Ibarretxe D, Cabre A, Gonzalez M, Ribalta J, Masana L. Circulating PCSK9 levels are positively correlated with NMR-assessed atherogenic dyslipidaemia in patients with high cardiovascular risk. Clin Sci (Lond) 2015;128(12):877-82.
215. Kwakernaak AJ, Lambert G, Dullaart RP. Plasma proprotein convertase subtilisin-kexin type 9 is predominantly related to intermediate density lipoproteins. Clin Biochem 2014;47(7-8):679-82.
216. Browning JD, Horton JD. Fasting reduces plasma proprotein convertase, subtilisin/kexin type 9 and cholesterol biosynthesis in humans. J Lipid Res 2010;51(11):3359-63.
217. Reyes-Soffer G, Pavlyha M, Ngai C, Thomas T, Holleran S, Ramakrishnan R, Karmally W, Nandakumar R, Fontanez N, Obunike JC and others. Effects of PCSK9 Inhibition with Alirocumab on Lipoprotein Metabolism in Healthy Humans. Circulation 2016.
218. Khovidhunkit W, Kim MS, Memon RA, Shigenaga JK, Moser AH, Feingold KR, Grunfeld C. Effects of infection and inflammation on lipid and lipoprotein metabolism: mechanisms and consequences to the host. J Lipid Res 2004;45(7):1169-96.
219. Levels JH, Marquart JA, Abraham PR, van den Ende AE, Molhuizen HO, van Deventer SJ, Meijers JC. Lipopolysaccharide is transferred from high-density to low-density lipoproteins by lipopolysaccharide-binding protein and phospholipid transfer protein. Infect Immun 2005;73(4):2321-6.

220. Levels JH, Abraham PR, van den Ende A, van Deventer SJ. Distribution and kinetics of lipoprotein-bound endotoxin. Infect Immun 2001;69(5):2821-8.
221. Walley KR, Thain KR, Russell JA, Reilly MP, Meyer NJ, Ferguson JF, Christie JD, Nakada TA, Fjell CD, Thair SA and others. PCSK9 is a critical regulator of the innate immune response and septic shock outcome. Sci Transl Med 2014;6(258):258ra143.
222. Topchiy E, Cirstea M, Kong HJ, Boyd JH, Wang Y, Russell JA, Walley KR. Lipopolysaccharide Is Cleared from the Circulation by Hepatocytes via the Low Density Lipoprotein Receptor. PLoS One 2016;11(5):e0155030.
223. Wouters K, Shiri-Sverdlov R, van Gorp PJ, van Bilsen M, Hofker MH. Understanding hyperlipidemia and atherosclerosis: lessons from genetically modified apoe and ldlr mice. Clin Chem Lab Med 2005;43(5):470-9.
224. Greeve J, Altkemper I, Dieterich JH, Greten H, Windler E. Apolipoprotein B mRNA editing in 12 different mammalian species: hepatic expression is reflected in low concentrations of apoB-containing plasma lipoproteins. J Lipid Res 1993;34(8):1367-83.
225. Grass DS, Saini U, Felkner RH, Wallace RE, Lago WJ, Young SG, Swanson ME. Transgenic mice expressing both human apolipoprotein B and human CETP have a lipoprotein cholesterol distribution similar to that of normolipidemic humans. J Lipid Res 1995;36(5):1082-91.
226. Yardeni T, Eckhaus M, Morris HD, Huizing M, Hoogstraten-Miller S. Retro-orbital injections in mice. Lab Anim (NY) 2011;40(5):155-60.
227. Golde WT, Gollobin P, Rodriguez LL. A rapid, simple, and humane method for submandibular bleeding of mice using a lancet. Lab Anim (NY) 2005;34(9):39-43.
228. Catimel B, Schieber C, Condron M, Patsiouras H, Connolly L, Catimel J, Nice EC, Burgess AW, Holmes AB. The PI(3,5)P2 and PI(4,5)P2 interactomes. J Proteome Res 2008;7(12):5295-313.
229. Krugmann S, Anderson KE, Ridley SH, Risso N, McGregor A, Coadwell J, Davidson K, Eguinoa A, Ellson CD, Lipp P and others. Identification of ARAP3, a novel PI3K effector regulating both Arf and Rho GTPases, by selective capture on phosphoinositide affinity matrices. Mol Cell 2002;9(1):95-108.
230. Dowler S, Kular G, Alessi DR. Protein lipid overlay assay. Sci STKE 2002;2002(129):pl6.
231. Busse RA, Scacioc A, Schalk AM, Krick R, Thumm M, Kuhnel K. Analyzing Protein-Phosphoinositide Interactions with Liposome Flotation Assays. Methods Mol Biol 2016;1376:155-62.
232. Julkowska MM, Rankenberg JM, Testerink C. Liposome-binding assays to assess specificity and affinity of phospholipid-protein interactions. Methods Mol Biol 2013;1009:261-71.
233. Sanchez SA, Gunther G, Tricerri MA, Gratton E. Methyl-beta-cyclodextrins preferentially remove cholesterol from the liquid disordered phase in giant unilamellar vesicles. J Membr Biol 2011;241(1):1-10.
234. Poirier S, Prat A, Marcinkiewicz E, Paquin J, Chitramuthu BP, Baranowski D, Cadieux B, Bennett HP, Seidah NG. Implication of the proprotein convertase NARC-1/PCSK9 in the development of the nervous system. J Neurochem 2006;98(3):838-50.
235. Hogarth CA, Roy A, Ebert DL. Genomic evidence for the absence of a functional cholesteryl ester transfer protein gene in mice and rats. Comp Biochem Physiol B Biochem Mol Biol 2003;135(2):219-29.
236. Yin W, Carballo-Jane E, McLaren DG, Mendoza VH, Gagen K, Geoghagen NS, McNamara LA, Gorski JN, Eiermann GJ, Petrov A and others. Plasma lipid profiling across species for the identification of optimal animal models of human dyslipidemia. J Lipid Res 2012;53(1):51-65.
237. Dillard A, Matthan NR, Lichtenstein AH. Use of hamster as a model to study diet-induced atherosclerosis. Nutr Metab (Lond) 2010;7:89.

238. Kapourchali FR, Surendiran G, Chen L, Uitz E, Bahadori B, Moghadasian MH. Animal models of atherosclerosis. World J Clin Cases 2014;2(5):126-32.
239. Greeve J, Altkemper I Fau - Dieterich JH, Dieterich Jh Fau - Greten H, Greten H Fau - Windler E, Windler E. Apolipoprotein B mRNA editing in 12 different mammalian species: hepatic expression is reflected in low concentrations of apoB-containing plasma lipoproteins. J Lipid Res 1993(0022-2275 (Print)).
240. Fan J, McCormick SP, Krauss RM, Taylor S, Quan R, Taylor JM, Young SG. Overexpression of human apolipoprotein B-100 in transgenic rabbits results in increased levels of LDL and decreased levels of HDL. Arterioscler Thromb Vasc Biol 1995;15(11):1889-99.
241. Fernandez ML, Volek JS. Guinea pigs: a suitable animal model to study lipoprotein metabolism, atherosclerosis and inflammation. Nutr Metab (Lond) 2006;3:17.

Appendix A – Mutagenesis Primers

Table A1: Sequences of forward (F) and reverse (R) primers used to mutate C-terminally FLAG-tagged wild-type human PCSK9. Bold, underlined letters indicate mutated base pairs, | indicates deletion site.

Mutant		Primer Sequence (5'→ 3')
Δ33-40	F:	GCGGGCGCCCGTGCGCAGGAG|CTGGTGCTAGCCTTGCGT
	R:	ACGCAAGGCTAGCACCAG|CTCCTGCGCACGGGCGCCCGC
Gly-Ser 41-45	F:	GGACGAGGACGGCGACTACGAGGAG**GGT**G**G**G**AGT**G**G**C**GG**G**A**GTTCCGAGGAGGACGGCCTGGCC
	R:	CTCCTCGTAGTCGCCGTCCTCGTCCTCCTGCGCACGGGCGCCCGCG
A44P	F:	GGAGCTGGTGCTA**C**CCTTGCGTTCCGAGG
	R:	CCTCGGAACGCAAGG**G**TAGCACCAGCTCC
R46L	F:	GGTGCTAGCCTTGC**T**TTCCGAGGAGGACGG
	R:	CCGTCCTCCTCGGAA**A**GCAAGGCTAGCACC
R496W	F:	GAGTGGGAAGCGG**T**GGGGCGAGCGCATG
	R:	CATGCGCTCGCCCC**A**CCGCTTCCCACTC
R469W	F:	CTCGGGGCCTACA**T**GGATGGCCACAGCCATC
	R:	GATGGCTGTGGCCATCC**A**TGTAGGCCCCGAG
F515L	F:	CCACAACGCTTT**A**GGGGGTGAGGGTG
	R:	CACCCTCACCCCC**T**AAAGCGTTGTGG
S127A	F:	CCTGGTGAAGATG**GC**TGGCGACCTGCTG
	R:	CAGCAGGTCGCCA**GC**CATCTTCACCAGG
S127R	F:	GGTGAAGATGAG**A**GGCGACCTGCTG
	R:	CAGCAGGTCGCC**T**CTCATCTTCACC
L108A	F:	CGCCGGGGATAC**GC**CACCAAGATCCTG
	R:	CAGGATCTTGGTG**GC**GTATCCCCGGCG
L108R	F:	CCGCCGGGGATACC**G**CACCAAGATCCTGC
	R:	GCAGGATCTTGGTG**C**GGTATCCCCGGCGG
D129G	F:	GAAGATGAGTGGCG**G**CCTGCTGGAGCTGG
	R:	CCAGCTCCAGCAGG**C**CGCCACTCATCTTC
mL44P	F:	GATTATGAAGAGC**C**GATGCTCGCCCTCC
	R:	GGAGGGCGAGCATC**G**GCTCTTCATAATC
mA47P	F:	GAAGAGCTGATGCTC**C**C**A**CTCCCGTCCCAGG
	R:	CCTGGGACGGGAG**T**G**G**GAGCATCAGCTCTTC
mS130R	F:	CTTGGTGAAGATG**C**G**T**AGTGACCTGTTGGG
	R:	CCCAACAGGTCACT**A**C**G**CATCTTCACCAAG
mD132G	F:	GAAGATGAGCAGTG**G**CCTGTTGGGCCTGG
	R:	CCCAACAGG**C**CACTGCTCATCTTCACC

Appendix B – Patient Characteristics

Table B1: Patient characteristics of hypertriglyceridemic study subjects.

Patient	Total cholesterol (mmol/L)	Plasma Triglyceride (mmol/L)	HDL-C (mmol/L)
1	6.4	16.5	0.78
2	6.1	8.2	1.44
3	6.7	4.8	1.18

HDL-C, high density lipoprotein cholesterol

Table B2: Patient characteristics of hypercholesterolemic study cohort.

Group	n (Male/Female)		Age	BMI	Total cholesterol (mmol/L)	Triglyceride (mmol/L)	LDL-C (mmol/L)	HDL-C (mmol/L)
Control (LDL<3 mM, TG<2.3mM)	42 (12/30)	Mean: (Range):	69 (40-90)	26.5 (18.6-36.0)	4.4 (3.4-5.9)	1.1 (0.5-2.1)	2.4 (1.7-3.0)	1.5 (0.8-3.0)
Hypercholesterolemia (LDL>4.9mM, TG<2.3mM)	42 (10/32)	Mean: (Range):	69 (30-90)	27.1 (20.0-35.9)	7.3* (6.6-8.5)	1.6* (0.6-3.4)	5.2* (4.9-6.0)	1.4 (0.8-2.4)

BMI - Body Mass Index; LDL-C - low-density lipoprotein cholesterol; HDL-C - high density lipoprotein cholesterol;
** - Statistically significant difference from control group, p≤0.05.*

Appendix C – Supplementary data

The work presented in this PhD thesis is an expansion on an MSc thesis previously written by the candidate (available at **http://dx.doi.org/10.20381/ruor-4155**). As such, some data presented in the MSc thesis (but as yet unpublished) is referred to in the text of this thesis. These data are included in this appendix as Figures C1, C2 and C4, while Figure C3 is supporting data for Figure 11 on page 50 of this thesis.

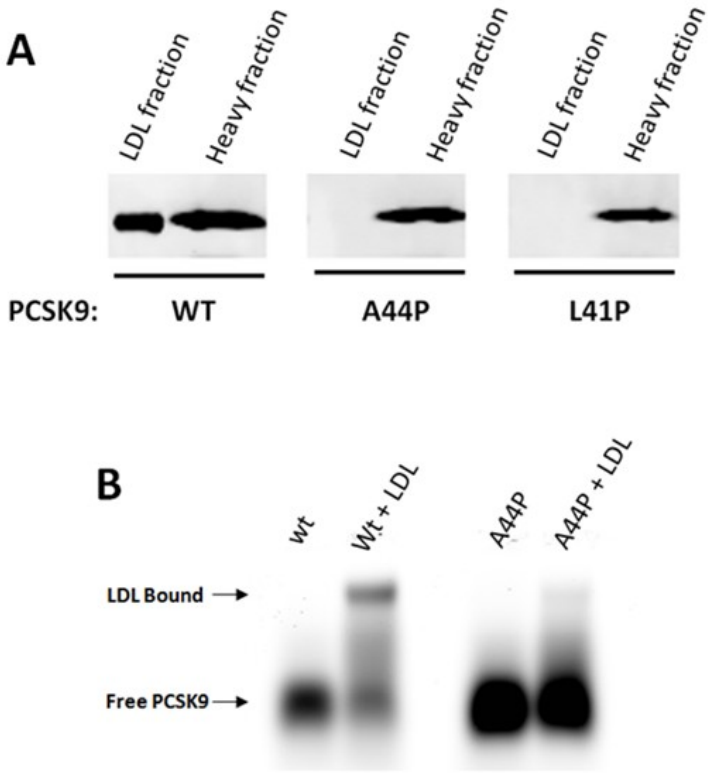

Figure C1: Introduction of helix-disrupting proline residues into PCSK9 prodomain N-terminal cause loss of LDL-binding. (A) Representative immunoblot (of n=3 experiments) of LDL and non-LDL (heavy) fractions of in vitro PCSK9-LDL binding reactions performed similar to experiments in Figure 3C. Probed for FLAG to detect recombinant C-terminally FLAG-tagged PCSK9. **(B)** Agarose gel shift assay of Dylight800-labelled wild-type or A44P-PCSK9 with LDL. 4µg/mL labelled PCSK9 was incubated with 500µg/mL LDL at 37°C for 1 hr. LDL-bound and unbound PCSK9 was resolved on 0.7% agarose. Fluorescently labelled proteins were directly visualized in the agarose on a LI-COR system.

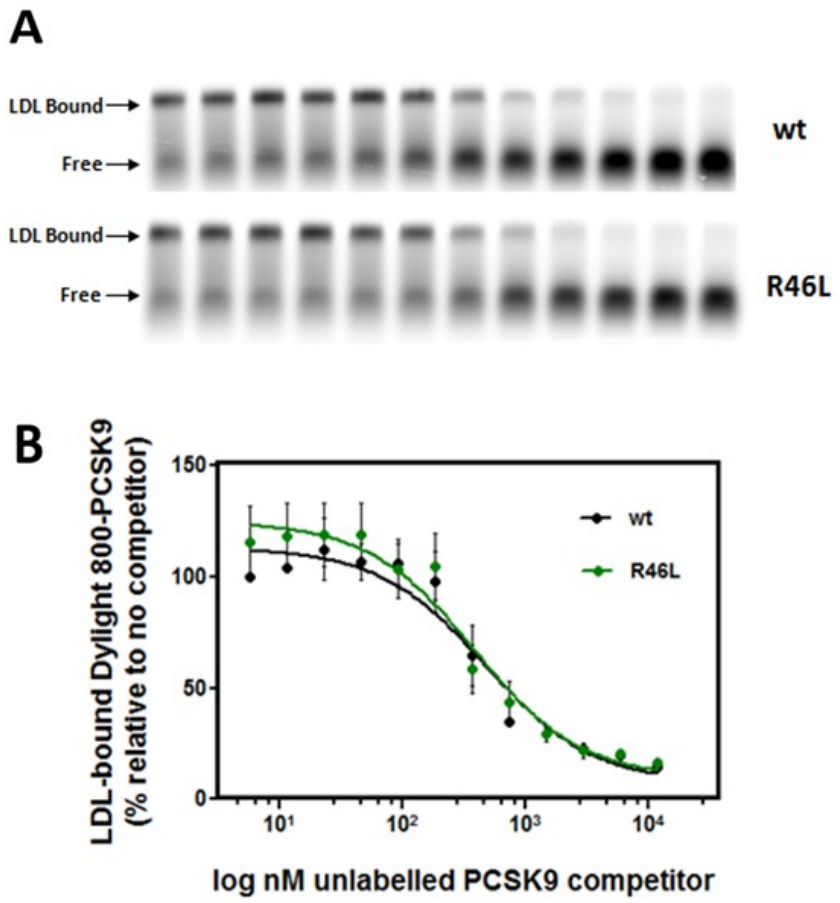

<u>Figure C2</u>: R46L PCSK9 competes for LDL binding with similar affinity to WT PCSK9 in agarose gel shift assay. 10.8nM IR-dye labelled PCSK9 was incubated with 500µg/mL LDL, in the presence of up to 500-fold excess unlabelled PCSK9, either wild-type or R46L. Bound and free complexes were resolved by electrophoresis on 0.7% agarose gels. Gels were visualized on a LI-COR Odyssey system. Bound labeled PCSK9 was quantified and fit to a one-site binding curve on Prism5 software using non-linear regression. Gel scan **(A)** is from one experiment representative of n=3. Mean data ± SEM for n=3 experiments is plotted in **(B)** for non-linear regression analysis. Mean inhibitor constant (Ki) values obtained for WT = 360.1±100.7 nM, for R46L = 357.9±96.7 nM. Difference between K_i's is not statistically significant according to student's t test.

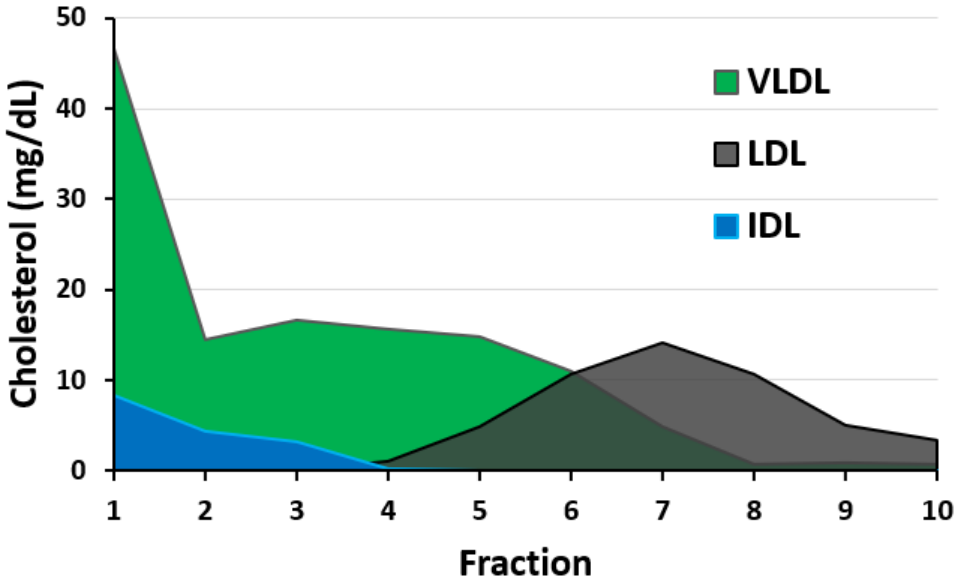

Figure C3: Cholesterol content of density ultracentrifugation fractions. Cholesterol content of the density ultracentrifugation fractions from Figure 11 (page 50) was measured as an indication of lipoprotein floatation within the density gradients. Fractions were obtained from the top to the bottom of the gradient (light to heavy density) covering the range of densities for each lipoprotein class. Portions of each fraction were subjected to a commercial colorimetric enzymatic plate assay to measure the cholesterol content.

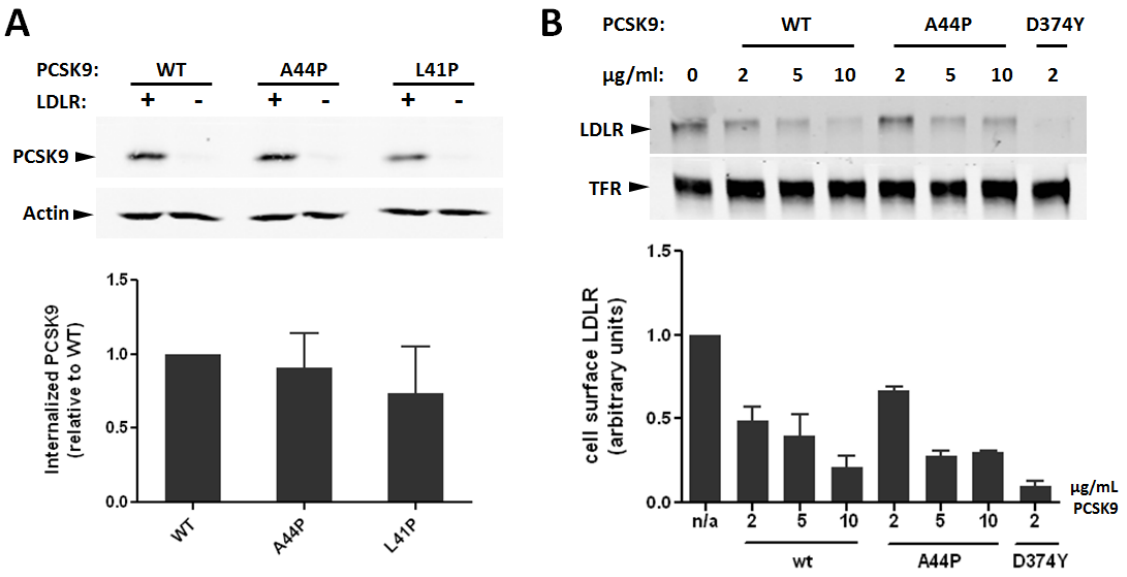

Figure C4: PCSK9 containing helix-disrupting proline mutaions in the N-terminal region can undergo cellular uptake and mediate LDLR degradation similar to wild-type PCSK9. (A) Cellular uptake of PCSK9-FLAG in HEK293 cells. HEK293 cells transfected (or not) with human LDLR were treated with 10µg/ml wild-type or mutant PCSK9-FLAG from conditioned medium for 2 hours at 37°C. Cells were lysed and proteins resolved by SDS-PAGE and detected by immunoblotting. Actin acts as loading control. Plotted means of n=3 with SEM, relative to wild-type. **(B) Cell-surface LDLR degradation by exogenous PCSK9.** HEPG2 cells induced to upregulate LDLR expression by pravastatin treatment were treated with purified exogenous wild-type or A44P-PCSK9-FLAG for 4 hours at 37°C. Cells-surface proteins were then biotinylated and isolated by pulldown with Neutravidin agarose beads, then resolved by SDS-PAGE and detected by western blot. Plotted means of n=3 with SEM, relative to no treatment (n/a). All lanes significantly different from no treatment ($p<0.05$) according to Dunnets post-test after one-way ANOVA.

Curriculum Vitae

SAMANTHA KHADIJA SARKAR

EDUCATION

Ph.D. in Biochemistry (2015 – present), University of Ottawa
- Working thesis title: "The regulation of PCSK9 structure and function by lipoprotein interactions"

M.Sc. in Biochemistry (2013 – 2015), University of Ottawa
- Thesis: "Association of PCSK9 with low density lipoproteins (LDL) in the regulation of LDL-cholesterol" (available at http://dx.doi.org/10.20381/ruor-4155)

B.Sc. Honors Specialization in Biochemistry with Co-op, Magna cum laude (2008 – 2013), University of Ottawa
- Thesis: "Mutagenesis of the prodomain of human Proprotein Convertase Subtilisin / Kexin Type 9 to identify residues important in low-density lipoprotein binding"

RESEARCH AND PROFESSIONAL EXPERIENCE

Lipoprotein Biology: Undergraduate and Graduate Research (May 2012 – present)
University of Ottawa Heart Institute; Atherosclerosis, Genetics and Cell Biology Group.
Supervisor: Dr. Thomas Lagace
- Discovered novel structural conformations of the protein PCSK9, an important regulator of blood cholesterol levels and target for therapeutic drug development, using mutagenesis, in vitro residue mapping and secondary structure studies.
- Characterized the biochemistry of PCSK9 associating with lipoproteins through protein binding assays, cell-based assays, and human plasma studies.
- Initiated *in vivo* work to evaluate different mouse models for the future study of PCSK9-lipoprotein interactions in circulation.

Clinical Biochemistry: Internship integrated in PhD program (July – October 2018)
The Ottawa General Hospital; Department of Pathology and Laboratory Medicine.
Supervisor: Dr. Ronald Booth
- Worked on survey research project aimed to improve physician-to-physician diagnostic consistency by comparing different methods of laboratory test result reporting.
- Shadowed clinical biochemists and technical laboratory staff to learn about the field of medical diagnostic testing.

Antibody Engineering: Undergraduate Co-op (January 2011-December 2011)
National Research Council; Institute of Biological Sciences, Antibody Engineering Group
Supervisors: Dr. Toya Nath Baral, Dr. Pejman Hanifi-Moghaddam
- Produced and tested the effects of humanized single-domain camelid antibodies against tumor markers in breast cancer cell lines using protein purification and cell proliferation assays.
- Tested alternative mechanisms of protein display in phage libraries to better maintain native antibody folding states in phage-display libraries using cloning, phage production, immunoassays and antibody library panning.

PUBLICATIONS

- **Samantha Sarkar,** Alex Foo, Angela Matyas, Tanja Kosenko, Natalie Goto, Ariela Vergera-Jaque and Thomas A. Lagace. A transient helix in the PCSK9 prodomain facilitates an interdomain interaction required for low-density lipoprotein binding (2019) *Manuscript in preparation.*

- **Samantha Sarkar**, Mia Golder, Tanja Kosenko, Angela Matyas, Ikhuosho Asikhia, Mathieu Bode, Ruth McPherson and Thomas A. Lagace. The S127R mutation in PCSK9 associated with autosomal-dominant hypercholesterolemia abolishes low-density lipoprotein binding (2019) *Manuscript in preparation*.

- Michael A. Iacocca, Jian Wang, Thomas Lagace, Jacqueline S. Dron, Samantha Sarkar, Adam D. McIntyre, Paulina Lau, John F. Robinson, Ping Yang, Joan H. Knoll, Henian Cao, Ruth McPherson, Robert A. Hegele. Whole-gene duplication of PCSK9 as a novel genetic mechanism for severe familial hypercholesterolemia (2018) Can J Cardiol. 2018 Oct; 34(10):1316-1324. doi: 10.1016/j.cjca.2018.07.479.

AWARDS AND HONORS

- Canadian Institutes of Health Research Travel Award, $1000 (2018)
- Graduate Poster Award, Canadian Lipoprotein Conference, $500 (multiple: Toronto 2018,Ottawa 2017,Saskatoon 2014)
- Top PhD Seminar Presenter, Biochemistry, Microbiology & Immunology Dept., University of Ottawa, $100 (2017)
- Ontario Graduate Scholarship, $15,000 (2015-2016)
- University of Ottawa Excellence Scholarship, $7000 (2015-2016)
- Faculty of Graduate and Postdoctoral Studies Dean's Scholarship, $1500 (2015)
- PhD Admission Scholarship, $21,000 (2015 – 2019)
- MSc Admission Scholarship, $15,000 (2013 – 2015)

CONFERENCE CONTRIBUTIONS (SELECTED)

Oral presentation
"Proprotein Convertase Subtilisin/Kexin Type-9 may associate with lipoproteins using lipid interactions"
Samantha Sarkar, Alex Foo, Natalie Goto, Thomas Lagace; **Canadian Lipoprotein Conference, 2016**

Poster presentations
"Association of PCSK9 with lipoproteins"
Samantha Sarkar, Tanja Kosenko, Alex Foo, Natalie Goto, Thomas Lagace; **Canadian Lipoprotein Conference, 2017**

"PCSK9 may associate with lipoproteins through lipid interactions"
Samantha Sarkar, Alex Foo, Natalie Goto, Thomas Lagace; **American Heart Association Scientific Sessions, 2016**

"Association of low density lipoproteins with PCSK9, and its role in regulating LDL cholesterol levels"
Samantha Sarkar, Mia Golder, Thomas Lagace; **Ottawa Heart Institute Annual Research Day and Canadian Lipoprotein Conference, 2014**

"Internalized PCSK9 dissociates from recycling LDL receptors in PCSK9-resistant SV-589 fibroblasts"
My-Anh Nguyen, Samantha Sarkar, Tanja Kosenko, Thomas Lagace; **Canadian Lipoprotein Conference, 2013**

Scientific Session Chairing

Chair: "Oral Presentation Session 3: Linkage to Brain and Heart Innovation Hub", **University of Ottawa Heart Institute Research Day 2018**.

Co-chair: "ORACLE Theme-2: Unlocking Novel Causes of Cardiovascular Disease", **University of Ottawa Heart Institute Research Day 2016**.

COMMITTEE MEMBERSHIPS

Graduate Student Representative (2015, 2018), Ottawa Heart Institute Research Day Planning Committee

- Critically evaluated applications for the Heart Institute Trainee of the Year Award.

Communications Officer (2014 – 2018), Ottawa Heart Institute Trainee Committee

- Organize trainee experience enrichment events at the institute e.g. career and scientific workshops and socials.
- Manage communications and record meetings between trainees, the trainee committee and the institute.

TEACHING EXPERIENCE

Laboratory Mentor to junior lab members (2016 – 2018), University of Ottawa Heart Institute

- Trained two undergraduate and one graduate student in performing and analyzing experiments.
- Advised undergraduates in their thesis writing.

Teaching Assistant and Laboratory Demonstrator (2014 – 2017), University of Ottawa

- Biochemistry, General Chemistry and Protein Structure and Function undergraduate courses.
- Supervised student experiments in-lab and assessed student assignments.

COMMUNITY AND VOLUNTEER ACTIVITIES

Heart Institute Science Outreach Team Leader and Classroom Volunteer Visitor (October 2013 – May 2018)
Let's Talk Science, University of Ottawa chapter.

Medical First Responder (January 2011 – April 2014)
Student Emergency Response Group, University of Ottawa, affiliated with St John's Ambulance, Ottawa, ON.

--End--